UNIVERSITÉ DE MONTRÉAL

INVESTIGATION OF NEW INTEGRATION AND INTERCONNECT TECHNIQUES FOR THREE DIMENSIONAL MICROWAVE AND MILLIMETER WAVE INTEGRATED CIRCUITS

JINBANG TANG
DÉPARTEMENT DE GÉNIE ELECTRIQUE
ET GÉNIE ET INFORMATIQUE
ÉCOLE POLYTECHNIQUE DE MONTRÉAL

THÉSE PRÉSENTÉE EN VUE DE L'OBTENTION
DU DIPLÔME DE PHILOSOPHIAE DOCTOR (Ph.D.)
(GÉNIE ELECTRIQUE)
OCTOBRE 2002

Your file Votre référence
ISBN: 0-612-80815-7
Our file Notre référence
ISBN: 0-612-80815-7

UNIVERSITÉ DE MONTRÉAL

ÉCOLE POLYTECHNIQUE DE MONTRÉAL

Cette thèse intitulée:

INVESTIGATION OF NEW INTEGRATION AND INTERCONNECT TECHNIQUES FOR THREE DIMENSIONAL MICROWAVE AND MILLIMETER WAVE INTEGRATED CIRCUITS

Présentée par: TANG Jinbang
en vue de l'obtention du diplôme de: Philosophiae Doctor
a été dûment accepté par le jury d'examen constitué de:

M. BOSISIO Renato-G, président
M. WU Ke, Ph.D., membre et directeur de recherche
M. AKYEL Cevdet, Ph.D., membre
M. CHEN David Z. Z., Ph.D., membre externe
M. CLÉMENT Bernard, Ph.D., représentant du doyen

ACKNOWLEDGEMENTS

Upon the time of completion of this thesis, I would like to express my sincere appreciation to my supervisor Professor Wu Ke, for his guidance and constant encouragement and support during the whole process of my research project. He has always been ready to give his time generously to discuss ideas and difficulties, and to provide invaluable advice. His keen technique insight and profound expertise have greatly benefited me and have been the driving force behind this research. I also wish to express special thanks to the members of my dissertation committee, Professor BOSISIO Renato-G, AKYEL Cevdet, CHEN David Z. Z., and CLÉMENT Bernard, for their invaluable suggestions and precious time spent in reviewing this thesis and participating in the oral defense.

I would like to express my appreciation to those people in the Poly-Grames Research Center, who have given me a great deal of help and support. My special thanks go to Professor Bosisio Renato G., Cevdet Akyel, Laurin Jean-Jacques and Channouchi Fadhel for their help and useful discussions during my graduate study. My thanks also to Mr. Dube Steve and Mr. Gauthier Jules for the fabrication and packaging of the circuits and to Mr. Archambault Rene for the computer and measurement system management.

I also thank my (former) colleagues in Poly-Grames Research Center, particularly Mr. Jean Daniel Richerd, Mr. Dominic Deslandes, Mr. Yves Cassivi, Mr. Jean Dallaire, Mr.

Pin Yang, Dr. Duochuan Li and Dr. Qinwei Shi, for their help and friendship.

I am indebted to my Master degree supervisor Professor Minsong Sun and Quanrang Yang of Southeast University, China. They introduced me into the wonderful world of microwave, millimeter wave technology and wireless communications. I would also like to thank all the people for their invaluable contributions to my personal and professional growth.

Finally, I am greatly indebted to my wife, son, parents and parents in law for their support, endurance and deep understanding. Their love is the impetus of my hard work.

RÉSUMÉ

Cette thèse présente de nouveaux concepts et de nouvelles technologies d'intégration hybride et d'interconnexion applicables aux circuits intégrés micro-onde et onde millimétrique. Les caractéristiques de propagation de ces nouvelles structures hybrides, qui sont réalisées sur un substrat diélectrique relativement mince, sont étudiées par méthode d'analyse numérique ainsi que par expérimentation. Il est démontré que ces structures guidées conservent les avantages de faibles pertes ohmiques et radiatives du guide d'onde diélectrique non-rayonnant (NRD) conventionnel. Les nouvelles méthodes d'intégration et d'interconnexion proposées consistent en une combinaison de deux structures différentes, soit un guide NRD et un circuit planaire, qui permet le contact direct du guide NRD au circuit planaire, le guide NRD étant placé directement sur celui-ci. Deux structures de base sont présentées, la première combinant une ligne microruban avec un guide NRD, l'autre combinant un guide coplanaire avec un guide NRD. Les modes dominants se propageant dans ces structures hybrides sont analysés. Les résultats pour les pertes de transmission et de retour sont présentés pour différentes transitions. Une technique essentielle pour supprimer les modes parasites dans les structures proposées est présentée avec des résultats analytiques et expérimentaux. Cette technique est simple et très efficace dans la suppression des modes parasites pour l'amélioration des performances des circuits intégrés hybrides planaire/guide NRD. Des exemples pratiques de ce suppresseur, combiné à des filtres NRD en onde millimétriques, sont mis à profit pour évaluer les performances de la technique proposée. À partir des résultats d'analyse

et d'expérimentation, il est démontré que le niveau de suppression pour tous les modes parasites, incluant les modes TE et LSE, est meilleur que 35dB pour une transition ligne microruban à guide NRD, et cela sur une très large bande de fréquence. Des techniques générales de suppression de modes parasites sont aussi présentées et étudiées. Pour la transition à performance améliorée entre ligne microruban et guide NRD superposé (le guide NRD est posé directement sur le circuit planaire utilisant un substrat diélectrique relativement mince), la perte de retour est meilleure que 20dB sur la bande d'intérêt, soit de 27.5GHz à 28.5GHz. Les modes parasites les plus fortement excités par cette transition sont les modes TE_{20} et LSE_{40}, mais ils sont atténués par plus de 35dB sur toute la bande de fréquence. Dans le cas de la transition à performance améliorée entre guide coplanaire et guide NRD superposé, tous les modes parasites peuvent être supprimés en utilisant une méthode simple impliquant un suppresseur intégré. Le niveau de suppression pour tous les modes parasites, incluant les modes TE et LSE, est meilleur que 50dB pour une seule transition et pour toute la large bande d'intérêt. Pour faciliter l'implémentation du suppresseur de mode, une technique compacte de suppression des modes parasites intégrée dans la conception de transition pour une structure hybride planaire/guide NRD est présentée et analysée. Finalement, un arrangement simple mais très efficace d'interconnexion par ruban est aussi proposé pour les modules multi-puces (MCM) sur même couche fonctionnant en micro-onde et en onde millimétrique.

ABSTRACT

This thesis presents new concept and technology of hybrid integration and interconnects for the applications in microwave and millimeter wave integrated circuits. Guided-wave characteristics of the new hybrid or composite structure, which is surface-mounted on a relatively thin dielectric substrate, are studied numerically and experimentally. It is demonstrated that this type of transmission line can preserve low-loss and almost non-radiating advantages of the conventional NRD (Non-Radiative Dielectric)-guide. New integration and interconnects approach utilizes co-layered arrangement of the two dissimilar structures, which allows the NRD-guide in direct contact with (or surface-mounted on) the planar circuits. Two basic building block schemes are presented that involve microstrip line and coplanar waveguide (CPW) with the NRD-guide. Principal modes generated in the hybrid planar/NRD-guide structure are modeled. Results for transmission and return loss are presented for different transitions. Key technique for suppressing spurious modes is presented with experiments and analysis results. It is simple and very effective in rejecting the spurious modes for performance enhancement of hybrid planar/NRD-guide integrated circuits. Practical examples in the design of millimeter-wave planar/NRD-guide filter are exploited to evaluate features of the proposed technique that yields expected good results. It is found through analysis and experiments that the rejection to all the spurious modes (including TE and LSE modes) can be better than –35 dB for a single microstrip-to-NRD-guide transition over a broadband frequency of interest. General spurious mode-suppressing techniques have

also been presented and investigated. For the performance enhanced integrated microstrip-to-surface-mounted NRD-guide transition (NRD-guide surface-mounted on the top of a relatively thin planar substrate), the return loss is better than -20 dB over the frequency band of interest from 27.5 to 28.5 GHz. The worst spurious modes excited in this case are TE_{20} and LSE_{40} modes but they are all suppressed to be better than –35 dB over the frequency range. For the performance enhanced integrated CPW-to-surface-mounted NRD-guide transition, all potential spurious modes related to CPW-to-NRD-guide transitions may be suppressed with a simple scheme that involves an integrated mode suppressor. The rejection to all of the spurious modes (including TE and LSE modes) is better than -50 dB for a single transition over a broadband frequency of interest. To facilitate the implementation of the mode suppressor, a compact spurious mode suppressing technique for the design of hybrid planar/NRD-guide integrated transition is then presented and analyzed. A very effective but rather simple scheme of ribbon interconnect is also proposed for co-layer multi-chip module (MCM) of microwave and millimeter-wave circuits.

LIST OF PUBLICATIONS

During the course of the Ph.D. program, the following publications have been produced.

[1] TANG J., and WU K. (2000), Co-layered integration and interconnect of planar circuit and non-radiative dielectric (NRD) wave-guide, IEEE Trans. Microwave Theory Tech., vol. 48, pp. 519-524.

[2] TANG J., DESLANDES, D., and WU K. Suppression of spurious modes for performance enhancement of hybrid planar/NRD-guide integrated circuits, has been accepted by IEE Proceedings - Microwaves, Antennas and Propagation for publication.

[3] TANG J., DESLANDES, D., ZENG X.; XU S.; WU K., Substrate-Mounted Non-Radiative Dielectric (NRD)-Guide For Low-Loss Millimeter-Wave Integrated Circuits, IEE Proceedings - Microwaves, Antennas and Propagation, Vol. 148, No. 5, pp. 291-294.

[4] TANG J., DESLANDES, D.; and WU K. (2000), Spurious mode suppressing technique for performance enhancement of hybrid planar/NRD-guide circuits, Microwave Conference, Asia-Pacific, pp. 140-143.

[5] TANG J., and WU K. (2000), Integrated microstrip to NRD-guide transition using a spurious mode suppressing technique, IEEE MTT-S International Microwave Symposium Digest, Volume: vol. 3, pp. 1805–1808.

[6] TANG J., ZENG X.; XU S.; WU K. (2000), Low-loss millimeter-wave propagation characteristics of NRD-guide surface-mounted on planar substrate for

hybrid integrated circuit, IEEE MTT-S International Microwave Symposium Digest, Volume: vol. 3, pp. 1679-1682.

[7] TANG J., and WU K. (1999), Three dimensional (3-D) integration scheme of surface mounted non-radiative dielectric (NRD) waveguide and coplanar waveguide (CPW), Microwave Conference, Asia-Pacific, vol. 2, pp. 262-265.

[8] TANG J., and WU K. (1999), Design technique of broadband planar interconnects for co-layer multi-chip module (MCM) of microwave and millimeter-wave circuits, Microwave Conference, Asia-Pacific, vol. 1, pp. 116-119.

[9] TANG J., and WU K. (2000), Modeling and properties of hybrid integration structures based on unbalanced nonradiative dielectric (NRD) waveguide, Proc. SPIE, Terahertz and Gigahertz Photonics II, vol. 4111, p. 267-275.

[10] TANG J., and WU K. (1999), New millimeter-wave circuit building block concept using innovative surface-mounted nonradiative dielectric (NRD) waveguide, Proc. SPIE, Terahertz and Gigahertz Photonics, vol. 3795, p. 631-638.

[11] TANG J., DESLANDES, D., BOONE F., DAMPHOUSSE S., and WU K. (2000), Hybrid microstrip/NRD-guide filter with enhanced upside stop-band rejection, Symposium on Antenna Technology and Applied Electromagnetics, ANTEM'2000, Winnepeg, Canada, Aug.

ÉTUDE DE NOUVELLES TECHNIQUES D'INTÉGRATION ET D'INTERCONNEXION POUR DES CIRCUITS INTÉGRÉS MICRO-ONDES ET ONDES MILLIMÉTRIQUES À 3 DIMENSIONS

Cette thèse présente de nouveaux concepts et de nouvelles technologies d'intégration hybride et d'interconnexion applicables aux circuits intégrés micro-onde et onde millimétrique. Le tout est basé sur une nouvelle classe de guide NRD à faible perte qui est déposé directement sur un circuit planaire.

1. Introduction

La poussée explosive du marché des systèmes de communication sans fil à large bande a amené le consommateur à demander des systèmes de qualité à faible coût. La technologie en onde millimétrique est le moteur principal derrière la croissance rapide d'une variété de services et des systèmes de communication sans fil plus élaborés. Par exemple, mentionnons les services LMDS/LMCS/MVDS opérant entre 24 et 42GHz, ainsi que les senseurs anti-collisions pour véhicules fonctionnant à 77GHz. Dans ces applications, des circuits intégrés monolithiques micro-ondes (MMIC) ainsi que des circuits multicouches miniaturisés à multiples MMIC sont largement utilisés pour réduire les coûts et augmenter les performances systèmes. L'aspect le plus important dans la conception de systèmes en onde millimétrique est l'utilisation de modules à faible coût ayant de haute performance et à haut rendement.

Dans la bande des ondes millimétriques, les circuits planaires comme la ligne microruban, le guide coplanaire (CPW), la ligne suspendue, la ligne à fente profilée et d'autres lignes de transmission traditionnelles ont été populaires dans la conception de circuits hybrides et monolithiques conventionnels. Les avancées récentes en recherche indiquent que la technologie multicouche planaire pourrait permettre la réalisation de modules à haut niveau d'intégration pouvant respecter les contraintes les plus difficiles, comme le coût, la compacité, ainsi que les capacités multi-fréquences et multi-fonctions. En particulier, de nouvelles techniques d'intégration ont démontrés des caractéristiques prometteuses pour la conception de circuits de très haute densité, soit les circuits MMIC à 3 dimensions (3D) et la technologie des céramiques fusionnées à basse température (LTCC). Des émetteurs/récepteurs onde millimétriques MMIC complètement intégrés, incluant amplificateur de puissance, amplificateur à faible bruit et les convertisseurs de fréquences, sont déjà largement utilisés dans la conception de systèmes de communication à onde millimétrique. Néanmoins la conception de circuits passifs intégrés se heurte toujours à des problèmes majeurs, comme par exemple pour les filtres passe-bande à faible perte, pour lesquels la technologie planaire n'est pas appropriée. Bien souvent, la seule solution pour ces circuits passifs est l'utilisation de la technologie guide d'onde qui est trop volumineuse. Des techniques avancées d'interconnexion entre ligne microruban et guide d'onde ont été publiées, ce qui indique un intérêt croissant dans les techniques hybrides associant les MMICs et les guide d'ondes dans la bande millimétrique. Présentement, un émetteur/récepteur MMIC intégré combiné avec un diplexeur hybride guide d'onde forme l'architecture typique la plus rencontrée dans les

radios millimétriques.

Des structures planaires multicouches alternatives ont été proposées pour permettre la réduction de taille de divers circuits micro-ondes. Elles emploient essentiellement les avantages cohérents et complémentaires de chaque technologie planaire, comme la ligne à fente avec le guide coplanaire, et comme la ligne microruban avec la ligne à ruban. Par conséquent ces deux différents groupes de structures peuvent être facilement conçus et intégrés dans un seul module avec différentes couches diélectriques, permettant une compacité tout en tirant avantage des propriétés de chaque ligne de transmission. Dans ce cas, différents types d'interconnexion entre les circuits a été utilisés. Cependant, il reste toujours plusieurs problèmes difficiles associés à cette technologie multicouche, comme les ondes de surface, le couplage parasite et la mise à la masse sur plusieurs niveaux.

Le guide d'onde diélectrique non-rayonnant (NRD) est connu comme une plate-forme de conception prometteuse pour les circuits intégrés à onde millimétrique parce que c'est un guide non-rayonnant, à faible perte et possiblement à faible coût. Néanmoins il reste toujours des problèmes à résoudre pour permettre une large utilisation de ce guide. Puisque le mode guidé à faible perte d'intérêt n'est pas le mode dominant, des suppresseurs sont nécessaires pour éliminer les modes non-voulus. Dans la plupart des cas, ils sont conçus pour couper le mode LSE. En pratique, des modes TE parasites associés au guide d'onde diélectrique à plaque parallèle qu'est le NRD peuvent être excités par des discontinuités. Par conséquent, la performance dans les bandes de rejet

d'un filtre NRD est habituellement détériorée, particulièrement dans la partie haute fréquence.

Un concept d'intégration hybride de circuit planaire avec un guide NRD a été proposé et développé qui vise à exploiter les avantages complémentaires inhérents des deux structures tout en éliminant (au moins partiellement si non complètement) les inconvénients potentiels de chaque structure. En pratique, des modes TE parasites associés au guide d'onde diélectrique à plaque parallèle qu'est le NRD peuvent être excités par des discontinuités. En ce qui concerne la technologie d'intégration hybride planaire/guide NRD, les transitions planaires à guide NRD présentent elles-mêmes des discontinuités qui sont nuisibles puisque les modes parasites non-voulus peuvent être générés. Donc, les caractéristiques attrayantes fondamentales de la technique hybride planaire/guide NRD proposée ne peuvent pas être entièrement exploitées. La suppression de mode est un des aspects fondamentaux autant pour la technologie du guide NRD standard que pour la technologie hybride planaire/guide NRD.

Il est difficile d'obtenir toutes les performances requises pour un circuit simultanément en optant pour une seule technologie. Cet argument suggère finalement qu'une technique hybride appropriée impliquant deux technologies ou plus fournit une possibilité d'accomplir toutes caractéristiques désirées en combinant leurs avantages pendant que chaque défaut inhérent individuel est éliminé. En grande partie, une technique efficace d'interconnexion et d'intégration horizontal et/ou vertical à faible perte et faible coût est

l'aspect fondamental à résoudre pour atteindre une conception de circuit à haute densité, laquelle semble être de plus en plus difficile lorsque la fréquence augmente.

L'objectif de ce travail est de résoudre les problèmes prohibitifs dans la conception de circuits micro-ondes et onde millimétriques multicouches à 3 dimensions (3D). Se basant sur le concept du guide diélectrique non-rayonnant (NRD) conventionnel, une famille de nouveaux circuits de base pour une technologie de guide diélectrique posé en surface ont été proposés, analysés et vérifiés. De nouvelles techniques d'intégration et d'interconnexion ont été proposées et leurs avantages ont été démontrés. Une nouvelle famille de techniques de suppression de modes parasites a aussi été proposée pour obtenir des augmentations de performance supplémentaires.

Puisque plusieurs parties des résultats de recherche de cette thèse ont été publiés ou soumis à des journaux ou conférences internationales avec comité de lecture, quelques chapitres de la thèse sont présentés sous la forme d'article avec quelque réorganisation structurelle.

2. Guide diélectrique non-rayonnant (NRD) posé sur substrat — Nouveau circuit de base en onde millimétrique

Le chapitre II présente le nouveau concept de circuit de base. Une famille de guide diélectriques posé sur substrat sont présentés et étudiés pour des applications en micro-onde et en onde millimétrique. La preuve de faisabilité est donnée avec les résultats

d'analyse. La variété des structures et les caractéristiques électriques/mécaniques uniques de la ligne de transmission diélectrique proposée, laquelle pourrait être réalisée avec les techniques d'intégration actuelles, promettent d'être instrumentaux dans la réalisation d'une famille de circuits intégrés 3D à haute performance.

3. Analyse théorique et vérification expérimentale du guide diélectrique non-rayonnant (NRD) posé sur substrat

Dans le chapitre III, les caractéristiques de propagation de la nouvelle structure hybride, laquelle est posé sur un substrat diélectrique relativement mince, sont étudiées par méthode d'analyse numérique ainsi que par expérimentation. Premièrement les expressions générales des champs des modes hybrides pour un guide NRD posé sur substrat sont dérivées, et ensuite les caractéristiques principales de la structure proposée sont discutées en se basant sur l'analyse théorique. Des résultats détaillés fournissent les indications nécessaires pour la conception de circuits ondes millimétriques hybrides planaire/guide NRD à faible perte utilisant cette technologie. Il est démontré que ce type de ligne de transmission peut conserver les avantages de faible perte ohmique et radiative d'un guide NRD conventionnel. Les résultats d'expérimentation permettent de vérifier les caractéristiques de faible perte de cette structure. De plus, les effets de la largeur des plans de masse sont aussi discutés pour montrer la faible ou même inexistante radiation de la structure. Un article, lequel est basé sur les résultats principaux de l'étude présenté dans ce chapitre, a été publié en octobre 2001 dans le journal IEE Proceedings – Microwaves, Antennas and Propagation.

4. Techniques d'interconnexion et d'intégration sur une même couche

Dans le chapitre IV, le nouveau concept d'intégration hybride entre un circuit planaire et un guide diélectrique non-rayonnant (NRD) est présenté avec des résultats d'essais préliminaires. Cette approche utilise deux structures dissemblables disposées sur une même couche, ce qui permet un contact direct entre le guide NRD et le circuit planaire. Deux arrangements de base sont présentés qui implique une ligne microruban ou un guide coplanaire (CPW) avec un guide NRD. Le premier consiste en la déposition du guide NRD sur le dessus d'un substrat microruban relativement mince, formant ainsi un circuit hybride NRD non-balancé, tandis que le second permet la gravure de circuit CPW directement sur les deux plans métalliques du guide NRD. Le guide NRD non-balancé est susceptible à des pertes par radiation, mais leur le niveau des pertes est négligeable, et même complètement inexistant dans certaine condition. Une telle technique d'intégration est jugée compatible avec le concept d'interconnexion en onde millimétrique à faible perte. En d'autres mots, simplement en déposant et couvrant le guide NRD sur des circuits planaires, le guide NRD peut être utilisé pour relier convenablement ces derniers. Les résultats de mesures de plusieurs transitions entre circuits hybrides sur même couche indiquent que des caractéristiques de transmission satisfaisantes peuvent être atteintes facilement. Ces nouveaux circuits de base pourraient fournir une approche alternative pour la conception de circuits et systèmes millimétriques multicouches à 3 dimensions. Un article se basant sur une partie des résultats de recherche présentés dans ce chapitre a été publié en avril 2000 dans le journal 'IEEE Transaction on Microwave Theory and Techniques'.

5. Modélisation et propriétés de structures hybrides intégrés basées sur le guide diélectrique non-rayonnant (NRD) posé sur substrat.

Dans le chapitre V, des transitions entre circuit planaire et guide hybride planaire/guide NRD, lesquelles fournissent une base pour la conception d'application large bande à haute performance, ont été étudié avec une emphase sur l'analyse de modes parasites potentiels. Les principaux modes générés dans la structure hybride planaire/guide NRD sont modélisés. Les résultats des pertes de retour et de transmission pour différentes transitions sont présentées. L'étude indique qu'une transition hybride planaire/guide NRD optimisée mais non compensée, présentée au chapitre IV, serait suffisamment performante pour plusieurs applications sur une certaine bande de fréquence. Cependant pour les applications larges bandes, des suppresseurs de modes parasites sont nécessaires pour éliminer les modes non voulus.

6. Suppression des modes parasites pour la conception de circuits intégrés hybrides ligne microruban et guide NRD

Dans le chapitre VI, une nouvelle technique de suppression de modes parasites est présentée qui englobe une transition ligne microruban à guide NRD et un suppresseur de mode. Les indications et les procédures de conception sont ensuite adressées. Les techniques générales de suppression de modes pour la transition ligne microruban à guide NRD posé sur un substrat (le guide NRD est posé sur un substrat planaire relativement mince) a aussi été étudié. Pour faciliter l'implémentation du suppresseur de mode, une technique compacte de suppression de mode pour la conception d'une transition hybride

planaire à guide NRD intégré est ensuite présentée et analysée. La structure plan métallique/film est utilisée dans la conception du suppresseur de mode, lequel est compacte et facile à réaliser. Notre étude a permis de trouver que le rejet de tous les modes parasites (incluant les modes TE et LSE) peut être meilleure que 32dB pour une seule transition sur une bande de fréquence d'intérêt. Ce résultat pourrait être amélioré davantage. Cette technique de conception compacte fournit aussi une solution alternative au problème inhérent de l'excitation de modes parasites (particulièrement les modes TE) dans les circuits standards à guide NRD. Plusieurs filtres en technologie hybride planaire et guide NRD ont été conçus et réalisés dans la bande de fréquence millimétrique pour évaluer les caractéristiques intéressantes de la technique proposée. Ces résultats expérimentaux montrent que le rejet de tous les modes parasites (incluant les modes TE et LSE) est meilleur que 35dB pour une seule transition sur la bande de fréquence d'intérêt. Un article basé sur une partie des résultats de l'étude de ce chapitre a été accepté pour publication dans le journal 'IEE Proceedings – Microwaves, Antennas and Propagation'.

7. Conception et applications des circuits hybrides intégrés guide NRD et CPW

Dans le chapitre VII, une antenne NRD innovatrice alimentée par CPW qui inclut la transition hybride CPW à guide NRD est présenté. Les résultats d'analyse démontre que de faible pertes d'insertion et de retour peuvent être obtenues avec le concept proposé. Dans la deuxième partie du chapitre, une technique de suppression de modes parasites pour améliorer les performances de la transition large bande entre CPW et guide NRD est

présentée. Ce travail révèle aussi quelques caractéristiques électriques et mécaniques intéressantes et uniques pour la structure proposée dans la conception de circuits 3D.

8. Techniques d'interconnexion planaires larges bandes pour les modules multi-puces (MCM) sur même couche fonctionnant en micro-onde et en onde millimétrique.

Dans le chapitre VIII, une nouvelle topologie d'interconnexion utilisant des liaisons à ruban est présentée. C'est un arrangement simple mais très efficace pour la conception large bande de module multi-puces (MCM) sur même couche fonctionnant en micro-onde et en onde millimétrique. D'excellentes performances ont été démontrées théoriquement et expérimentalement.

9. Conclusions et suggestions de travaux futurs

De nouvelles techniques d'intégration et d'interconnexion ont été présentées, étudiées et validées. Les caractéristiques avancées associées à ces nouvelles techniques ont été démontrées. Les travaux futurs devraient porter sur le développement d'applications pratiques en utilisant des procédés de fabrication existants. Dans le chapitre IX fournit plusieurs conclusions et suggestions pour les travaux futurs.

TABLE OF CONTENTS

LIST OF FIGURES

LIST OF ACRONYMS

3D	Three Dimensional
BWA	Broadband Wireless Access
CAD	Computer Aided Design
CPW	Co-planar Waveguide
H(M)MIC	Hybrid/Monolithic Microwave Integrated Circuit
HTCC	High Temperature Co-fired Ceramic
LMDS	Local Multipoint Distribution Service
LMCS	Local Multipoint Communication System
LNA	Low Noise Amplifier
LSE	Longitudinal Section Electric
LSM	Longitudinal Section Magnetic
LTCC	Low Temperature Co-fired Ceramic
MEMS	Micro-Electro-Mechanical system
MIC	Microwave Integrated Circuit
MMIC	Monolithic Microwave Integrated Circuit
MVDS	Multichannel Multipoint Distribution Service
NRD	Non-Radiative Dielectric
PA	Power Amplifier
PCS	Personal Communication Services
TE	Transverse Electric

TEM	Transverse ElectroMagnetic
TM	Transverse Magnetic
TRL	Thru-Return-Line
WLAN	Wireless Local Area Network
λ_g	Guided wavelength
λ_0	Free space wavelength
k_0	Free space propagation constant
α	Attenuation constant
β	Phase constant
ε	Dielectric constant
ε_r	Relative dielectric constant
μ	Permeability
μ_r	Relative permeability

CHAPTER I

INTRODUCTION

Explosive growth in the broadband wireless access market has led to consumer demand for low-cost, high-quality systems. Millimeter wave technology is one of the principal driving forces behind the rapid development of a variety of advanced wireless communications and services, for example, LMDS/LMCS/MVDS operating from 24 and 42 GHz, and vehicle collision warning sensor at 77 GHz. In these applications, monolithic microwave integrated circuits (MMICs) as well as multi-layer, multi-chip miniaturized circuits have been widely used for the cost reduction and system performance enhancement. One of the most important issues in dealing with the design of the millimeter-wave systems is to make use of a high-yield and high-performance circuit building block at low-cost.

1.1 Brief review of the existing millimeter-wave circuit building block technology

Over the millimeter-wave range, planar circuits on the basis of microstrip, coplanar waveguide (CPW), suspended stripline, finline and other traditional transmission lines have been popular for conventional hybrid and monolithic integration designs. Recent research progress indicates that multi-layer planar technology may provide a high-level module integration achieving some of these stringent requirements such as low-cost and

compactness as well as multi-frequency and multifunction operation. In particular, newly emerging integration schemes have shown promising features for high-density circuit designs, namely, three-dimensional (3D) MMICs, and low-temperature co-fired ceramic (LTCC) technology [1, 2]. Fully integrated millimeter wave MMIC transceivers (including MMIC PA, LNA, up and down-converters) have already been widely employed in millimeter-wave communications system designs. Multi-chip Modules (MCMs) as a group of highly functional electronic devices provide reliable low-cost integration technology, which allows integrating several ICs from various processing technologies into a system. Nevertheless, there are still bottleneck problems in the design of low-loss passive integrated circuits, just to name an example, a high-Q band-pass filter, to which the planar geometry is fundamentally not amenable. Quite often, the bulky metallic waveguide technique is necessary in the design of passive blocks to overcome these inherent difficulties of the planar structures. Advanced interconnects between the microstrip line and metallic waveguide have been reported [3, 4], which indicate the growing interests in the hybrid technique involving MMICs and wave-guide at millimeter wave frequencies. Integrated MMIC transceiver combined with hybrid waveguide diplexer is the typical architecture observed in most of current millimeter wave radios.

Alternative multi-layered planar structures have been proposed for application to compact different microwave circuits [5], which exploit essentially the coherent and complementary advantages of each planar topology such as CPW/slotline and mictostrip/stripline. As a result, these two different groups of structures can be designed

and integrated well into a single building block with alternated dielectric layer so that the compactness and advantages of each line can be benefited, in this case, different kind of interconnects between the circuits have been used. However, there are still several challenging problems coming from the proposed multi-layer topology such as surface-wave and parasitic coupling, multi-level grounding.

The non-radiative dielectric (NRD)-guide has been known as a very promising design platform for millimeter-wave integrated circuits because of its non-radiating, low-loss transmission properties at potentially low cost [6-9]. Nevertheless, there are still problems to be solved for its wide application. Since the low-loss guided mode of interest is not the lowest mode, suppressors for eliminating unwanted modes are required. In most cases, they are designed to reject the LSE mode as shown, for example, in [10-11]. In practice, spurious TE modes in view of a parallel-plate dielectric waveguide may be excited by discontinuity. As a result, the stop-band or out-of-band performance (especially the higher portion) of NRD-guide filter is usually deteriorated.

A hybrid integration concept of planar circuit and NRD-guide has been proposed and developed that aims at exploiting inherent complementary advantages of both planar circuit and NRD-guide while eliminating (at least partly if not completely) potential drawbacks of each building block [12]. Similarly, spurious TE modes in view of a parallel-plate dielectric waveguide may also be excited by discontinuity. With regard to the hybrid planar/NRD-guide integration technology, the planar line-to-NRD-guide

transitions present themselves certain discontinuities that are harmful since the unwanted spurious modes may be generated. Therefore, the underlying attractive features of the proposed hybrid planar/NRD-guide technique may not be fully exploited. Mode suppressing is one of the key aspects in both the standard NRD-guide technology and the hybrid planar/NRD-guide technology.

Today there are more dielectric material options. Low loss, high performance commercial dielectric materials are available for the NRD-guide based circuit design. Several commonly used materials are listed in Table 1.1.

Table 1.1 Typical dielectric properties

	Dielectric Constant @10GHz	Loss δ @10GHz
ECCOSTOCK	2.54	0.0005
Rogers TMM 3	3.27	0.0016
Rogers TMM 6	6.0	0.0018
Rogers TMM 10i	9.8	0.0015
Rogers RT/Duroid 5880	2.2	0.0009
Rogers RT/Duroid 5870	2.33	0.0012

It is difficult to achieve simultaneously overall required circuit performance by utilizing a single technology framework. This argument eventually suggests that an appropriate hybrid scheme involving two or more technologies provide a possibility of accomplishing all desired features by combining their advantages while each individual inherent shortcoming are eliminated. To a large extent, effective, low-loss and low-cost horizontal and/or vertical integration and interconnect technique is the key issue in achieving a high-density integration of circuit design, which seems to be more and more difficult as

frequency increases.

1.2 Objective and outline of the thesis

The objective of this work is to address the bottleneck problems in the design of multi-layer 3D-microwave and millimeter wave circuits. Based on the concept of the conventional non-radiative dielectric (NRD) guide, a class of new circuit building blocks — surface mounted dielectric guide based structures have been proposed, analysed and verified. New integration and interconnects techniques have been proposed and the advantages have been demonstrated. A class of spurious mode suppressing techniques have been proposed for further performance enhancement design.

The thesis consists of eight chapters. Chapter II presents the new concept of circuit building block. A class of surface mounted dielectric guides has been presented and investigated for microwave and millimeter wave applications. The proof of concept has been provided with analysis results. The variety of the structures and the unique electrical/mechanical features of the proposed dielectric transmission line, which could be realized with the available integration technique, promise to be instrumental in constructing a class of high performance 3-D integrated circuits.

In chapter III, guided-wave characteristics of the new hybrid or composite structure, which is surface-mounted on a relatively thin dielectric substrate, are studied numerically

and experimentally. We first derive general expressions for hybrid-mode fields of the typical surface-mounted NRD-guides, and then the basic characteristics of the proposed structure are discussed based on theoretical analysis. Detailed results provide us a basic guideline for the design of low-loss hybrid planar/NRD-guide millimeter-wave circuits using such a composite building block. It is demonstrated that this type of transmission line can preserve low-loss and almost non-radiating advantages of the conventional NRD-guide. Our experiments further verify the low-loss characteristics of the structure. In addition, effects of the width of ground plane are also discussed to show its low or non-radiating guided-wave properties. One paper, which is based on the main investigation results of this chapter, was published in October 2001 issue of IEE Proceedings - Microwaves, Antennas and Propagation.

In chapter IV, the new concept of hybrid integration between planar circuits and non-radiative dielectric (NRD) waveguide is presented with preliminary experiments. This approach utilizes co-layered arrangement of the two dissimilar structures, which allows the NRD-guide in direct contact with (or surface-mounted on) the planar circuits. Two basic building block schemes are presented that involve microstrip line and coplanar waveguide (CPW) with the NRD-guide. The first is to deposit the NRD-guide on the top of a relatively thin microstrip substrate, thus forming unbalanced NRD-guiding hybrid circuits while the second is to design CPW circuits directly etched on the ground planes of the NRD-guide. The unbalanced NRD-guide is subject to a certain leakage loss but at a negligible level, and it may even be suppressed completely in certain circumstances. Such

an integration technique is found consistent with the concept of low-loss interconnects at millimeter-wave frequencies. In other words, the NRD-guide can be used for viable interconnects of co-layered planar circuits with a simple "put and cover" procedure. Measured results of several co-layered hybrid transitions/baluns indicate that satisfactory transmission properties can readily be achieved. The new building blocks are expected to provide an alternative design approach to 3-D multilayered millimeter-wave circuits and systems. One paper, which is based on part of the investigation results of this chapter, was published in April 2000 issue of IEEE Transaction on Microwave Theory and Techniques.

In chapter V, transitions of planar circuit to surface-mounted NRD-guide have been studied with emphasis on the analysis of potential spurious modes, which provides a basis for the performance-enhanced broadband design and applications. Principal modes generated in the hybrid planar/NRD-guide structure are modeled. Results for transmission and return loss are presented for different transitions. The investigation indicates that an optimized but uncompensated hybrid planar/NRD-guide integrated transition as presented in chapter IV should be good enough for many applications over a certain frequency band. For broadband applications, however, spurious mode suppressors in the design of eliminating unwanted modes are required.

In chapter VI, a new spurious mode suppressing technique is first presented, concerned with an integrated microstrip-to-NRD-guide transition and a mode suppressor. The

design guideline and procedures are then addressed. With some simple modifications, this spurious mode-suppressing concept can be extended and applied to a class of integrated planar to surface-mounted NRD-guide transitions. General spurious mode-suppressing techniques for the integrated microstrip-to-surface-mounted NRD-guide transition (NRD-guide surface-mounted on the top of a relatively thin planar substrate) have also been investigated. To facilitate the implementation of the mode suppressor, a compact spurious mode suppressing technique for the design of hybrid planar/NRD-guide integrated transition is then presented and analyzed. The metallic plate/film mode suppressing structure is used in the design, which is compact and easy to implement. It is found through our investigation that the rejection to all the spurious modes (including TE and LSE modes) can be better than -32 dB for a single transition over a broadband frequency of interest, and the performance could be further enhanced. This compact design technique also provides an alternative solution to the inherent problem of spurious mode (especially TE modes) in the standard NRD-guide circuit design. Several planar/NRD-guide filters are designed and implemented over millimeter-wave frequency band to evaluate the interesting features of the proposed technique. Those obtained experimental results indicate that the rejection to all the spurious modes (including TE and LSE modes) can be better than –35 dB for a single proposed transition over a broadband frequency of interest. One paper, which is based on part of the investigation results of this chapter, has been accepted by IEE Proceedings - Microwaves, Antennas and Propagation for publication.

In chapter VII, an innovative CPW-fed surface-mounted NRD-guide antenna that includes hybrid CPW/NRD-guide transition has been presented. Analysis results demonstrate that low transmission loss and good return loss can be achieved with the proposed concept. In the second part of this chapter, a spurious mode suppressing technique for the performance enhancement in the design of a broadband CPW-to-NRD-guide transition is presented. This work also reveals some interesting and unique electrical and mechanical features of the proposed building blocks in 3-D design.

Despite the emergence of new packaging and interconnect technologies, wire bonding remains the dominant conventional low cost, high reliability and high manufacturability chip connection technology. A novel ribbon bond interconnect topology has been proposed, and excellent performance has been theoretically and experimentally demonstrated, this is presented in Chapter VIII. It is a very effective but rather simple technique for applications in the broadband design of co-layer multi-chip module (MCM) of planar circuits at microwave and millimeter-wave frequencies.

Chapter IX provides conclusions and suggestions for the future work. The future work should be associated with the available advanced processing techniques, and should focus on the practical applications.

CHAPTER II

SUBSTRATE-MOUNTED NON-RADIATIVE DIELECTRIC (NRD)-GUIDE — NEW MILLIMETER-WAVE CIRCUIT BUILDING BLOCK

2.1 Introduction

In recent years, there has been growing interest in finding new transmission media for use in the higher frequency range microwave and millimeter wave circuits. Non-radiative dielectric (NRD) waveguide has been known as a very promising transmission line for use in designing passive and active millimeter-wave integrated circuits because of its non-radiating discontinuity, low-loss transmission and easy mechanical fabrication [6, 7, 9]. Figure 2.1 shows the geometrical view of the conventional NRD-guide. However, an effective integration with active devices may be difficult in the original version of the proposed NRD-guide technology in light of potential ductile and/or brittle problems as well as required precision mechanical assembling and/or alignment of multi dielectric strips.

In this chapter, a class of surface mounted dielectric guides have been proposed and briefly analyzed. The structures are proposed in particular to facilitate their application in the multi-layer/three dimension (3-D) microwave and millimeter wave integrated circuits.

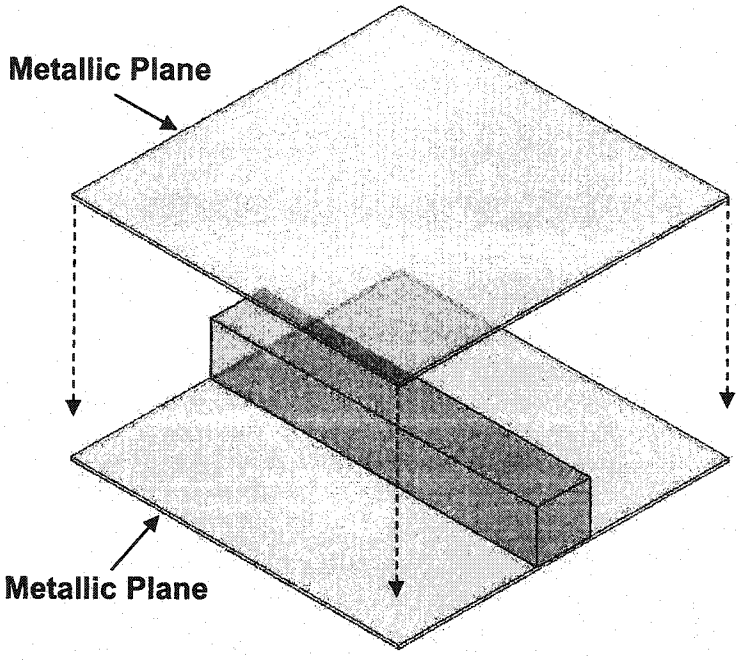

Fig. 2.1 Three-dimension (3D) geometrical view of a conventional NRD-guide

2.2 The proposed structures and numerical analysis

The surface mounted dielectric guides proposed in this research can be based on the concept of the conventional NRD-guides, with some modifications, new structures have been proposed for use as a class of integrated millimeter wave building blocks. Compared to the conventional NRD-guide, the proposed structures are suited to the design of a new class of line-to-line interconnects and hybrid integration design of planar circuit/NRD-guide. The new 3D integrated schemes will be detailed in the following sections.

2.2.1 Unbalanced NRD-guide and balanced NRD-guide

Figure 2.2 shows the three-dimension (3D) geometrical view of the proposed unbalanced NRD-guides, which consist of a core dielectric strip deposited on top of a relatively thin dielectric substrate layer. The whole structure is sandwiched between two parallel metallic plates as in the conventional NRD-guide.

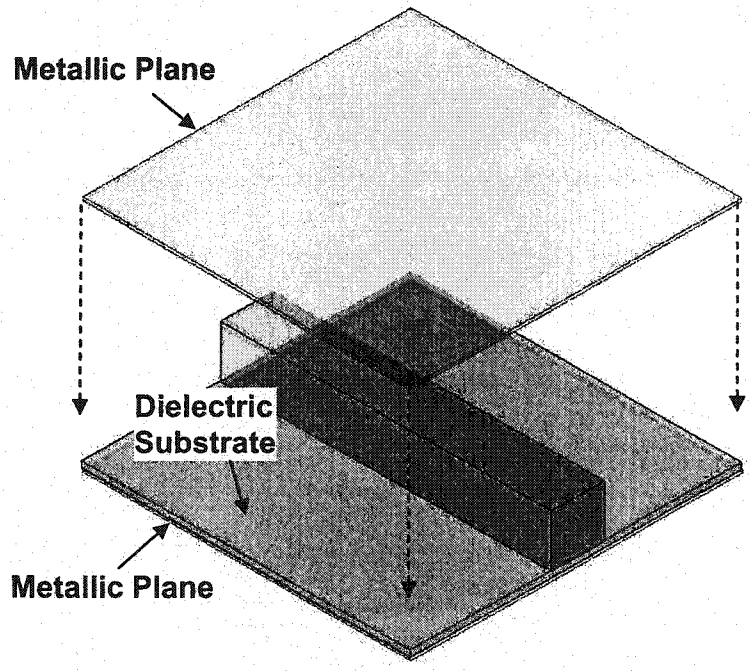

Fig. 2.2 Three-dimension (3D) geometrical transparent view of the proposed unbalanced NRD-guide

Figure 2.3 shows the three-dimension (3D) geometrical view of the balanced NRD-guide, which looks very similar to the previously proposed insulating NRD-guide [8]. Note that the insulating NRD-guide was originally proposed to accommodate a dielectric strip with a high dielectric constant. Our proposed balanced structure may incorporate two relatively thin dielectric substrates with different dielectric constant and/or thickness.

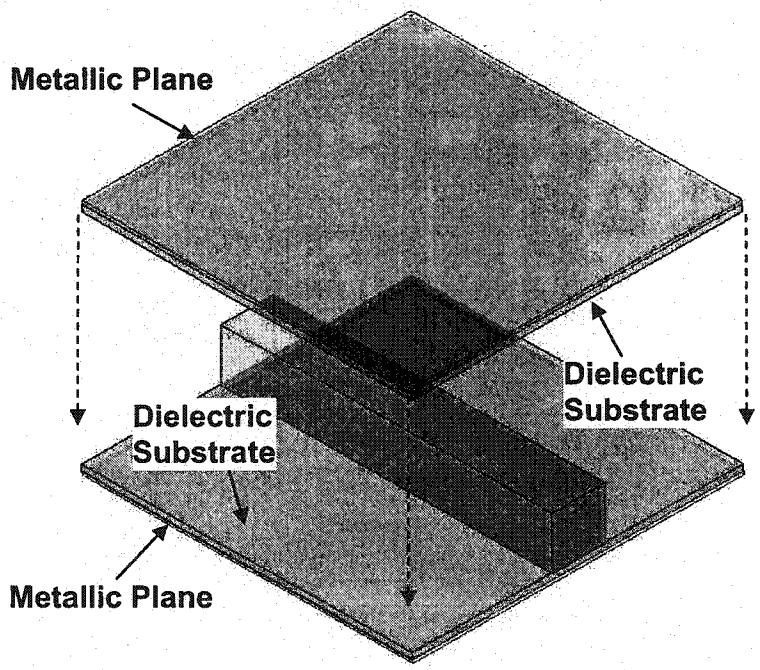

Fig. 2.3 Three-dimension (3D) geometrical transparent view of the proposed balanced NRD-guide

Possible leakage may be generated from these proposed structures if the vertical symmetry of the structures cannot be guaranteed. However, this unwanted scenario might be corrected with two possible remedies. First, some special geometrical asymmetry may not always generate a leakage within certain frequency ranges because of a cancellation of the LSM and LSE modes [13, 14]. Secondly, bilateral packaging/shielding structures may be used to eliminate the circuit-to-circuit coupling due to leakage even though there is an issue of effectiveness. In general, the leakage may be rather small or even negligible if adequate dimensions of the asymmetric structures are chosen, which require a careful modeling and design, detailed analysis will be presented in the following chapters. As a matter of fact, the proposed structures will become useful if their transmission losses are remarkably lower than planar transmission lines at millimeter-wave frequencies.

Regardless of the proposed balanced or unbalanced NRD-guide structures, a quasi-LSM_{01} fundamental mode should be considered along the new NRD-guides because of the introduction of the thin dielectric substrate(s). First of all, look at the unbalanced structure with a core dielectric strip placed on an electrically thin substrate layer. In this case, potential leakage due to the asymmetry of the structure is supposed to be negligible or relatively small at certain frequency range. The vertical height of the core dielectric block can thus be used to design an NRD-guide with a similar rule as used for the conventional NRD-guide but in the presence of the dielectric substrate. With the help of an numerical simulation package HFSS, Figure 2.4 plots the field profiles of an unbalanced NRD-guide made of 20 mil thick Duroid substrate (ε_r= 2.33) and

Polystyrene core dielectric strip (ε_r = 2.56) with a height of 138 mil at f = 30 GHz. Figure 2.4 (a) shows the E-field vectors (designated by arrows) on the cross-section in the y-z plane while Figure 2.4 (b) gives the E-field vectors in the longitudinal section cut through a half of the core dielectric strip block over the x-y plane.

Propagation characteristics of the two new structures are quite similar to the conventional NRD-guide since the thin dielectric layer(s) modifies little field profiles and guided-wave features as indicated in Figure 2.4. Therefore, the proposed structures may be able to preserve a great deal of the desired features of the conventional NRD-guide. This observation will be further verified numerically and experimentally in the following chapters.

2.2.2 Dielectric filled unbalanced NRD-guide, balanced NRD-guide and NRD-guide

If the air regions of the unbalanced NRD-guide are filled with lower dielectric constant material, this structure provides an option for different mass production technique. If the dimensions and the materials are chosen properly, similarly, this kind of structure may be able to preserve a great deal of the desired features of the standard NRD-guide. The geometrical view of the dielectric filled unbalanced NRD-guide is shown in Figure 2.5.

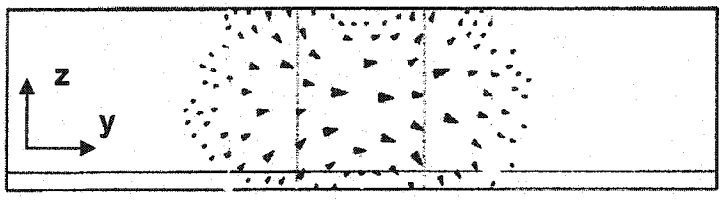

(a)

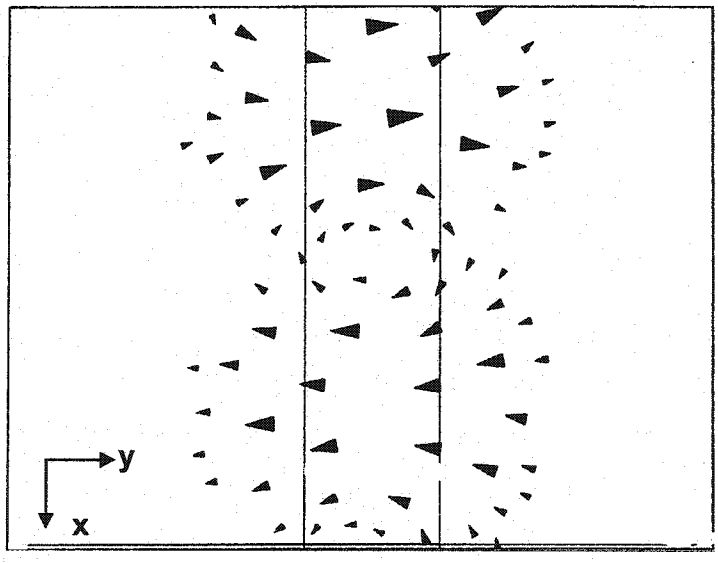

(b)

Fig. 2.4 Field distributions over the unbalanced NRD-guide for the quasi-LSM_{01} mode. (a) E-field vector plot (designated by arrows) over the transverse plane (parallel to the y-z plane); (b) E-field vector plot over the longitudinal plane parallel to the x-y plane cut through a half of the core dielectric strip

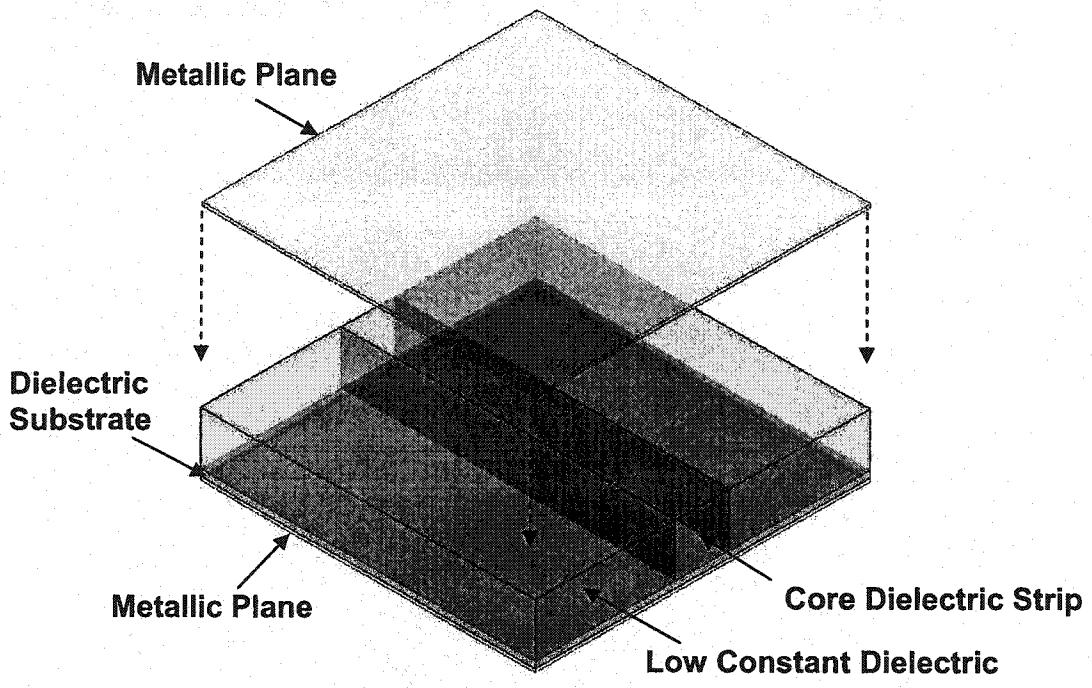

Fig. 2.5 Three-dimension (3D) geometrical transparent view of the proposed dielectric filled unbalanced NRD-guide

As an example, Figure 2.6 plots the field profiles of a dielectric filled unbalanced NRD-guide made of 20 mil Rogers TMM3 (ε_r=3.27) and Rogers TMM (ε_r=6) core dielectric strip with a height of 140 mil at f =20 GHz, the filled lower dielectric constant material is chosen to be polystyrene (ε_r=2.56). Figure 2.6 (a) shows the E-field vectors (designated by arrows) on the cross-section in the y-z plane while Figure 2.6 (b) shows the E-field contour lines over the same plane. No obvious field distribution difference can be observed between the proposed structure and the standard NRD-guide.

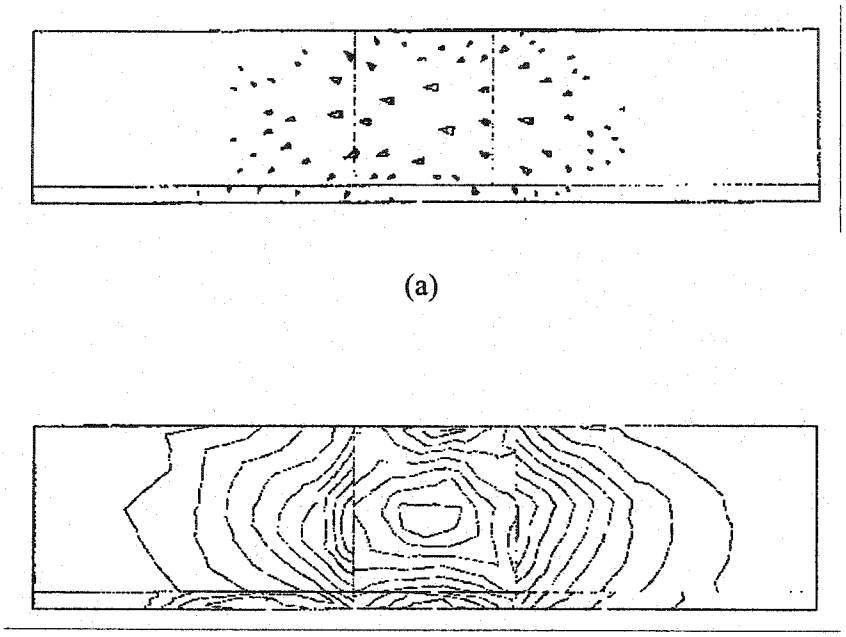

(a)

(b)

Fig. 2.6 Field distributions over the dielectric filled unbalanced NRD-guide for the quasi-LSM_{01} mode. (a) E-field vector plot (designated by arrows) over the transverse plane (parallel to the y-z plane); (b) E-field magnitude contour line plot over the same plane

Similarly, the air regions of balanced NRD-guide and the conventional NRD-guide may be filled with dielectric material, which has a relatively lower dielectric constant, compared to the core dielectric strip. By doing so, the modified structure could retain the advantageous characteristics of the original one.

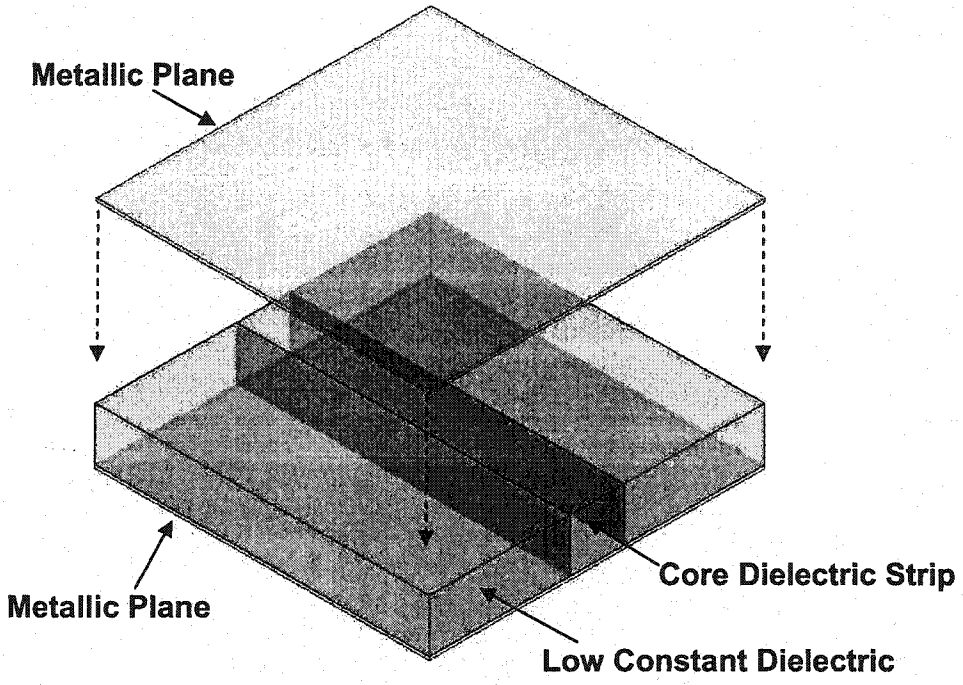

Fig. 2.7 Three-dimension (3D) geometrical view of the dielectric filled NRD-guide

The schematic picture of the dielectric filled NRD-guide is shown in Figure 2.7, the air regions of the conventional NRD-guide are now filled with a dielectric material, which has a relatively lower dielectric constant, compared to the core dielectric strip. As that in the conventional NRD-guide, LSM_{01} mode is considered as the operating mode in the dielectric filled NRD-guide. As our first example, the filled lower dielectric constant material and the core dielectric strip are chosen to be polystyrene (ε_r=2.56) and Rogers TMM (ε_r=6), respectively. As our second example, the core dielectric strip was chosen to be Rogers TMM (ε_r=9). In both cases, field profiles of the fundamental mode are

similar to that as shown in Figure 2.6 in each frequency band, except that the field is more concentrated in the core dielectric strip in the second case.

Surface mounted dielectric guides are very suited to the design of a new class of line-to-line interconnects and hybrid integration techniques of planar circuit/NRD-guide. These new 3D integrated schemes will be addressed in the following chapter.

2.3 Conclusions

In this chapter, a class of surface mounted dielectric guides has been presented for microwave and millimeter wave applications. The proof of concept has been provided with analysis results. The variety of the structures and the unique electrical/mechanical features of the proposed dielectric transmission line schemes should be able to help circuit designer to employ the optimum characteristics of each particular structure.

The proposed surface mounted dielectric guides, which could be realized with the available integration technique, promise to be instrumental in constructing a class of high performance 3-D integrated circuits.

CHAPTER III

THEORETICAL ANALYSIS AND EXPERIMENTAL VERIFICATION OF SUBSTRATE-MOUNTED NON-RADIATIVE DIELECTRIC (NRD)-GUIDE

3.1 Introduction

In chapter II, a new hybrid or composite structure that consists of a non-radiative dielectric (NRD) waveguide surface-mounted on the top of a relatively thin dielectric substrate has been presented. This structure allows for a direct hybrid integration of planar microstrip circuit with NRD-guide, thus providing an alternative design building block to a class of 3-D multi-layered millimeter-wave circuits. However, as mentioned in the previous chapter, the proposed structure is no longer a conventional NRD-guide because its asymmetry may potentially generate unwanted leakage loss. Our initial investigation indicated that one of the most interesting features is that it can still preserve a great deal of the desired properties of the conventional NRD-guide under certain circumstances. In this chapter, general expressions for hybrid-mode fields of the typical surface-mounted NRD-guides are derived and then the basic characteristics of the proposed structure are discussed based on theoretical analysis. Our observations are further verified by numerical and experimental results.

3.2 Mathematical formulations for fields expressions

The propagation characteristics of this new structure constitute a variety of phenomena, including the potential leakage of guided energy and leakage-related resonance effects under appropriate circumstances.

Figure 3.1 shows the cross section of the surface-mounted unbalanced NRD-guide, the region under consideration (right half of the cross section) is divided into two sub regions. The media are designated as: thin dielectric substrate ε_1 and core dielectric strip ε_2.

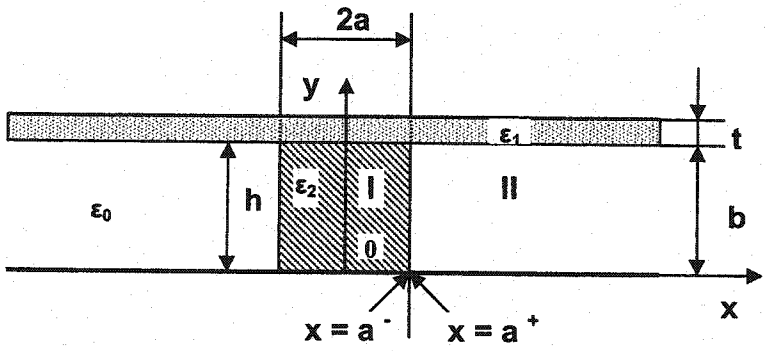

Fig. 3.1 Cross section of the surface-mounted unbalanced NRD-guide

The modes can be classified as TM or TE with respect to the y-direction [16]. One important phenomenon is the coupling produced between TE and TM waves at geometrical discontinuities. Similarly, rigorous mode-matching procedure [17] can also be used for the analysis of the leaky properties of the unbalanced NRD-guides. The following analysis is based on the expansion of the field in each subregion of the cross

section of the structure into a complete set of functions and the consequent matching at the boundaries.

Considering the symmetry of the structure with respect to the plane, symmetric (even) and antisymmetric (odd) modes can propagate in the structure. If E_y is even (or H_y is odd), we can insert a magnetic wall at x = 0 plane without affecting the field distribution. Similarly, if E_y is odd (or H_y is even), an electric wall can be introduced at x = 0 plane without affecting the field distribution. In both cases, we need to consider only half of the cross section of the structure. In the following investigation, our focus is the leakage properties of the quasi-LSM_{01} mode, which is the fundamental mode in the unbalanced NRD-guide. Therefore, only the antisymmetric case will be considered and studied.

The fields in each region will be expanded in terms of its eigenfunctions. The fields at the interface x = a (the width of the core dielectric strip is w = 2a) are then matched and solved for the leakage constant.

3.2.1 Modes in the structure

The fields can be expressed in terms of the scalar potential functions $f^e(x,y)$ and $f^h(x,y)$ as follows:

1) Field Expressions for TM Modes:

$$E_{xm} = \frac{1}{\varepsilon(y)} \frac{\partial^2 f_m^e(x,y)}{\partial x \partial y}$$

$$E_{ym} = \frac{1}{\varepsilon(y)} (k_z^2 - \frac{\partial^2}{\partial x^2}) f_m^e(x,y)$$

$$E_{zm} = \frac{-jk_z}{\varepsilon(y)} \frac{\partial f_m^e(x,y)}{\partial y}$$

$$H_{xm} = -\omega k_z \varepsilon_0 f_m^e(x,y)$$

$$H_{ym} = 0$$

$$H_{zm} = j\omega\varepsilon_0 \frac{\partial f_m^e(x,y)}{\partial x} \tag{3.1}$$

The potential of the *mth* TM mode is separable and can be written as

$$f_m^e(x,y) = \phi_m^e(y) \sin(k_{xm} x) \tag{3.2}$$

and

$$\phi_m^e(y) = \begin{cases} \cos(k_{y2m} y) \\ a_m^e \cos\left[k_{y1m}(y-b-t)\right] \end{cases} \tag{3.3}$$

in which

$$\alpha_m^e = \frac{\cos(k_{y2m} b)}{\cos(k_{y1m} t)}$$

$$k_{y1m} = (\varepsilon_1 k_0^2 - k_{xm}^2 - k_z^2)^{1/2}$$

$$k_{y2m} = (\varepsilon_2 k_0^2 - k_{xm}^2 - k_z^2)^{1/2}$$

$$k_0^2 = \omega^2 \mu_0 \varepsilon_0$$

In region I, $\varepsilon_1, \varepsilon_2$ are relative dielectric constants of the thin dielectric substrate, core guiding dielectric strip, respectively. The eigenvalue equation for $k_x^2 + k_z^2$ is

$$(k_{y1m}/\varepsilon_1)\tan(k_{y1m} t) + (k_{y2m}/\varepsilon_2)\tan(k_{y2m} b) = 0 \tag{3.4}$$

2) Field expressions for TE Modes:

$$E_{xmi} = \omega k_z \mu_0 f_m^h(x, y)$$

$$E_{ym} = 0$$

$$E_{zm} = -j\omega\mu_0 \frac{\partial f_m^h(x,y)}{\partial x}$$

$$H_{xm} = \frac{\partial^2 f_m^h(x,y)}{\partial x \partial y}$$

$$H_{ym} = (k_z^2 - \frac{\partial^2}{\partial x^2}) f_m^h(x,y)$$

$$H_{zm} = -jk_z \frac{\partial f_m^h(x,y)}{\partial y} \tag{3.5}$$

The potential function of *mth* TE mode, $f_m^h(x,y)$, is also separable and can be written as

$$f_m^h(x,y) = \phi_m^e(y)\cos(k_{xm}' x) \tag{3.6}$$

and

$$\phi_m^h(y) = \begin{cases} \sin(k_{y2m}' y) \\ \alpha_m^h \sin\left[k_{y1m}'(y-b-t)\right] \end{cases} \tag{3.7}$$

in which

$$\alpha_m^h = -\frac{\sin(k'_{y2m}b)}{\sin(k'_{y1m}t)}$$

$$k'_{y1m} = (\varepsilon_1 k_0^2 - k'^2_{xm} - k_z^2)^{1/2}$$

$$k'_{y2m} = (\varepsilon_2 k_0^2 - k'^2_{xm} - k_z^2)^{1/2}$$

The eigenvalue equation for $k'^2_x + k'^2_z$ is

$$\tan(k'_{y1m}t)/k'_{y1m} + (\tan(k'_{y2m}b)/k'_{y2m}) = 0 \qquad (3.8)$$

Similarly, setting $\varepsilon_2 = 1$, and assuming leaky mode boundary conditions, the modes in Region II can be obtained.

The modes listed above have five field components instead of three normally possessed by TE and TM modes. These modes are no longer TE or TM, but they are characterized by the absence of an electric or a magnetic field component in the y direction. Such modes are known as LSE or LSM modes [18], or a H-type and E-type modes with respect to the y direction [19], if $E_y = 0$ or $H_y = 0$, respectively.

3.2.2 Fields expansion and matching

The fields in each of the two regions I and II are first expanded in the terms of the TE- and TM-Mode functions. The expansion coefficients and the propagation constant k_z are then obtained by matching the tangential components of the fields at the interface plane $x = a$.

Fields expansion in the region I:

$$E_y = \sum_{m=1}^{M} (k_{xm}^2 + k_z^2) \frac{\sin(k_{xm} x)}{\sin(k_{xm} a)} \frac{\phi_m^e(y)}{\varepsilon(y)} A_m$$

$$H_y = \sum_{m=1}^{M'} (k_{xm}^{'2} + k_z^2) \frac{\cos(k_{xm}^{'} x)}{\cos(k_{xm}^{'} a)} \phi_m^h(y) B_m$$

$$E_z = \sum_{m=1}^{M} (-jk_z) \frac{\sin(k_{xm} x)}{\sin(k_{xm} a)} \frac{1}{\varepsilon(y)} \frac{\partial \phi_m^e(y)}{\partial y} A_m + \sum_{m=1}^{M'} (j\omega\mu_0 k_{xm}^{'}) \frac{\sin(k_{xm}^{'} x)}{\cos(k_{xm}^{'} a)} \phi_m^h(y) B_m$$

$$H_z = \sum_{m=1}^{M} (j\omega\varepsilon_0 k_{xm}) \frac{\cos(k_{xm} x)}{\sin(k_{xm} a)} \phi_m^e(y) A_m + \sum_{m=1}^{M'} (-jk_z) \frac{\cos(k_{xm}^{'} x)}{\cos(k_{xm}^{'} a)} \frac{\partial \phi_m^h(y)}{\partial y} B_m \tag{3.9}$$

where A_m's, B_m's and complex number k_z are constants to be determined.

Fields expansion in the region II:

$$E_y = \sum_{m=1}^{N} (\bar{k}_{xm}^2 + k_z^2) \exp\left[-j\bar{k}_{xm}(x-a)\right] \frac{\bar{\phi}_m^e(y)}{\bar{\varepsilon}(y)} C_m$$

$$H_y = \sum_{m=1}^{N'} (\bar{k}_{xm}'^2 + k_z^2) \exp\left[-j\bar{k}_{xm}'(x-a)\right] \bar{\phi}_m^h(y) D_m$$

$$E_z = \sum_{m=1}^{N} (-jk_z) \exp\left[-j\bar{k}_{xm}(x-a)\right] \frac{1}{\bar{\varepsilon}(y)} \frac{\partial \bar{\phi}_m^e(y)}{\partial y} C_m$$
$$+ \sum_{m=1}^{N'} (-\omega\mu_0 k_{xm}') \exp\left[-j\bar{k}_{xm}'(x-a)\right] \bar{\phi}_m^h(y) D_m$$

$$H_z = \sum_{m=1}^{N} (\omega\varepsilon_0 k_{xm}) \exp\left[-j\bar{k}_{xm}(x-a)\right] \bar{\phi}_m^e(y) C_m$$
$$+ \sum_{m=1}^{N'} (-jk_z) \exp\left[-j\bar{k}_{xm}'(x-a)\right] \frac{\partial \bar{\phi}_m^h(y)}{\partial y} D_m \qquad (3.10)$$

Where the barred characters are used to distinguish the values in region II from those in region I, and C_m's, D_m's are constant to be determined.

3.2.3 Matching of tangential field components at x = a

Required continuity of the field components E_y, H_y, E_z and H_z, as given in the above equations across x = a leads to

$$\sum_{m=1}^{M} (k_{xm}^2 + k_z^2) \frac{\phi_m^e(y)}{\varepsilon(y)} A_m - \sum_{m=1}^{M'} (\bar{k}_{xm}^2 + k_z^2) \frac{\bar{\phi}_m^e(y)}{\bar{\varepsilon}(y)} C_m = 0$$

$$\sum_{m=1}^{N}(k_{xm}^{'2}+k_z^2)\phi_m^h(y)B_m-\sum_{m=1}^{N'}(\bar{k}_{xm}^{'2}+k_z^2)\bar{\phi}_m^h(y)D_m=0$$

$$\sum_{m=1}^{M}\frac{1}{\varepsilon(y)}\frac{\partial\phi_m^e(y)}{\partial y}A_m+\sum_{m=1}^{M'}\frac{(-\omega\mu_0 k_{xm}^{'})}{k_z}\tan(k_{xm}^{'}a)\phi_m^h(y)B_m$$

$$-\sum_{m=1}^{N}\frac{1}{\bar{\varepsilon}(y)}\frac{\partial\bar{\phi}_m^e(y)}{\partial y}C_m-\sum_{m=1}^{N'}\frac{(-j\omega\mu_0\bar{k}_{xm}^{'})}{k_z}\bar{\phi}_m^h(y)D_m=0$$

$$\sum_{m=1}^{M}\frac{(-\omega\varepsilon_0 k_{xm})}{k_z}\cot(k_{xm}a)\phi_m^e(y)A_m+\sum_{m=1}^{M'}\frac{\partial\phi_m^h(y)}{\partial y}B_m \qquad (3.11)$$

$$-\sum_{m=1}^{N}\frac{(j\omega\varepsilon_0\bar{k}_{xm})}{k_z}\bar{\phi}_m^e(y)C_m-\sum_{m=1}^{N'}\frac{\partial\bar{\phi}_m^h(y)}{\partial y}D_m=0$$

Equations yield an exact solution for the fields and propagation constants if M, N, M′ and N′ are infinite. However, in practice, we have to limit these to finite numbers. As a consequence of this approximation, the fields matching at the interface is not perfect and there is a residual discontinuity of the tangential fields as one traverses the interface.

The following orthogonal relations hold and are utilized in solving the above equations,

$$\int_0^{b+t}\frac{1}{\varepsilon(y)}\phi_m^e(y)\phi_n^e(y)dy=0$$

$$\int_0^{b+t} \phi_m^h(y)\phi_n^h(y)dy = 0$$

$$\int_0^{b+t} \frac{1}{\bar{\varepsilon}(y)}\bar{\phi}_m^e(y)\bar{\phi}_n^e(y)dy = 0$$

$$\int_0^{b+t} \bar{\phi}_m^h(y)\bar{\phi}_n^h(y)dy = 0 \qquad \text{For } m \neq n \tag{3.12}$$

Please note that no cross-orthogonal relations exist between the different potential functions. All above four of the orthogonal relations can be used in setting up a system of homogeneous equations. Then, we can choose an equal number of TM modes in the two regions and also equal number of TE modes. The zeros of the determined of this system of equations can calculate an accurate leakage constant of the quasi-LSM_{01} mode in the unbalanced NRD-guide.

3.3 Leakage suppression features of the proposed structure

In the presence of a thin planar dielectric substrate, a leakage wave may be generated from the proposed structure, and such a potential leakage makes the propagation constant κ_z complex. Our emphasis is on its potential leakage. With attenuation constant α being used for measure of the leakage, influences of different parameters on the leakage characteristics of the structure are described in Figures 3.2–3.4, and the dielectric constant of the thin dielectric substrate is 2.33.

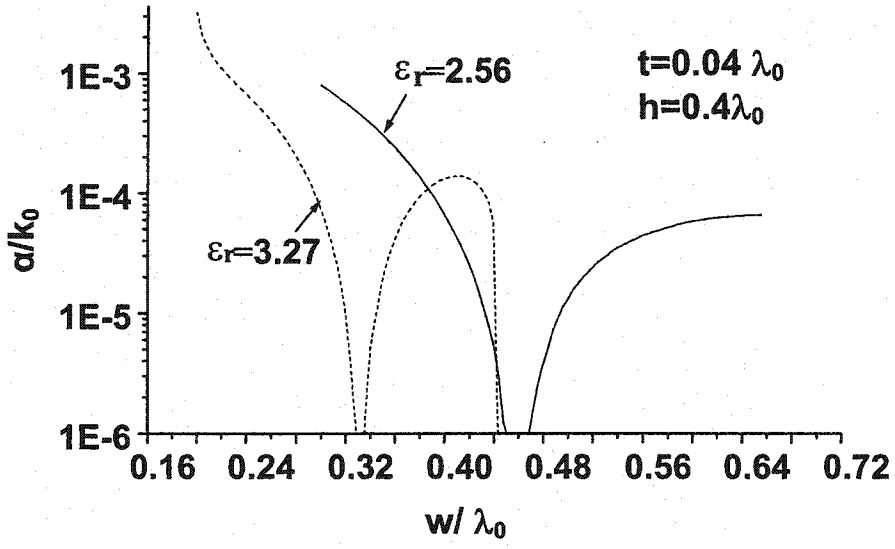

Fig. 3.2 Parametric influence of w/λ_0 on leakage properties with $w = 0.04\lambda_0$, $h = 0.4\lambda_0$. The geometrical parameters are defined in Figure 3.1; in which t refers to the substrate thickness; w and h are the width and height of the core NRD strip, respectively

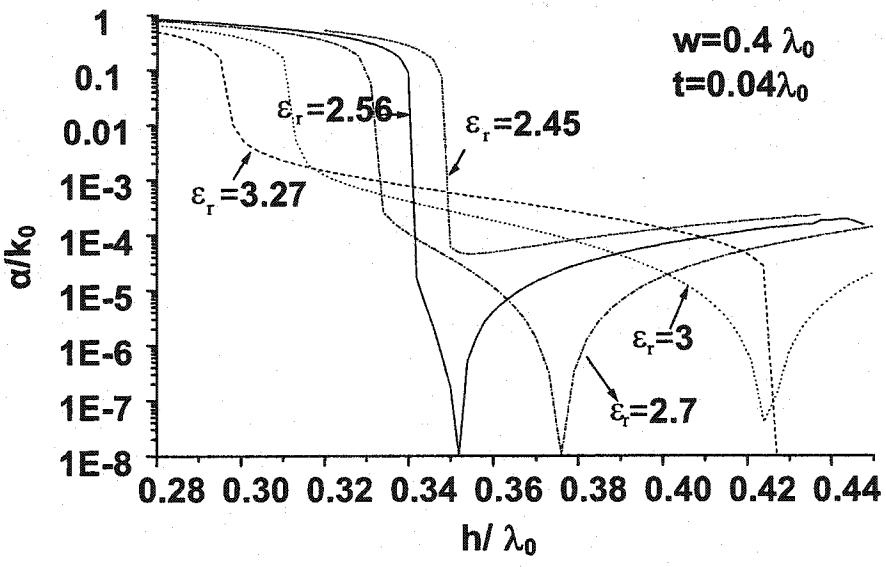

Fig. 3.3 Parametric influence of h/λ_0 on leakage properties with $w = 0.4\lambda_0$, $t = 0.04\lambda_0$. Parameters of structure are defined in the same way as in Figure 3.1 and Figure 3.2

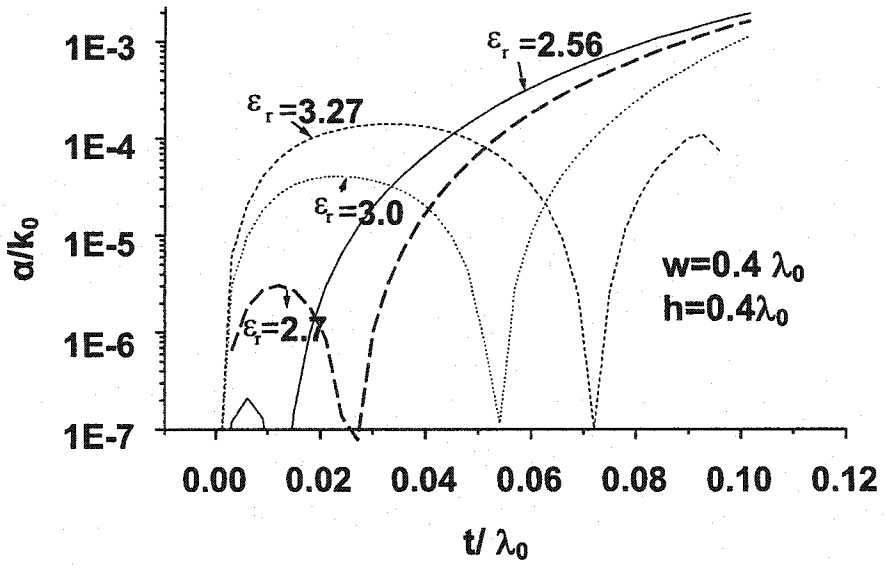

Fig. 3.4 Leakage characteristics as a function of t/λ_0 with $w = 0.4\lambda_0$, $h = 0.4\lambda_0$. Parameters of structure are defined in the same way as in Figure 3.1 and Figure 3.2

We can observe that there are some dips along the curves, where α drops sharply. Qualitatively speaking, the leakage loss may even disappear completely in these cases. This suggests that such an asymmetrical structure be able to uphold the guided signal within its dielectric strip bounds. In fact, it is due to the well-documented cancellation effect coming from the interaction between the two-step discontinuities in the transverse cross section through the coupling of the LSM and LSE modes in the guide.

From a simple calculation, such a cancellation condition may approximately be stated as follows [14, 20, 21]:

$$\kappa_x w = 2\pi \tag{3.13}$$

$$\kappa_0^2 \varepsilon_r = \beta^2 + \kappa_x^2 + \kappa_y^2 \tag{3.14}$$

in which ε_r is the dielectric constant of the core NRD strip. The cancellation effect is actually not only due to the coupling of the fundamental LSM and LSE modes, but also of a number of hybrid modes excited by the step discontinuities, even though the fundamental modes are dominant. Therefore we can only say equation (3.13) is approximately correct.

Figure 3.2 plots two curves of α as functions of width w, as well as the dielectric constant ε_r of the core dielectric strip. In this example, $h = 0.4\lambda_0$, $t = 0.04\lambda_0$ that stand for the height of the core dielectric strip and the thickness of the thin dielectric substrate,

respectively. It is seen that the larger the dielectric constant becomes, the smaller the width w where dip appears. This is because the increase of ε_r leads to the increase of κ_x. In order to meet the requirement of equation (3.13), w must be decreased. Besides, the leakage suddenly decreases to zero around 0.45, and the reason for this phenomenon is that the guided wave becomes a bounded wave but the structure is not a fast-wave guiding structure ($\beta/\kappa_0 > 1.0$), therefore, the leakage disappears.

Figure 3.3 shows the effect of h related to the core dielectric strip on the leaky characteristics. In this example, $w = 0.4\lambda_0$, $t = 0.04\lambda_0$ that represent the width of the core dielectric strip and the thickness of the thin dielectric substrate, respectively. It is seen that the larger the dielectric constant ε_r becomes, the larger h for which dip appears. This can be explained by the fact that increasing h will lead to the increase of β and decreasing κ_y slightly. In order to keep κ_x unchanged such that the cancellation condition (3.13) can approximately be satisfied, ε_r must be increased judging from equation (3.14).

Figure 3.4 plots a number of curves of α/κ_0 as a function of thickness t/λ_0 of the dielectric substrate versus dielectric constant ε_r of the core dielectric strip. In this example, $w = 0.4\lambda_0$ and $h = 0.4\lambda_0$ that represent the width and the height of the core dielectric strip, respectively. We can also find out from them that the larger the dielectric constant ε_r is, the larger the parameter t becomes for which the dip appears. This is due to the fact that increasing t will lead to the increasing of β and a slight decreasing of κ_y. In order to keep

κ_x unchanged (in the present case where w is fixed), ε_r must be increased such that the cancellation condition (3.14) can be maintained.

The interesting observation made in the above discussion of results is that, if the dimensions of structure and the value of dielectric constant are adequately selected, the leakage can be maintained at a very low level (usually a negligible level) or even can disappear in certain circumstances. In all the above figures, the leakage constant great than 10^{-4} or 10^{-3} takes place over below-cutoff regions where the attenuation is caused by evanescent effect instead of the leakage loss.

3.4 Single mode conditions

Due to the existence of the thin dielectric substrate, the radiation suppression condition of the unbalance NRD-guide is different from that for the standard NRD-guide. By imposing the cutoff condition for TE and TM waves between two conducting plates, the condition for the suppression is given by

$$\tan(k_0 h) + \frac{\tan(\sqrt{\varepsilon_1} k_0 t)}{\sqrt{\varepsilon_1}} = 0 \tag{3.15}$$

In which, h is the height of the core dielectric strip and t is the thickness of the thin dielectric substrate respectively. While ε_1 is the dielectric constant of the substrate, k_0 is

the free space wave number. If t is very small $(\sqrt{\varepsilon_1}k_0 t << 1)$, the radiation suppression condition of the unbalanced NRD-guide is approximately the same as that of the standard NRD-guide.

Figure 3.5 shows the numerical results of suppression condition of unbalanced NRD-guide as a function of t/λ_0. It indicates that the distance of the two separate metal plates with respect to the free space wavelength $(h + t)/ \lambda_0$ for the radiation suppression condition of the unbalanced NRD-guide decreases as the t/ λ_0 increases.

In addition to being non-radiative

$$h + t < \lambda_0 / 2$$

The requirement that the unbalanced NRD-guide operates in the dominant quasi-LSM_{11} mode is met by the condition

$$\lambda_{g01}/2 < h + t < (\lambda_{g01}, \lambda_{g11}/2) \qquad (\lambda_{g02}/2 = \lambda_{g01})$$

In which λ_{g01}, λ_{g11}, λ_{g02} are the guided wavelengths of the quasi-LSM_{01}, quasi-LSM_{11} and LSM_{02} modes, respectively. λ_0 is the free space wavelength.

The figure 3.6 shows the single-mode operation conditions for the unbalanced NRD-guide. The results are approximately the same as that of the standard NRD-guide. This is

because the quasi-LSM_{01} and quasi-LSM_{11} slab modes are hardly affected by the presence of the substrate, because the field of each mode is mainly concentrated within the core dielectric strip.

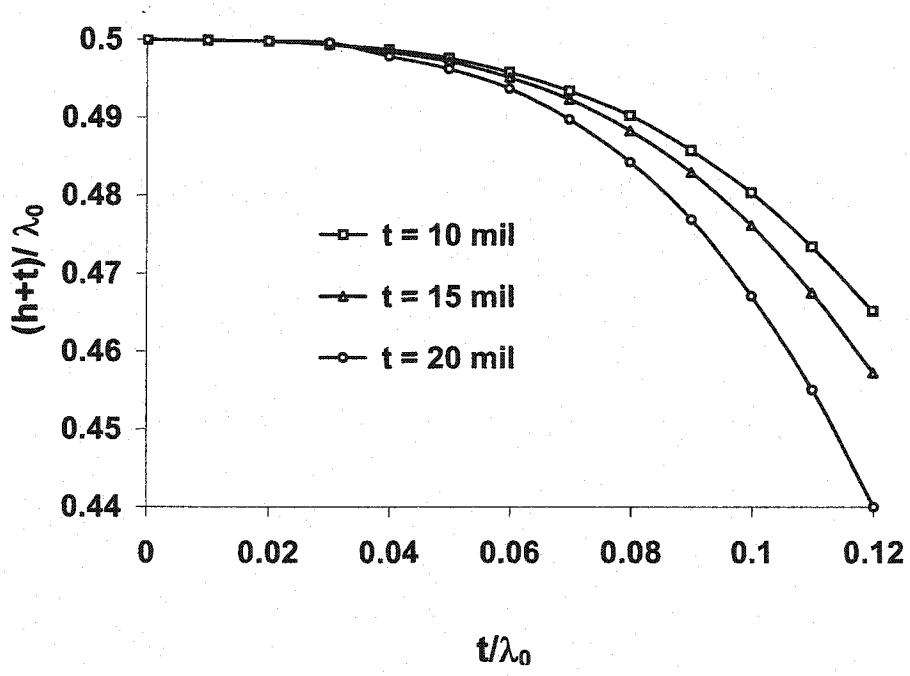

Fig. 3.5 Numerical results of suppression condition of unbalanced NRD-guide as a function of t/λ_0

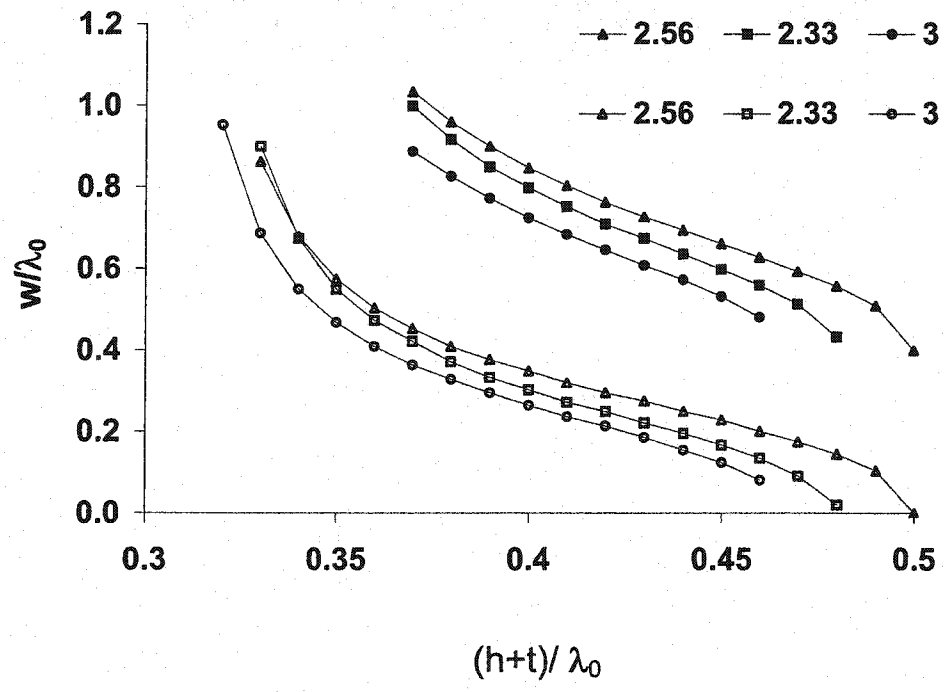

Fig. 3.6 Single-mode operation conditions for the unbalanced NRD-guide for different dielectric core strip

3.5 Low-loss propagation properties

In Figure 3.7, a thin substrate is chosen with $\varepsilon_r = 2.33$, t = 10 mil, and the height h of the core NRD strip is fixed, while the width of the ground plane is 1250 mil. The leakage constant α/κ_0 is below 2×10^{-5} when the width is between 160 and 195 mil over the frequency range of interest. In Figure 3.8, a slightly thicker substrate is used with ε_r = 2.33, t = 20 mil, the height h of the core NRD-guide strip is also fixed in this case. The leakage constant α/κ_0 is found to be also below 2×10^{-5} when the width is designed between 180 and 195 mil over the frequency range of interest. Such leakage loss levels are in fact much lower than the loss caused by the metallic conductor and dielectric. To be specific, Figure 3.9 gives the attenuation constant caused by dielectric losses compared with that due to the leakage effect, in which the core strip w = 210, h = 157.5, (unit = mil), ε_r = 2.56, and loss tangent = 0.0005. In this case, the thin dielectric substrate t = 20 mil, ε_r = 2.33 and loss tangent = 0.0012. We find that the dielectric loss constant α/κ_0 stays around 10^{-3}, which is much higher than the leakage constant. Therefore, the proposed composite structure should be very useful for low-loss hybrid integration of planar circuit and NRD-guide at millimeter-wave frequencies.

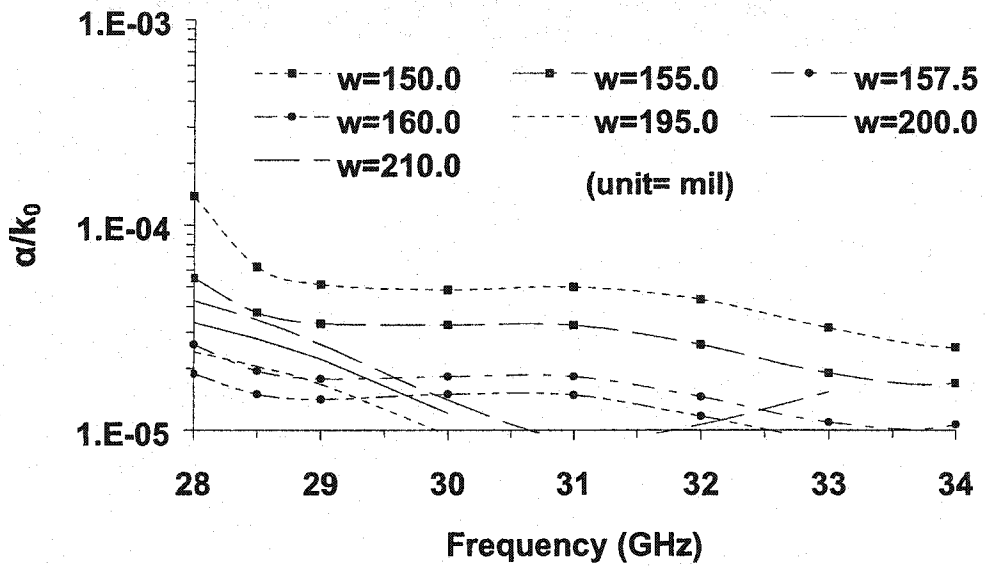

Fig. 3.7 Leakage characteristics as a function of w with h = 157.5 mil, t = 10 mil, ε_r = 2.33, and the dielectric constant of the core NRD strip is 2.56

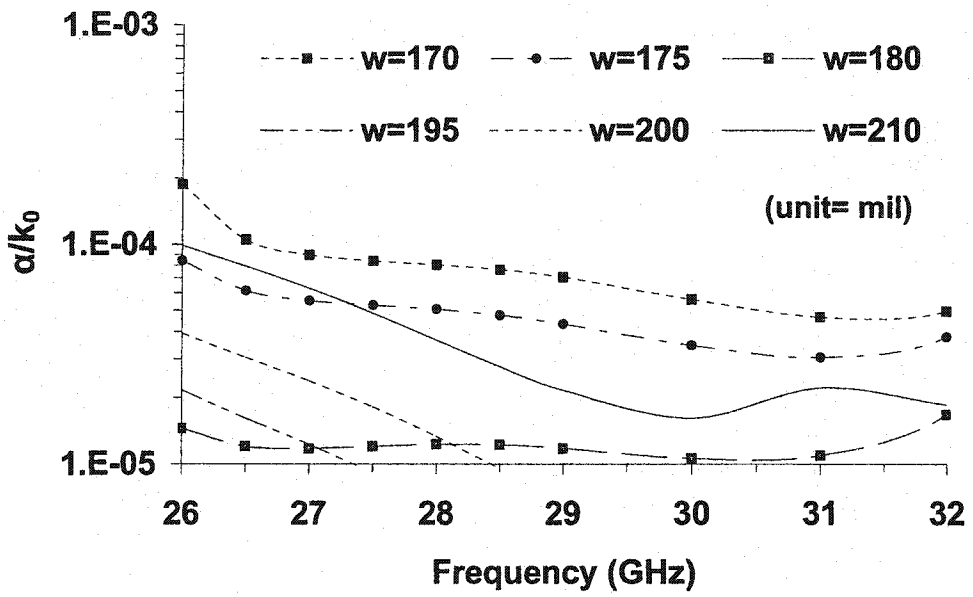

Fig. 3.8 Parametric effect of w on leakage properties with h = 157.5 mil, t = 20 mil and ε_r = 2.33, and the dielectric constant of the core NRD strip is 2.56

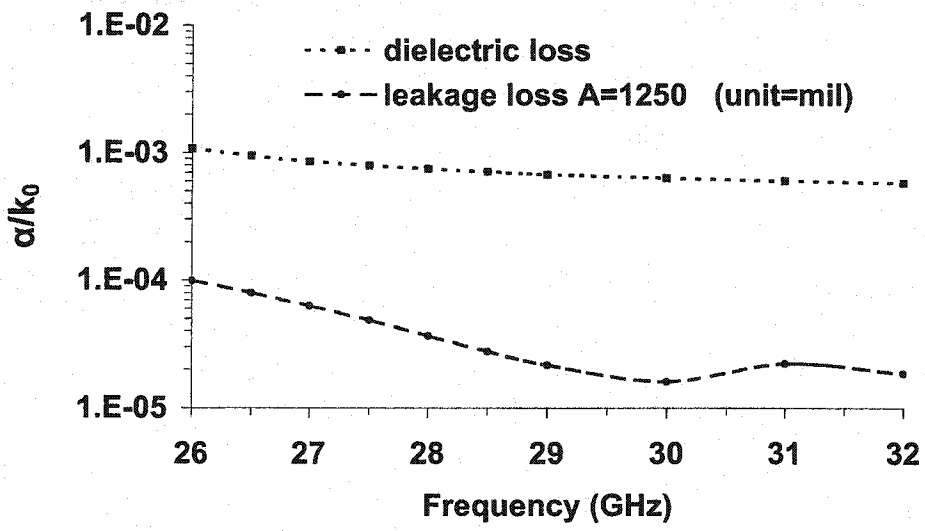

Fig. 3.9 Quantitative comparison of propagation attenuation due to dielectric and leakage losses

3.6 Effect of finite width of the ground plane

In practice, the structure is always truncated that results in a finite-width ground plane. It is expected that such a truncation should yield a negligible impact on the guided-wave characteristics because of the negligible leakage effects. To verify such a statement, Figure 3.12 shows α as a function of finite ground width A as described in Figure 3.1. In the calculations, the width w and height h of the core NRD strip is fixed at 210 and 157.5 mil, respectively. The dielectric constant ε_r of the core NRD strip is 2.56. A thin substrate is considered with ε_r = 2.33, t = 20 mil. To make more visible the influence of the finite width on guided-wave characteristics, we intentionally avoid the choice of the optimized dimension of structure that yields the lowest leakage loss. We find from the plotted curves of the leakage constant have small ripples because of a multiple reflection caused by the finite ground width (assuming radiation boundary condition at the open surface in the analysis). Nevertheless, the magnitude is rather small because of the weak leakage, and the difference of the curves has no much significant meaning, as α is much lower than the phase constant, at least in the order of 3. On the other hand, the loss due to imperfect conductors and dielectrics should prevail in the attenuation of guided waves.

3.7 Experimental verification

To verify our above discussions on the basis of theoretical results, two simple qualitative experiments were made to evaluate its low- or non-radiating features of the proposed structure. The test arrangement is illustrated in Figure 3.11. The thin planar substrate is

selected with ε_r = 2.22, t = 10 mil. The width w and the height h of the core NRD strip are fixed at 180 and 168 mil respectively. In addition, the finite ground width A is 950 mil, and the dielectric constant of the NRD strip is 2.56. Transmission and return loss of a straight surface-mounted NRD-guide were measured for both the open and shielded scenarios (two cross-sectional sides are open and closed, respectively). Two conventional aperture-coupled microstrip-to-surface-mounted NRD-guide transitions were used as shown in Figure 3.11. Thus, the leakage influence of structure may easily be assessed without using the direct microstrip-NRD contact scheme.

The shielding metallic plate in the two transition sections is used to reduce spurious modes, which may be generated in the surface-mounted NRD-guide [8]. In this way, the input and output remain in the form of microstrip lines that can easily be used in connection with our HP8510C vector network analyzer (VNA) for measurements. The thru-reflect-line (TRL) calibration technique is applied in the measurements. The standards are fabricated with the same substrate used for the input/output microstrip substrate with ε_r = 10.2, t=10 mil. The reference planes for the measurements are selected at A as shown in Figure 11, at the edge of coupling slot.

In the first experiment, the length L of the surface-mounted NRD-guide is 500 mil. Both bilaterally open and shielded structures are measured to evaluate the potential leakage effects. The results are presented in Figure 3.12. We find that no significant leakage effect can be observed over 26-29 GHz. There is a minor difference of S-parameters

between the two cases around 26.9 GHz that may be caused by some spurious boxing effects. Three points should be observed. First, the transitions have a limited operating bandwidth that allows us to evaluate a portion of the whole operating frequency bandwidth of the substrate-mounted NRD-guide. Secondly, some of the spurious modes may become leaky since they appear out of the transition-operating band. At higher frequencies, the non-radiating condition of the core dielectric strip is no longer satisfied, and leakage effects are observed in this frequency range. This may be well pronounced by the fact that the transition discontinuities are directly responsible for the mode conversion from the microstrip quasi-TEM mode to the leaky modes of structure. This can also be evidenced by the difference of the open and shielded cases over the higher frequency range. Third, the best insertion loss of structure is roughly 1.4 dB that consists of those contributed by two back-to-back microstrip-to-substrate-mounted NRD-guide transitions (including a length of 2500 mil NRD-guide). It indicates that the metallic and dielectric losses become dominant over the operating non-radiating band designed over 25.5-28.5 GHz. In other words, no obvious leakage effect can be observed. In the second experiment, the length of the substrate-mounted NRD-guide L is 700 mil, and also different transitions were used while the other conditions remain the same. Measured results are given in Figure 3.13 that suggests the same arguments.

3.8 Conclusion

Low-loss propagation characteristics of NRD-guide, which is surface-mounted on a relatively thin dielectric substrate, are studied analytically and experimentally. Detailed

results provide us a basic guideline for the design of low-loss hybrid planar/NRD-guide millimeter-wave circuits using such a composite building block. It is demonstrated that this type of transmission line can preserve low-loss and almost non-radiating advantages of the conventional NRD-guide. This new structure may give designer a much-needed freedom for integration and interconnects between planar circuits and NRD-guide.

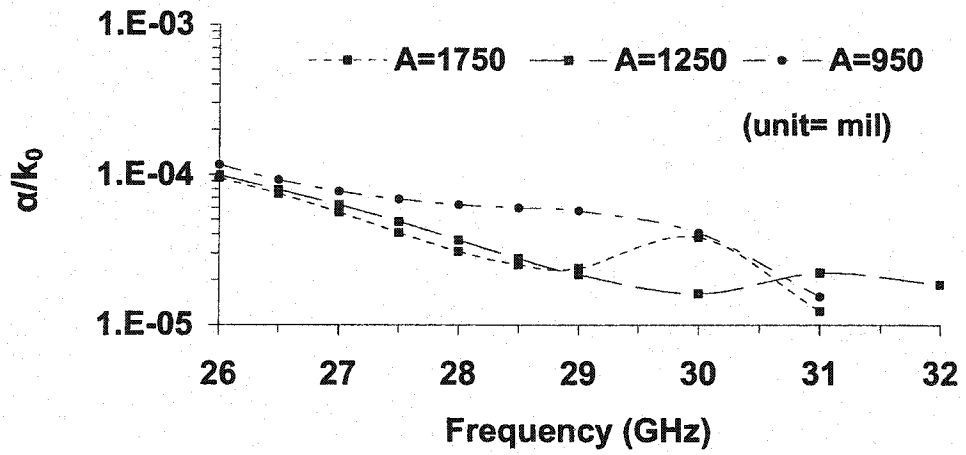

Fig. 3.10 Effects of truncated finite ground width A on leakage properties with w = 210 mil, h = 157.5 mil and the dielectric constant of NRD strip = 2.56, t = 20 mil and ε_r = 2.33 for the substrate

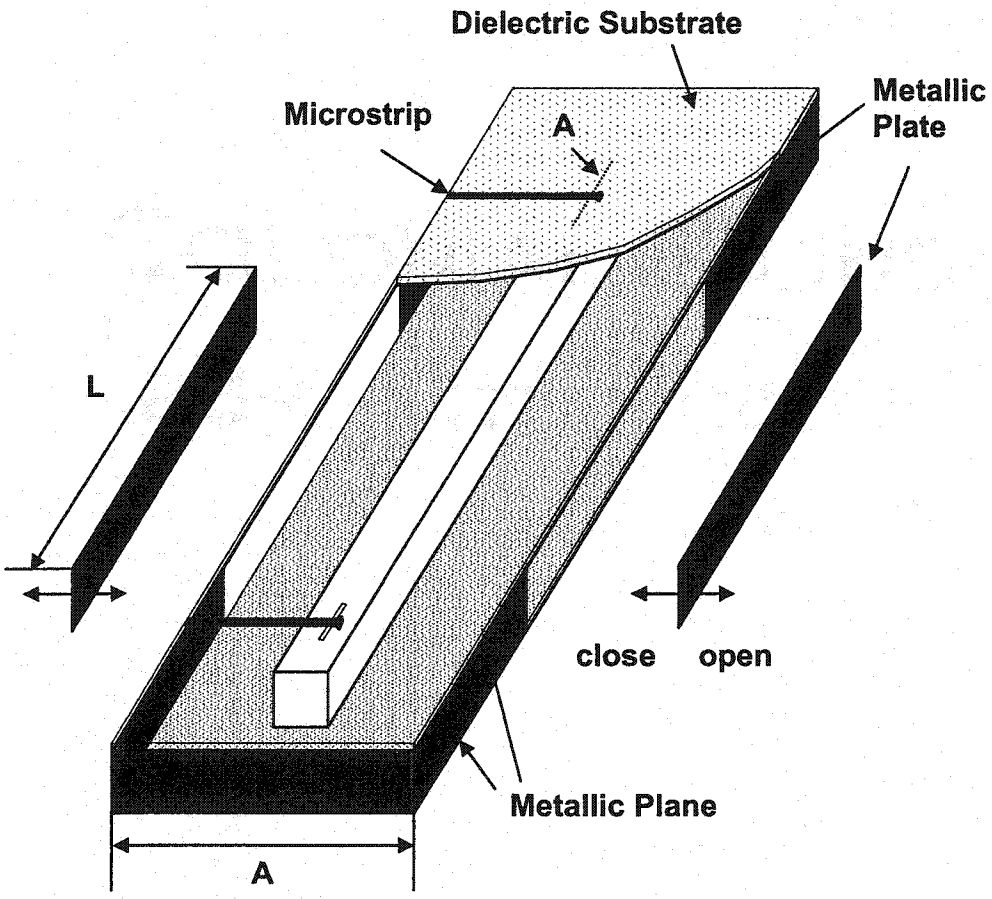

Fig. 3.11 Test arrangement for assessing potential leakage effects on low-loss substrate-mounted NRD-guide propagation characteristics

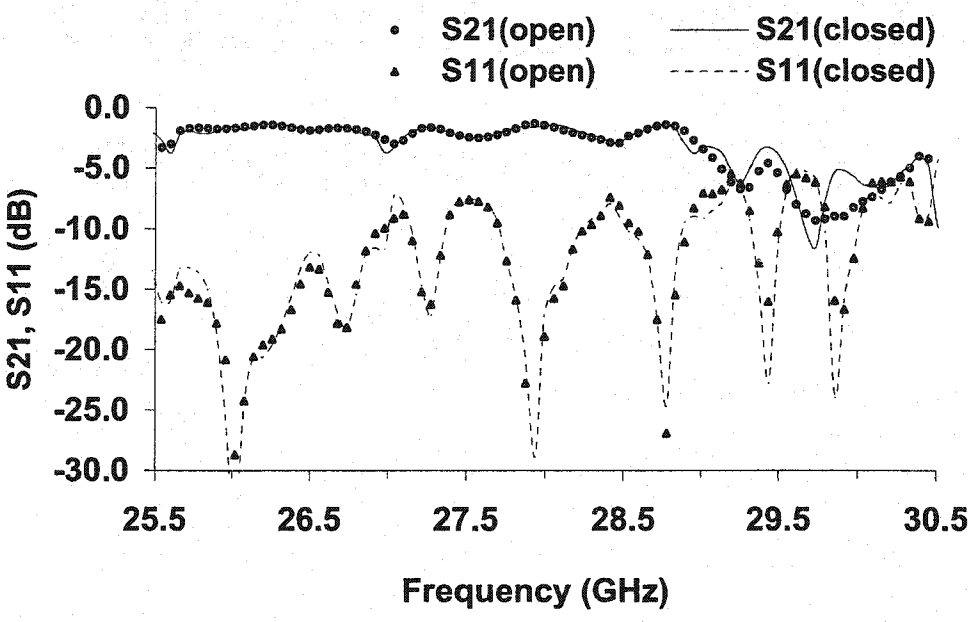

Fig. 3.12 Measured results of potential leakage effects on the propagation characteristics. Length of the substrate-mounted NRD-guide L is 500 mils

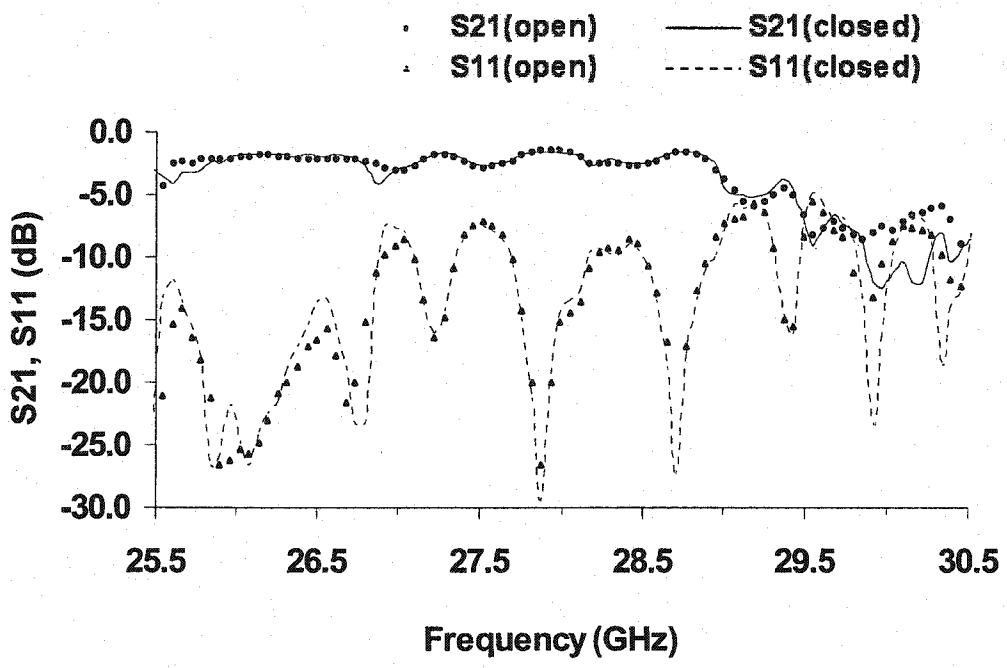

Fig. 3.13 Measured results of potential leakage effects on the propagation characteristics. Length of the substrate-mounted NRD-guide L is 750 mils

CHAPTER IV

CO-LAYERED INTEGRATION AND INTERCONNECT TECHNIQUES

4.1 Introduction

As discussed in the previous chapter, the proposed surface-mounted NRD-guide should be able to help circuit designer to employ the optimum characteristics of each particular structure.

The question remains how to achieve the expected advantages. One of the key issues related to the millimetre wave integrated circuit building block is the integration and interconnects technique. In this chapter, based on the introduction of the surface-mounted NRD/planar structures, a concept is presented for the circuit design of the proposed structures, which features co-layered hybrid integration of the two dissimilar structures without resort to intermediate aperture couplings as reported in [12]. Two classes of structures, microwave-to-NRD-guide and CPW-to-NRD-guide transitions/baluns are presented, which provides a basis for our proposed integration and interconnect technique. The NRD-guide can be used for viable interconnects of co-layered planar circuits with a simple "put" and "cover" procedure. Preliminary experiments are made to validate the new schemes. Our proof of concept has been completed with a successful demonstration of two classes of microstrip-to-NRD-guide and CPW-to-NRD-guide transitions/baluns. Measured results show that satisfactory transmission properties can

readily be obtained. This concept is rather useful if monolithic circuits are required to integrate with the NRD-guide. In addition, this concept points to a possibility of designing unique low-loss interconnects of adjacent interface-to-interface or layer-to-layer planar circuits via NRD-guide. In the following, the proposed 3-D integration and interconnect schemes are presented and discussed with respect to transmission efficiency between these structures.

4.2 Co-layered integration and interconnect schemes

4.2.1 Co-layered integration of unbalanced NRD-guide with microstrip circuits

4.2.1.1 Design of microstrip-to-unbalanced NRD-guide transition/balun

Without involving planar lines and circuits, the geometry of an unbalanced NRD-guide is shown in Figure 2.2, which consists of a core dielectric strip deposited on the top of a relatively thin dielectric substrate. The whole structure is then placed between two parallel metallic plates in the same way as required in the conventional NRD-guide. The core dielectric block can thus be used to design an NRD-guide with a similar rule as used for the conventional NRD-guide but in the presence of the dielectric substrate. As discussed in chapter III, characteristics of the unbalanced NRD-guide are expected similar to the original NRD-guide since the electrically thin dielectric layer may modify solely little field profiles and guided wave features.

Of course, a possible leakage may be generated from the proposed structure since the vertical symmetry of structure cannot be guaranteed. However, this unwanted scenario may be corrected with two possible remedies. First, some specific geometrical asymmetry may not always generate a leakage loss within certain frequency ranges because of modal cancellation effects as reported in [13]. Secondly, bilateral packaging/shielding structure could be used to eliminate circuit-to-circuit couplings due to the leakage even though there is an issue of effectiveness. Generally, such a leakage loss may be very small or even negligible within certain frequency ranges if adequate dimensions of the structure are chosen, which require in any case a careful field-theory-based modeling and design.

Figure 4.1 shows the new integration scheme of unbalanced NRD-guide with microstrip circuits. This is made possible by a geometrical arrangement in that the microstrip circuits are formed on a relatively thin dielectric substrate and the circuit integration is achieved by a line-to-guide coupling as described in Figure 4.1(a). In this case, the planar line is oriented perpendicularly with respect to the NRD-guide, similar to the transition of a strip line to NRD-guide as reported in [22], such that the two dissimilar structures are designed with a great freedom except for the coupling section. Excellent coupling characteristics are expected from this transition/balun, which will be discussed in a subsequent section. Underlying advantages of the proposed technique can be simply postulated by the fact that the planar circuits are useful for the design of active circuits while the NRD-guide can be exploited for high-Q low-loss passive and other types of

components. Figure 4.1(b) shows a back-to-back interconnect of two distant microstrip lines on the same substrate for the purpose of experiments. Obviously, the removal of the upper metallic plate cover and NRD-guide will disconnect the two lines.

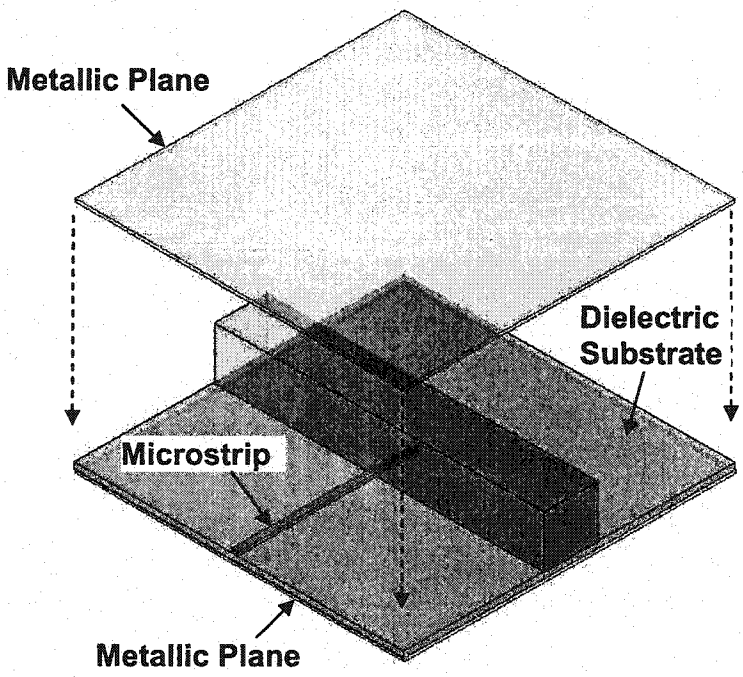

(a)

Fig.4.1. Co-layered integration and interconnect scheme of the unbalanced NRD-guide with a microstrip planar circuit. (a) Transparent view of the 3-D geometry for the integration of the two dissimilar structures

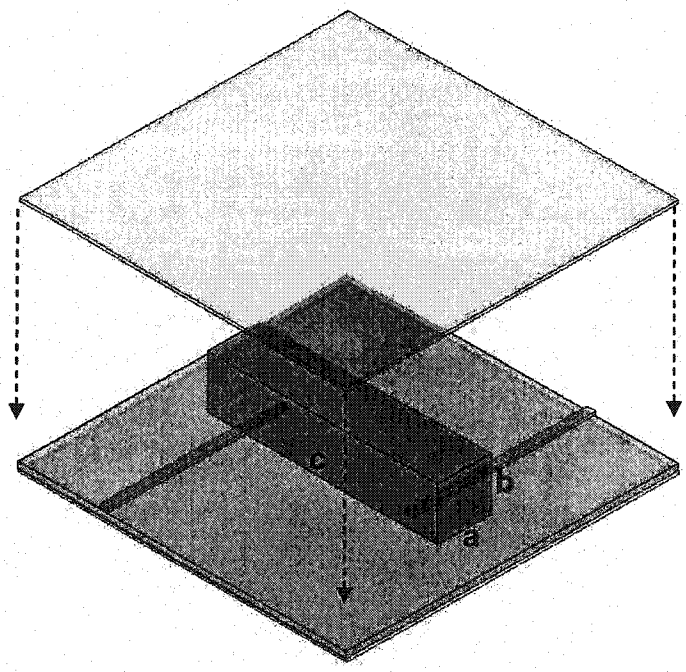

(b)

Fig.4.1. Co-layered integration and interconnect scheme of the unbalanced NRD-guide with a microstrip planar circuit. (b) The experimental back-to-back arrangement of two microstrip line-to-unbalanced NRD-guide transitions/baluns

This observation suggests that the NRD-guide can effectively serve as a low-loss interconnect for the two separate microstrip lines.

Successful integration and interconnect of the microstrip lines with the unbalanced NRD-guide rely on the design of a good transition/balun that links the two dissimilar structures. Such a design procedure is crucially important that requires a low signal-path loss and a miniaturized coupling section. In our transition/balun design as highlighted in Figure 4.2(a), the width of microstrip line is W; the penetration depth of the open-ended microstrip line into the core dielectric block is L_s; and the NRD open-end distance with respect to the center of the microstrip line is L_w. The adequate choice of L_s and L_w is critical in exciting the quasi-LSM_{01} mode in this unbalanced NRD-guide and also in obtaining a good impedance matching. As described in Figure 4.2(b), electrical performance of the transition/balun may be improved by appropriately reshaping the microstrip line open-end, which needs further detailed investigations. In our case studies, the microstrip line and the unbalanced NRD-guide are made of 20 mil Duroid substrate ($\varepsilon_r = 2.33$) and Polystyrene block ($\varepsilon_r = 2.56$), respectively.

This new scheme is different from our previously studied hybrid integration of planar circuits/NRD-guide, in which a magnetic coupling is used via aperture, which is subject to a potential resonance. In the present case, the coupling is made through the direct line-to-guide contact that has a strong magnetic coupling. This transition is expected to yield

satisfactory transmission characteristics between the two dissimilar structures over a broad bandwidth.

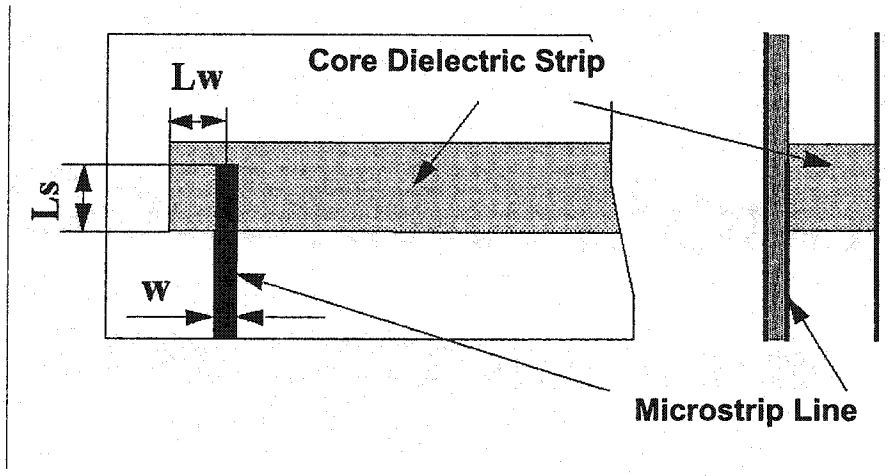

(a)

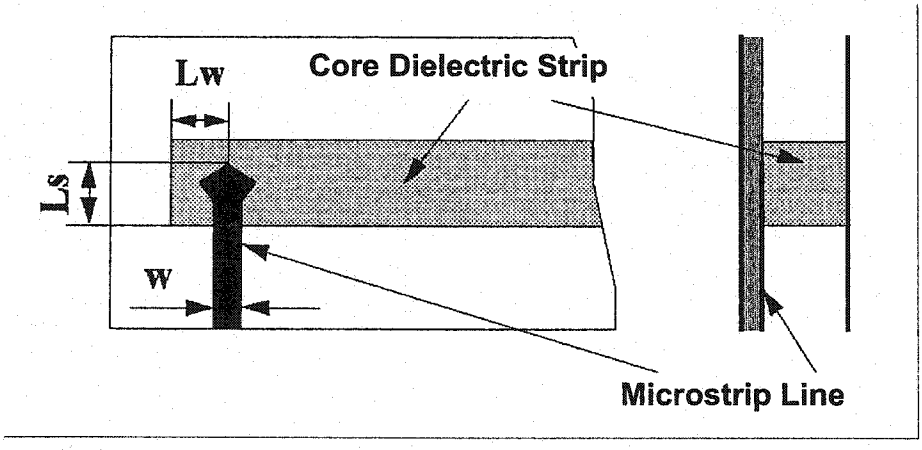

(b)

Fig.4.2 Straightforward arrangement of the microstrip line to the unbalanced NRD-guide transition/balun with geometrical details. (a) Basic coupling section; and (b) Modified coupling section with potential improvement of performance

4.2.2 Co-layered integration of surface-mounted NRD-guide with CPW

4.2.2.1 New scheme of integration

Figure 4.3 presents the proposed scheme of integrating an NRD-guide with a CPW structure. In this case, the NRD-guide is surface-mounted on the uniplanar ground plane of the CPW in a straightforward manner, and the uniplanar ground plane also serves as one of the parallel plates for the NRD-guide. Therefore, the original NRD-guide geometry is perfectly preserved. This new scheme is especially useful for MMICs and multilayered ICs.

The significant difference between the proposed integration/interconnect technique and the previous version of the hybrid NRD-guide/CPW geometry [23] lies in the arrangement of planar circuit with respect to the NRD-guide. In [23], the planar circuits were inserted into the NRD-guide. While in the new scheme, the NRD-guide is integrated in the form of a direct contact and layered format with the CPW circuits. This is a simple "put and cover" procedure, which potentially provides a low-loss and low-cost solution for millimeter-wave ICs.

4.2.2.2 Design of CPW-to-surface-mounted NRD-guide transition/balun

In this work, the CPW and the surface-mounted NRD-guide are made of 10 mil Duroid (Rogers^{TM}) substrate (ε_r = 2.94) and TMM6 (Rogers^{TM}) dielectric block (ε_r = 6), respectively. In the similar manner, the core dielectric strip of the NRD-guide is orthogonal in space with respect to the CPW in order to excite the LSM_{01} mode. As

illustrated in Figure 4.4, the distance from the open end of the NRD-guide to the center of the CPW (the open-end position of the NRD-guide) is L_w. In our case studies, a CPW step discontinuity is utilized in the design to achieve a better coupling between the two structures. The penetration depth of the CPW end into the core dielectric strip is L_s. The CPW end dimensions as denoted by L_{s1}, L_{s2}, W_1, W_2, W and D are also critical in exciting the wanted LSM_{01} mode in the NRD-guide and in obtaining good transmission properties between the two dissimilar structures.

4.3 Preliminary experiments and measured results

It is difficult to design the proposed transitions/baluns in a very neat way because they involve the complex 3-D planar/non-planar geometry. The proposed structures may be modeled with full-wave electromagnetic simulators but such modeling tasks are usually tedious to come up with optimized design results. In our concept proof experiments, the transitions/baluns are first simulated with those electromagnetic simulators in order to gain certain insight into their electrical properties. To verify the new concept of hybrid integration and interconnect techniques, several transitions are fabricated in the Ka-band, and measured with a HP8510C vector network analyzer (VNA). Note that a low-cost rough mechanic fabrication was deployed for our experimental samples in the laboratories and tolerance errors are of course inevitable with regards to the designed dimensions. In any case, our objectives are to experimentally demonstrate and prove the proposed new concept. Properties of an unbalanced NRD-guide bend are also experimentally studied to show its low- or non-radiative features. A thru-reflect-line

(TRL) calibration technique is applied in the measurements, and the standards are fabricated with the same substrate as used for the planar circuits.

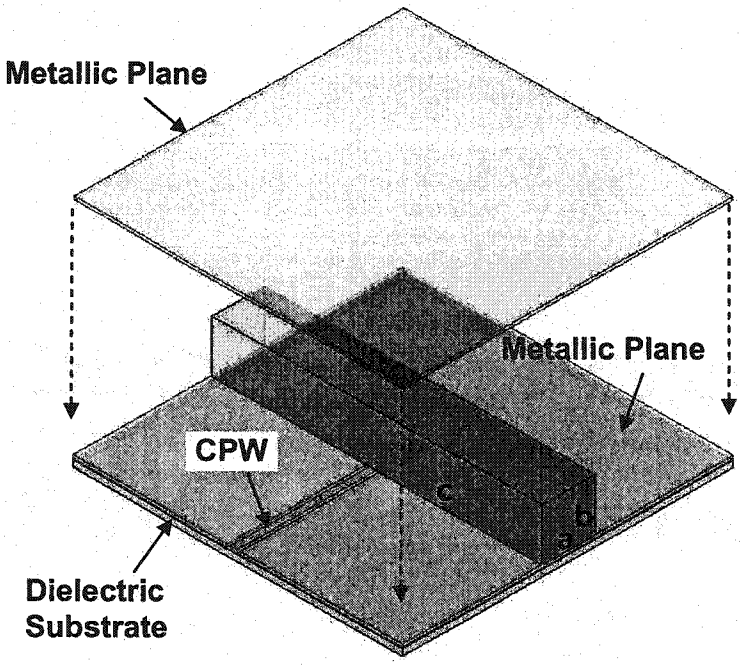

Fig.4.3 Proposed integration scheme of an NRD-guide with coplanar waveguide (CPW). The NRD-guide is surface-mounted on one of the uniplanar CPW ground planes

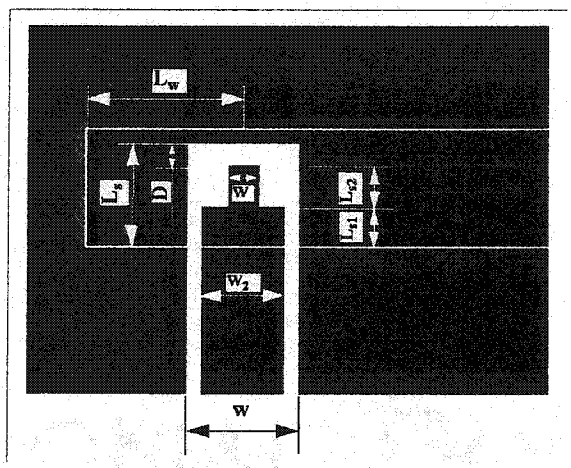

Fig.4.4 Graphical sketch of an improved integration scheme with geometrical parameters for the CPW-to-NRD-guide transitions/baluns

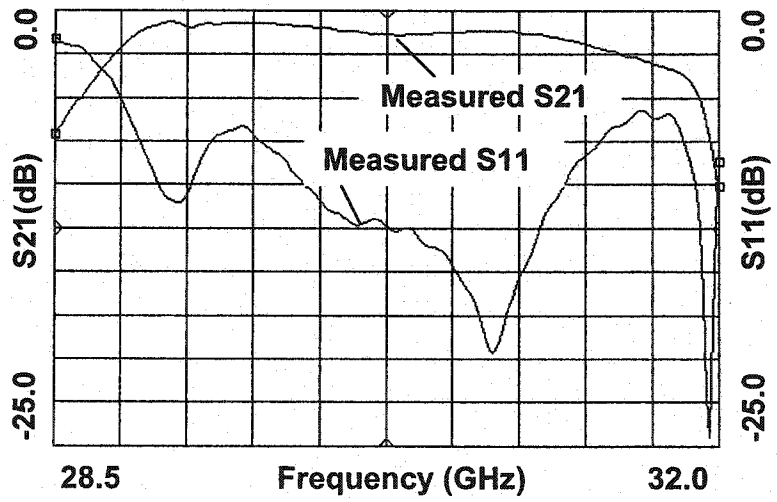

Fig.4.5 Measured insertion and return losses of a back-to-back experimental arrangement of two microstrip line-to-unbalanced NRD-guide transitions/baluns and the length of the unbalanced NRD-guide is 620 mil in this experiment

4.3.1 Back-to-back transition/balun of microstrip to unbalanced NRD-guide

To begin with, a back-to-back arrangement of Figure 4.1(b) with two identical transitions/baluns is considered that involves two separate microstrip lines interconnected via an unbalanced NRD-guide. In this way, the input and output remains in the form of the microstrip line that can easily be used in connection with the VNA for measurements. As our first experimental sample, the core NRD-guide is designed with dimensions of its cross-section $a \times b = 158 \times 138$, and length $c = 620$ (unit = mil). Measured results of this arranged structure are shown in Figure 4.5 for its insertion and return losses. It can be found that the measured results for the insertion loss present a relatively flat and wide frequency response, indicating a broadband feature with a low transmission loss. In our experiments, the insertion loss is observed to be less than 1.2 dB for the complete block that consists of the two back-to-back transitions and interconnecting lines over the effective frequency range. Such attractive properties come from the strong magnetic coupling between the two direct-contact structures, as mentioned in the above section. On the other hand, the return loss is reasonably good except a small rise around 29.4 GHz, which can be reduced with further studies.

Our second experimental sample is made of a core NRD-guide with its cross-section dimensions $a \times b = 150 \times 138$, and length $c = 500$ (unit = mil). Measured insertion and return losses of its back-to-back structure are given in Figure 4.6, the best insertion loss in the frequency range is about 0.5 dB obtained around 32.5 GHz, and the return loss is better than 20 dB, thereby showing very promising characteristics at millimeter-wave

frequencies. Similar frequency responses are observed in Figure 4.6 with reference to Figure 4.5 except that the low end of the effective frequency band is pushed up. This is because the cutoff frequency of the unbalanced NRD-guide is effectively modified with the change in dimension.

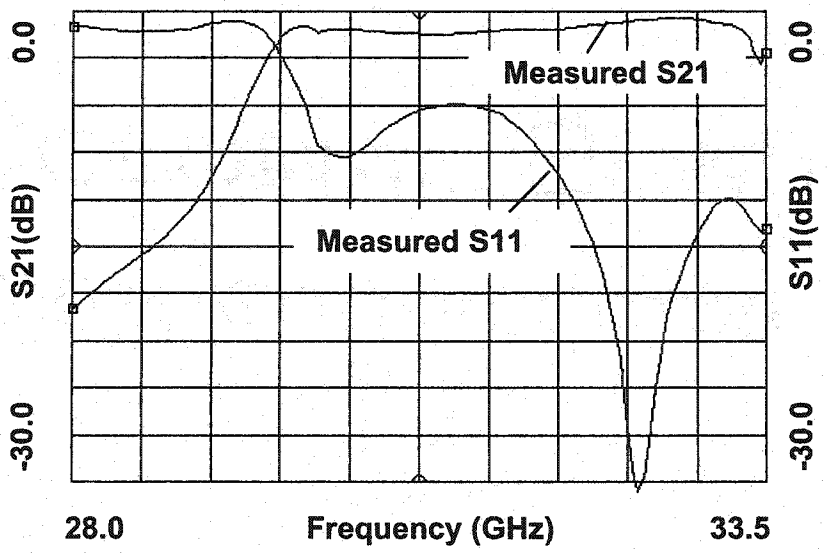

Fig.4.6 Measured frequency response of the insertion and return losses of a back-to-back experimental arrangement that consists of two microstrip line-to-unbalanced NRD-guide transitions and the length of the unbalanced NRD-guide is 500 mils

4.3.2 Unbalanced NRD-guide interconnect

Interconnects of planar circuits at millimeter-wave frequencies can be realized by the proposed unbalanced NRD-guide with a "put & cover" procedure. To illustrate this proposal, a special back-to-back interconnect as sketched in Figure 4.7 is fabricated and measured for two microstrip lines on the top of a TMM3 (Rogers^{TM}) substrate of 15 mil (ε_r = 3.27) that are connected through an unbalanced NRD-guide. In this case, the scheme is achieved with aperture-based feed-through couplings of the microstrip lines to the NRD-guide, similar to our previous hybrid integration technique except the use of an unbalanced NRD-guide. In this case, the core NRD-guide is made of Polystyrene with dimensions of its cross-section $a \times b = 158 \times 138$, and length $c = 620$ (unit = mil). Measured results are displayed in Figure 4.8, also showing good characteristics, and the transmission loss is slightly higher but the frequency response of the return loss looks satisfactory over a wider bandwidth of frequency.

The removal of the unbalanced NRD-guide will obviously disconnect the two lines. This useful interconnect may be made at low-cost and it also may be more convenient than wire bonding and other pragmatic approaches at millimeter-wave frequencies. This points to the convergence of the two usually separate high-frequency design aspects: integration and interconnects that are in fact consistent with each other.

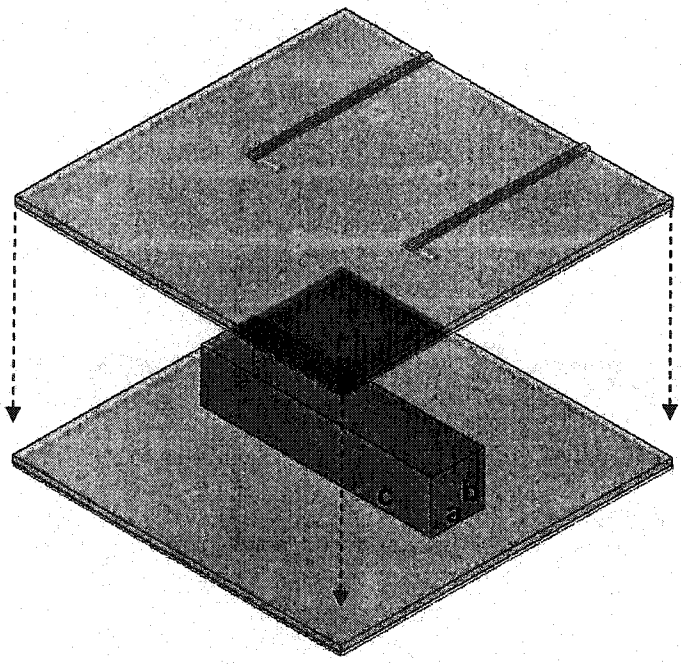

Fig.4.7 Interconnect and integration demonstrations of two electrically separate microstrip lines on the same planar substrate using an unbalanced NRD-guide. The microstrip lines are coupled to the unbalanced NRD-guide via two slot apertures

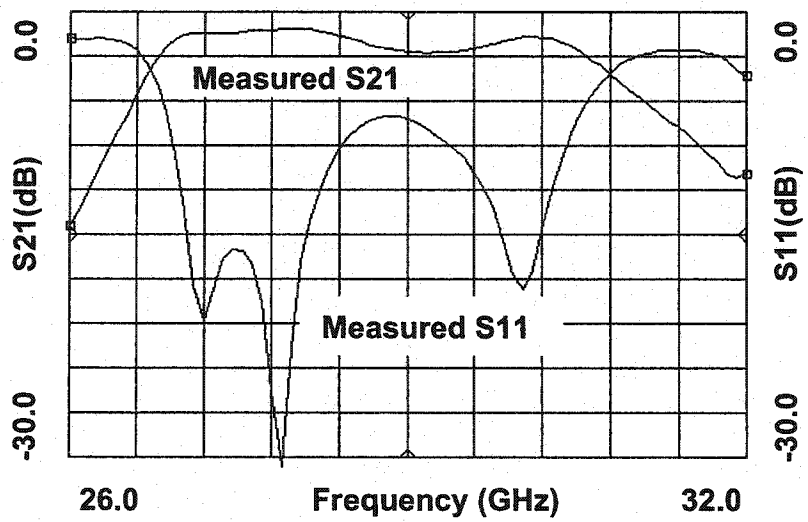

Fig.4.8 Measured frequency response of the insertion and return losses of two interconnected microstrip lines (see Figure 4.7) via a length of 620 mil unbalanced NRD-guide

4.3.3 Unbalanced NRD-guide bend

To show potential radiation and leakage losses due to the use of unbalanced NRD-guide, one experiment is made for two microstrip lines that are connected with each other via an unbalanced NRD-guide bend as shown in Figure 4.9. The two transitions are designed with reference to Figure 4.2. This bend spans a sectorial angle of 90 degree and its radius of curvature is 500 mil. Dimensions of its cross-section are selected as $a \times b = 158 \times 138$ (unit = mil). Measured results are shown in Figure 4.9 for the insertion and return losses over the bandwidth of interest. Compared to our first two examples that are made of the similar but a straight unbalanced NRD-guide, the results of Figure 4.9 indicate that any potential leakage loss due to the bend is truly negligible in this example. If the leakage is present in the structure, the resulting loss would be much smaller than its conductor counterpart if the NRD-guide is replaced by a curved microstrip line judging from Ka-band loss parameters known in the literature for the microtrip line.

4.3.4 Back-to-back transition/balun of CPW to surface-mounted NRD-guide

Our final experiment showcases a back-to-back arrangement of two CPW lines that are interconnected via a length of a surface-mounted NRD-guide. In this way, the input and output remains in the form of CPW that can easily be used in connection with VNA for our measurements. The CPW lines and the surface-mounted NRD-guide are made of 10 mil Duroid (Rogers^{TM}) substrate (ε_r=2.94) and TMM6 (Rogers^{TM}) dielectric block (ε_r=6), respectively. The CPW end step is designed with L_{s1}=30, L_{s2}=30, D=15, W_1=12,

W_2=58, and W=70 (unit = mil) with reference to Figure 4.4. Two NRD-guides are designed and fabricated with dimensions of same cross-section $a \times b = 100 \times 150$, and with two different length $c = 580$, and $c = 600$ (unit = mil), respectively. Measured results are presented in Figure 4.10 for the complete experimental block consisting of the two back-to-back transitions/baluns and interconnecting lines. For the 600 mil NRD-guide, it is found that the best insertion loss is about 1.0 dB obtained around 27.75 GHz, and the return loss is better than 20 dB. As for the 580 mil NRD-guide, the best insertion loss is about 1.2 dB around 28 GHz, and the return loss is also better than 20 dB. Such preliminary results, once again, demonstrate very promising characteristics of the proposed schemes for millimeter-wave applications.

4.4 Conclusion

A concept of hybrid integration and interconnects is presented for the design of millimeter-wave ICs. The proposed concept consists of two distinct schemes that involve the hybrid integration of NRD-guide in direct-contact coupling with microstrip and CPW circuits. In essence, the first scheme makes use of an NRD-guide deposited on a relatively thin dielectric substrate, thus forming an unbalanced NRD-guide. Co-layered microstrip circuits are designed on the same dielectric substrate. This approach is inspired by the fact that the susceptible leakage loss due to the NRD asymmetry may be very small or even completely suppressed with some adequate geometrical arrangement as compared to the conductor loss if the NRD-guide is replaced with planar lines. The second scheme is developed on the basis of a hybrid integration of NRD-guide and CPW

circuits, both of which share the same ground plane. In this case, the NRD-guide can be regarded as a surface-mounted structure on the top of the CPW, and the original geometry of the NRD-guide is well preserved with the known advantageous features.

Our preliminary experiments have firmly validated the proposed concept and also the usefulness of the new schemes, which are shown with distinct advantages. One of the most interesting and also fundamental observations in this work is that the integration and interconnect can be unified and handled in the same manner, and in fact they present the same design aspects. The present studies show that the proposed co-layered transitions/baluns are promising with low signal loss between the two dissimilar structures. Further work should be done for in-depth understanding of comprehensive properties of the new schemes, which are critically important for successful design. This new concept features added advantages in our hybrid integration technology of planar circuits/NRD-guide [12] for the design of 3-D multilayered ICs and millimeter-wave MMICs.

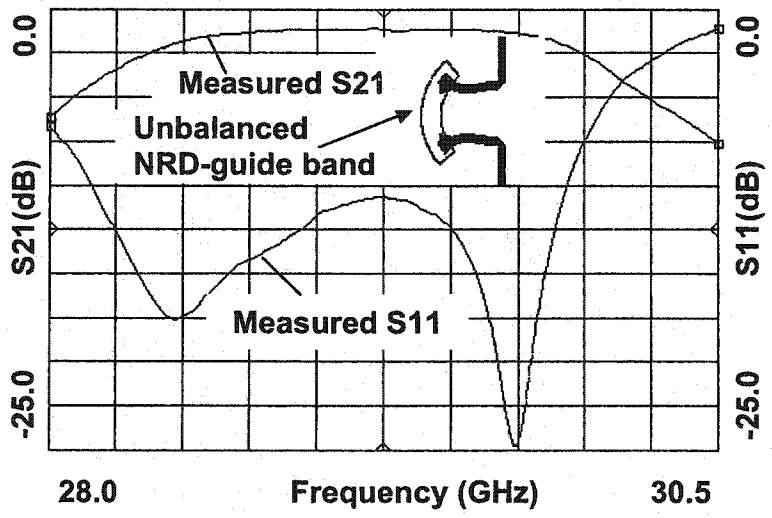

Fig.4.9 Measured insertion and return losses of the complete experimental building block for two interconnected microstrip lines that involves the depicted topology of a length of 90 degree unbalanced NRD-guide bend. In this experiment, the microstrip lines are in direct contact with the unbalanced NRD-guide as shown in Figure 4.1(b)

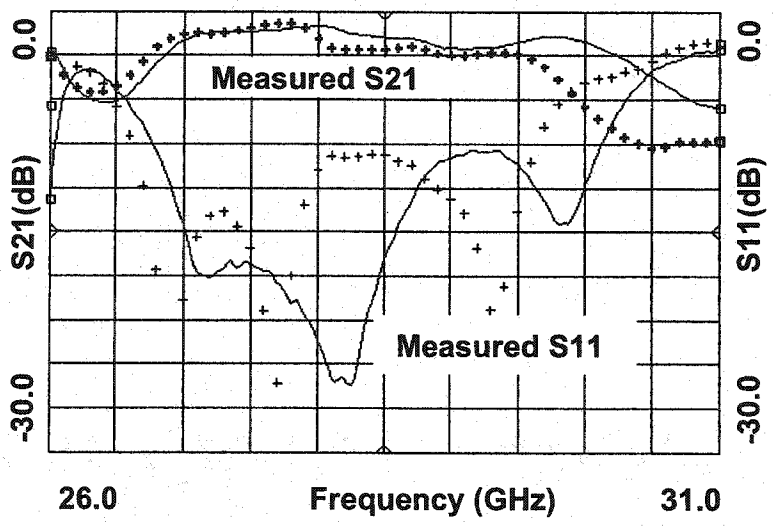

Fig.4.10 Measured insertion and return losses of two back-to-back experimental arrangements that consist of two CPW-to-surface-mounted NRD-guide transitions/baluns with the lengths of the unbalanced NRD-guide are chosen as 580 mil (solid lines), 600 mil ("+" lines), respectively. The improved coupling section as shown in Figure 4.4 is used in the experiments with the parameters: L_{s1}=30, L_{s2}=30, D=15, W_1=12, W_2=58, and W=70 (unit = mil)

CHAPTER V

MODELING AND PROPERTIES OF HYBRID INTEGRATION STRUCTURES BASED ON SURFACE-MOUNTED NON-RADIATIVE DIELECTRIC (NRD) WAVEGUIDE

5.1 Introduction

In previous chapters, surface-mounted NRD-guide has been presented, and a class of integration and interconnects structures have been investigated with preliminary experiments. The integration of planar circuits with surface mounted NRD-guide is very flexible in topology; NRD-guide may be in direct contact with planar circuits that are fabricated on the thin dielectric substrate such as microstrip circuits. Besides, surface mounted NRD-guide may be easily integrated with the microstrip circuits on a separate layer by aperture coupling, which is similar to that reported in [12]. The proposed hybrid integration scheme and its basic operating principle and usefulness were initially reported in [14, 24, 25].

In this chapter, we start with the analysis of an integration structure of an NRD-guide to a microstrip with emphasis on the analysis of the spurious mode effects. Then, the microstrip to surface-mounted NRD-guide transitions are studied. The aim is to provide a theoretical basis for performance-enhanced broadband designs and applications. Since unwanted modes are also excited, the main modes generated in the hybrid planar/NRD-

guide structures are modeled, modal transmission and return loss results are presented for different type of transitions. Investigation results indicate that an optimized hybrid planar/NRD-guide integrated transition without additional compensatory measures may be good enough for some application over a certain frequency band. However, for many broadband applications, spurious mode suppressors are required to eliminate unwanted modes for performance enhancement. The critical spurious mode suppressing techniques will be addressed in the following chapter.

5.2 Modeling of transition of NRD-guide to microstrip

Figure 5.1 shows the integration scheme of an NRD-guide with a microstrip circuit, which is designed using the similar geometrical arrangement and the same technique as addressed before. The coupling is achieved through a rectangular slot etched on the ground plane that separates the NRD-guide and the planar circuit. In this study, the microstrip line and the NRD-guide are made of 10 mil Duroid substrate (ε_r= 10.2) and ECCOSTOCK 0005 (ε_r= 2.54), respectively. The width w and the height h of the NRD-guide strip are 168 mil and 180 mil, respectively, which are selected using the same method as that we reported as in [27].

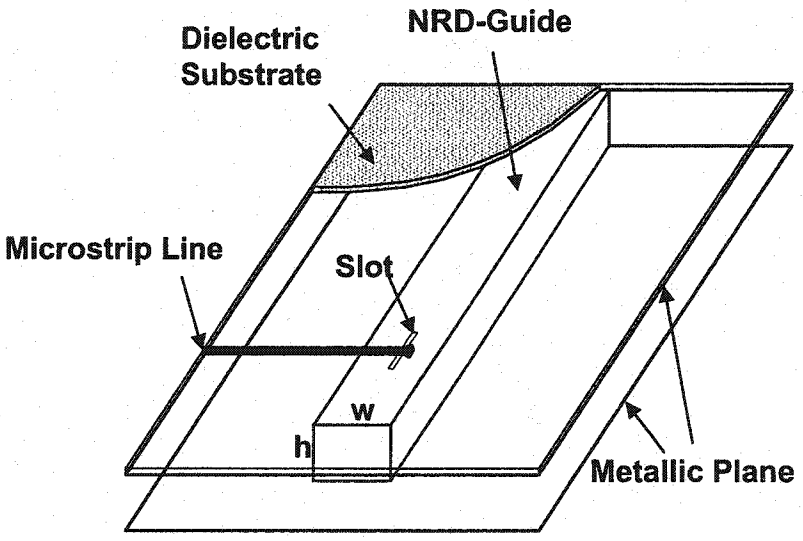

Fig. 5.1 Three-dimension (3-D) topological view of a conventional integrated microstrip-to-NRD-guide transition

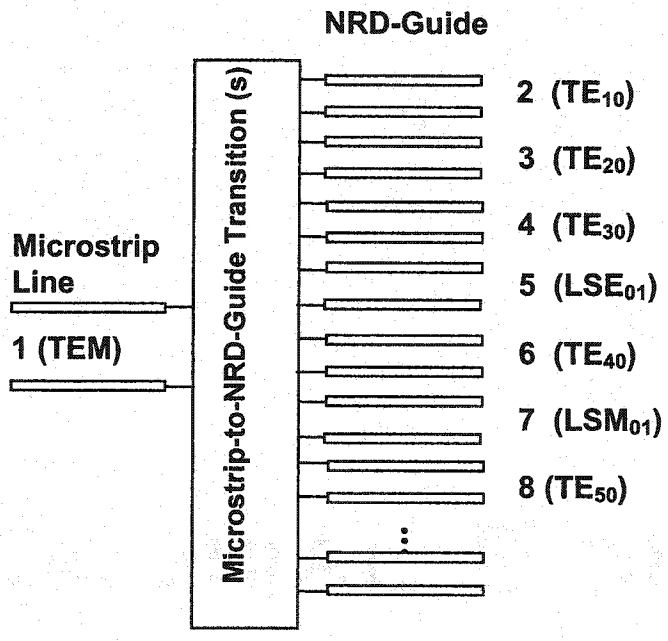

Fig. 5.2 Equivalent network for the microstrip-to-NRD-guide transition that accounts for the quasi-TEM mode in the microstrip line coupled to multiple NRD-guide modes

Susceptible principal modes excited in the NRD-guide depend on the hybrid structure configuration (especially the coupling section that includes the NRD-guide) and the dielectric materials. In this case, the quasi-TEM mode in the microstrip line will potentially excite TE_{10}, LSE_{01}, TE_{20}, LSM_{01}, TE_{30}, TE_{40}, and LSM_{02} modes in the NRD-guide, although the other less important modes may be also induced by the transition discontinuities. To represent this particular microstrip-to-NRD-guide transition, an equivalent one-to-multi-port network as shown in Figure 5.2, which reflects the concerned main modes, should be considered.

The principal modes generated in this hybrid planar/NRD-guide structure are modeled and extracted for the equivalent network. With emphasis on the feasibility of the proposed technique, we make little attempt for the circuit design aspects. In Figure 5.3, parameters S_{21}, S_{31}, S_{41}, S_{51}, S_{61}, and S_{71} stand for the conversion losses from the input quasi-TEM mode to TE_{10}, TE_{20}, TE_{30}, LSE_{01}, TE_{40} and LSM_{01} modes along the NRD-guide, respectively. Figure 5.3 plots transmission and return losses of the modes for the transition from microstrip to NRD-guide as described in Figure 5.1. We can observe that the return loss S_{11} is better than -17 dB over the frequency band of 27-29 GHz. The worst spurious modes excited over this structure seem to be TE_{20} mode and TE_{40} mode with a lower than –15dB frequency response that may be good enough for some applications. However, such spurious modes appear to quickly rise up and become extremely harmful beyond the center frequency band. These spurious modes are responsible for making the filter upside stop-band performance deteriorated that is not acceptable for the required

isolation of channels located within the Ka-band. Interestingly, such a planar/NRD-guide transition is able to inherently reject some spurious modes, namely, LSE_{01} mode that may be generated by discontinuity in the conventional NRD-guide.

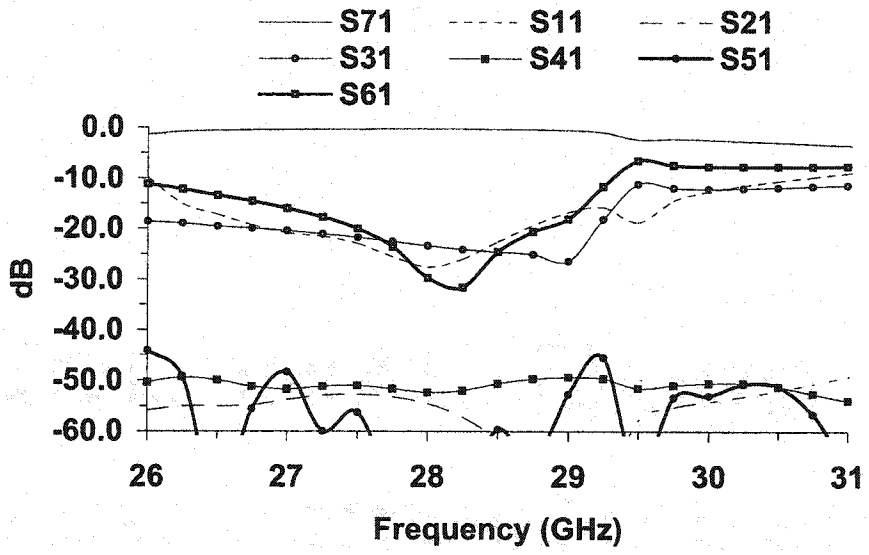

Fig. 5.3 Transmission and return losses of an optimized transition as shown in Figure 5.1, considering the modal transfer and conversion as described by the equivalent network of Figure 5.2

5.3 Modeling of transition of surface-mounted NRD-guide located on a separate layer

Figure 5.4 shows an integration scheme of the surface-mounted NRD-guide with a microstrip circuit located on a separate layer, which are designed with the technique similar to the transition of an NRD-guide to a microstrip circuit. In this geometrical arrangement, the planar microstrip line is perpendicularly oriented with respect to the NRD-guide. The coupling is achieved through a rectangular slot etched on the ground plane that separates the NRD-guide and the planar circuit on a separate layer. This structure is developed for potential compatibility in multilayer process, and it is also a perfect candidate for the study of modal effects because of the absence of a microstrip line on the thin dielectric layer. Electrical performance of such a transition may be improved by appropriately reshaping the microstrip line open-end, as explained in chapter 4, which was initially reported in [25]. In the following modeling analysis, the microstrip line and the NRD-guide are made of 10 mil Duroid substrate (ε_r = 10.2) and ECCOSTOCK 0005 (ε_r = 2.54), respectively. The width w and the height h of the NRD-guide strip are 155 mil and 185 mil, respectively. The thin dielectric substrate is made of 10 mil duroid substrate (ε_r =2.22).

The coupling between the microstrip line and the surface mounted NRD-guide involves two dissimilar structures. In this case, the quasi-TEM mode in the microstrip line will potentially excite TE_{10}, LSE_{01}, TE_{20}, LSM_{01}, TE_{30}, TE_{40}, LSM_{02}, and TE_{50} modes along the surface-mounted NRD-guide, although other less important modes may be also

induced by the transition discontinuities. We use the same equivalent one-to-multi-port network as shown in Figure 5.2 to represent the microstrip-to-surface-mounted-NRD-guide transition as described in Figure 5.4.

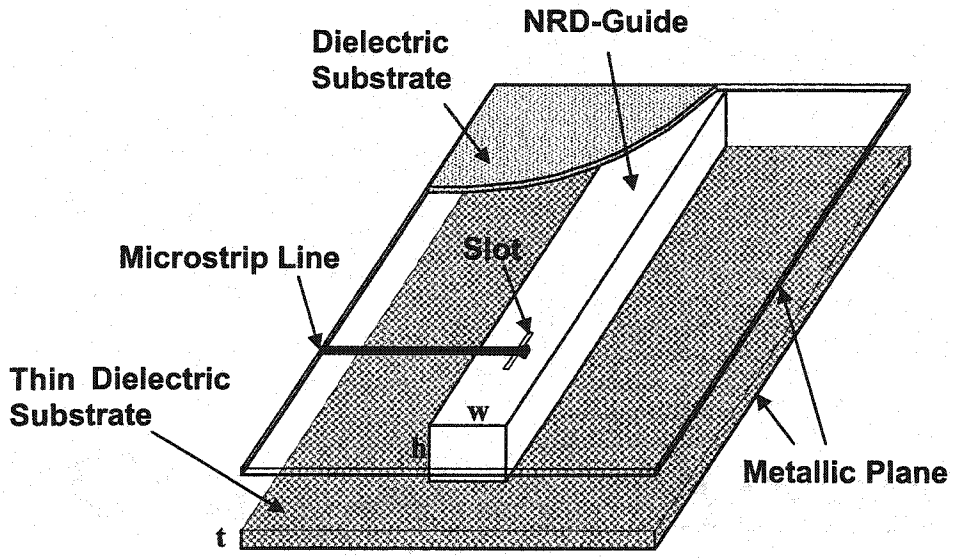

Fig. 5.4 Three-dimension (3-D) topological view of a conventional transition of microstrip-to-surface-mounted NRD-guide, with microstrip located on a separate Layer

The principal modes generated in this hybrid planar/NRD-guide structure are modeled and extracted for the equivalent network. Figure 5.5 plots transmission and return losses

of the principal modes for the transition from microstrip to surface-mounted NRD-guide as described in Figure 5.4, parameters S_{21}, S_{31}, S_{41}, S_{51}, S_{61}, and S_{71} stand for the conversion losses from the input quasi-TEM mode to TE_{10}, TE_{20}, TE_{30}, LSE_{01}, TE_{40} and LSM_{01} modes along the surface-mounted NRD-guide, respectively.

We can observe that the return loss S_{11} is better than -17 dB over the frequency band of 26.5-29 GHz. The worst spurious modes excited over this structure seem to be TE_{20} mode and TE_{40} mode with a lower than –12dB frequency response. Similar to the transition of a standard NRD-guide to microstrip, the spurious modes appear to quickly rise up and become extremely harmful beyond the center frequency band. This planar/NRD-guide transition is also able to inherently reject some spurious modes, namely, LSE_{01} mode.

5.4 Modeling of transition of surface-mounted NRD-guide to microstrip located on thin dielectric substrate

Figure 5.6 shows an alternative integration scheme of the surface-mounted NRD-guide with a microstrip circuit located on the thin dielectric substrate. Figure 5.7 plots transmission and return losses of the modes for the transition.

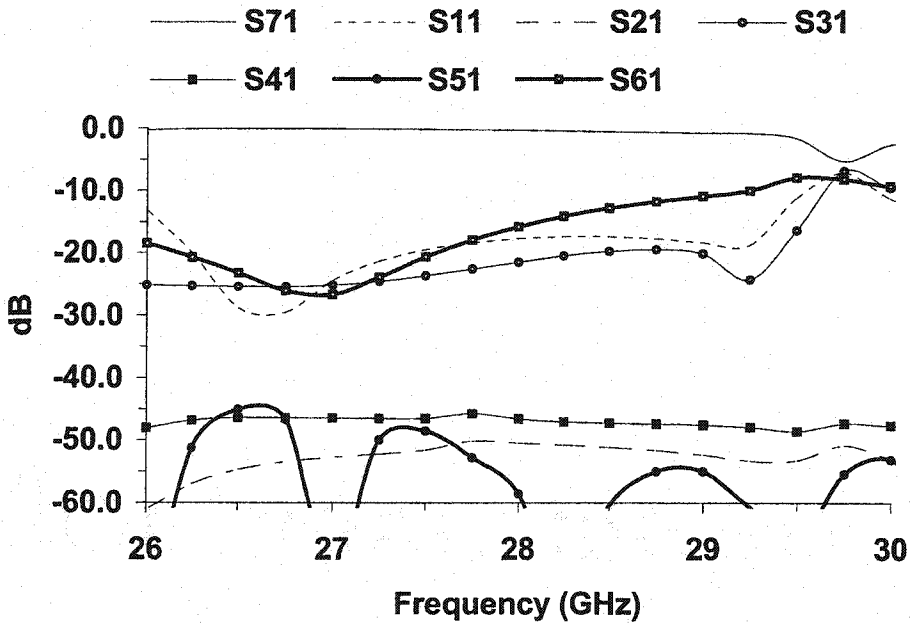

Fig. 5.5 Transmission and return losses of an optimized transition as shown in Figure 5.4, considering the modal transfer and conversion as described by the equivalent network of Figure 5.2

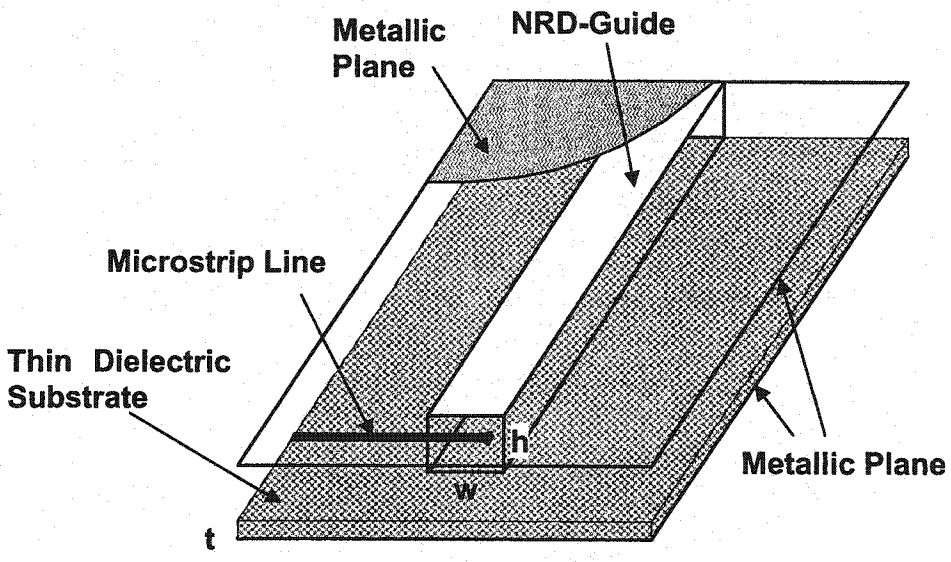

Fig. 5.6 Three-dimension (3-D) topological view of a conventional transition of microstrip-to-surface-mounted NRD-guide, with a microstrip line located on the thin dielectric substrate

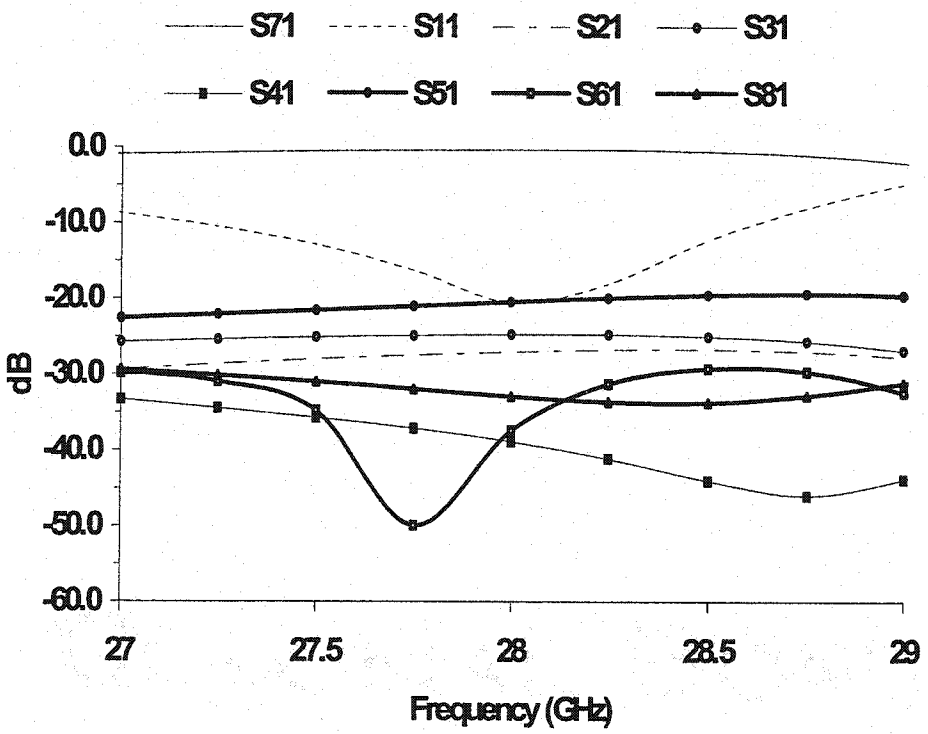

Fig. 5.7 Transmission and return losses of an optimized transition as shown in Figure 5.6, considering the modal transfer and conversion as described by the equivalent network of Figure 5.2

In this example, the NRD-guide is made of ECCOSTOCK 0005 (ε_r = 2.54). The width w and the height h of the NRD-guide strip are 155 mil and 185 mil, respectively. The thin dielectric substrate is made of 20 mil duroid substrate (ε_r =2.33). Parameters S_{21}, S_{31}, S_{41}, S_{51}, S_{61}, S_{71}, and S_{81} stand for the conversion losses from the input quasi-TEM mode to TE_{10}, TE_{20}, TE_{30}, LSE_{01}, TE_{40}, LSM_{01}, and TE_{50} modes along the surface-mounted NRD-guide, respectively. We can observe again that an optimized hybrid planar/surface-mounted NRD-guide integrated transition may be good enough for some applications over a certain frequency band. However, for broadband applications, a spurious mode suppressor is often required for eliminating unwanted modes; the related issues will be addressed in the following chapters.

5.5 Conclusions

Transitions of planar circuit to NRD-guide have been studied with numerical results and with emphasis on the spurious mode effects. This investigation provides a basis for the performance-enhanced broadband design and applications. Principal modes generated in a hybrid planar/NRD-guide structure are modeled. Results for modal transmission and return loss are presented for different transitions. Our study indicates that a normal hybrid planar/NRD-guide integrated transition without compensatory measures may be good enough for some applications over a certain frequency band. However, for broadband applications, spurious mode suppressors are required for eliminating unwanted modes in many cases. The principal modes generated in the surface-mounted NRD guides are

determined by the transition structure, dimension. Effective mode suppressing techniques are critical for the performance enhancement of the proposed hybrid planar/ NRD circuits.

CHAPTER VI

SUPPRESSION OF SPURIOUS MODES FOR THE DESIGN OF HYBRID MICROSTRIP PLANAR/NRD-GUIDE INTEGRATED CIRCUITS

6.1 Introduction

As mentioned in the previous chapter, emerging technologies present promising features for high-density design of radio-frequency integrated circuits (RFICs), namely, 3-D MMICs and low-temperature co-fired ceramic (LTCC) schemes [2]. Nevertheless, challenging problems are often encountered in the design of low-cost millimeter-wave high-Q integrated circuits such as band-pass filter, to which the planar geometry is fundamentally not amenable. NRD-guide structure provides a promising solution, however, there are still problems to be solved for its wide application. Since the low-loss guided mode of interest is not the lowest mode in the NRD-guide, in many cases, the spurious mode problem is often responsible for deteriorating electrical performance. Suppressors for eliminating unwanted modes are usually required. So far, they are designed to reject the LSE mode as shown, for example, in [9, 10, 12]. The reported mode suppressors are designed with specifically shaped metallic strips/films that are usually inserted into the center plane of NRD-guide. It is not convenient to implement although this is a very effective approach.

A hybrid integration concept of planar circuit and NRD-guide has been proposed and developed [12]. As demonstrated in chapter V, an optimized hybrid planar/NRD-guide integrated transition without additional compensatory measures may be good enough for some application over a certain frequency band. However, spurious TE modes in view of a parallel-plate dielectric waveguide may also be excited by discontinuity. With regard to the hybrid planar/NRD-guide integration technology, the planar transmission line-to-NRD-guide transitions present themselves certain discontinuities that are harmful since the unwanted spurious modes may be generated. As a result, the stop-band or out-of-band performance (especially the higher end of pass band) of a planar NRD-guide filter is usually deteriorated. Therefore, the underlying attractive features of the proposed hybrid planar/NRD-guide technique have not been fully exposed. Similar to the standard NRD-guide applications, spurious mode suppressors are also required to eliminate unwanted modes for performance enhancement.

In this chapter, a new spurious mode suppressing technique is first presented, concerned with an integrated microstrip-to-NRD-guide transition and a mode suppressor. The design guideline and procedures are then addressed. With some simple modifications, this spurious mode-suppressing concept can be extended and applied to a class of integrated planar to surface-mounted NRD-guide transitions. General spurious mode-suppressing techniques for the integrated microstrip-to-surface-mounted NRD-guide transition (NRD-guide surface-mounted on the top of a relatively thin planar substrate) have also been investigated.

To facilitate the implementation of the mode suppressor, a compact spurious mode suppressing technique for the design of hybrid planar/NRD-guide integrated transition is then presented and analyzed. The metallic plate/film mode suppressing structure is used in the design, which is compact and easy to implement. It is found through our investigation that the rejection to all the spurious modes (including TE and LSE modes) can be better than -32 dB for a single transition over a broadband frequency of interest, and the performance could be further enhanced. This compact design technique also provides an alternative solution to the inherent problem of spurious mode (especially TE modes) in the standard NRD-guide circuit design.

Several planar/NRD-guide filters are designed and implemented over millimeter-wave frequency band to evaluate the interesting features of the proposed technique. Those obtained experimental results indicate that the rejection to all the spurious modes (including TE and LSE modes) can be better than –35 dB for a single proposed transition over a broadband frequency of interest. Our proposed spurious mode-suppressing scheme for the hybrid planar/NRD-guide integrated circuits was initially reported in [26].

6.2 Mechanism of spurious mode suppression and modeling

Without mode suppressor, the integration scheme of NRD-guide with microstrip circuit is shown in Figure 5.1, Figure 5.3 plots transmission and return losses of the modes for the

transition from microstrip to NRD-guide. It is observed that spurious modes appear to quickly rise up and become extremely harmful beyond the center frequency band.

In this design, the microstrip line and the NRD-guide are made of 10 mil Duroid substrate ($\varepsilon_r = 10.2$) and ECCOSTOCK 0005 ($\varepsilon_r = 2.54$), respectively. The width w and the height h of the NRD-guide strip are 168 mil and 180 mil, respectively.

Figure 6.1 illustrates our proposed transition of two dissimilar structures to handle the spurious modal responses, which involves a conventional transition combined with a mode suppressor. The concept for this technique is very simple. As we can find out from results and discussion in chapter V, the planar/NRD-guide technique has a feature inherent to reject the unwanted LSE_{01} and TE_{10} modes. Thus, the subsequent consideration in the design is focused to how to suppress the spurious TE_{20}-mode, which is in fact very simple to implement. The easiest way is to use a section of a cutoff waveguide relative to the TE mode together with match sections, while this suppressor has little or negligible effect on the fundamental LSM_{01} mode in the NRD-guide. This requires the selection of a distance between the two metallic blocks of the suppressor to ensure a cutoff of the spurious TE-modes. Two metallic blocks are located at the two sides of the NRD-guide mode launcher from the microstrip line.

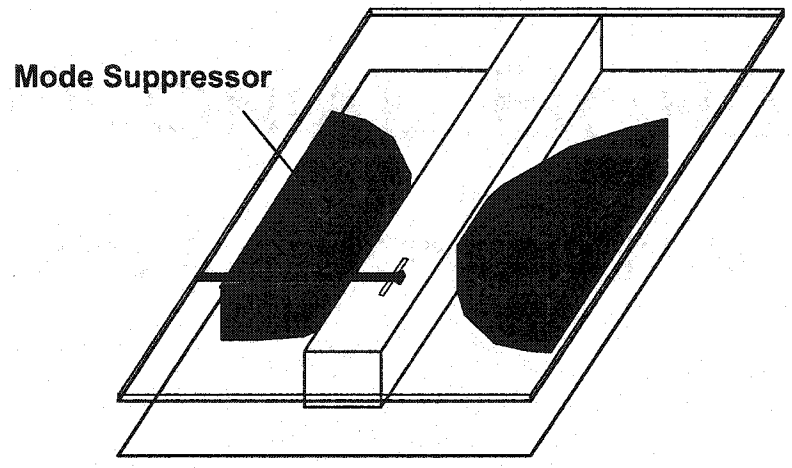

Fig. 6.1(a) 3-D transparent view of the microstrip-to-NRD-guide integrated transition involving the proposed spurious mode suppressor

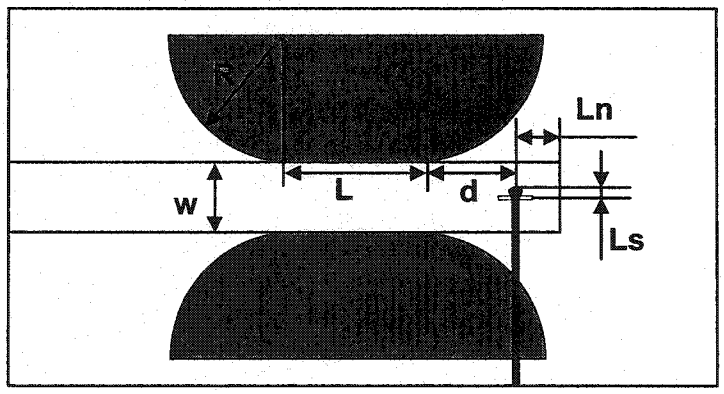

Fig. 6.1(b) Geometrical parameters for the new hybrid microstrip-to-NRD-guide integrated transition

In the design, the NRD open-end distance Ln with respect to the center of the microstrip line is 91 mil; the distance between the microstrip open-end and the center of the NRD-guide (also the center of slot) Ls is 41 mil. The slot dimensions are 180 ×17 (mil). The proposed mode suppressor is designed to suppress the remaining higher-order spurious modes, especially the TE_{20} and TE_{40} modes in this case. The design of such a mode suppressor requires no metallic sheet insertion into the NRD-guide strip in this case. The suppressor configuration shown in Figure 6.1(b) is used to facilitate the fabrication. The distance between the two mode suppressor blocks is selected to reject the TE_{20} mode, in our case, equal to the width of the NRD-guide. The center straight length L is designed to be about a half wavelength of the fundamental LSM_{01} mode, that is, 385mil. The matched input and output sections are designed with R = 391 mil. The position of the mode suppressor is then optimized to match with the fundamental LSM_{01} mode, and d is 314 mil.

Figure 6.2 plots simulated transmission and return losses for this performance-enhanced transition, equivalent network for the microstrip-to-NRD-guide transition is the same as that shown in Figure 5.2. We can observe now that the return loss is better than -18 dB over the frequency band of interest from 27.5 to 28.5 GHz. The worst spurious modes excited in this case are TE_{10} and LSE_{01} modes but they are all suppressed to be better than –39 dB over the frequency range. Therefore, the proposed technique should be useful for low-loss hybrid integration of planar and NRD-guide at millimeter-wave

frequency band, and in particular for hybrid planar NRD filter design that requires a stringent out-of-the-band rejection.

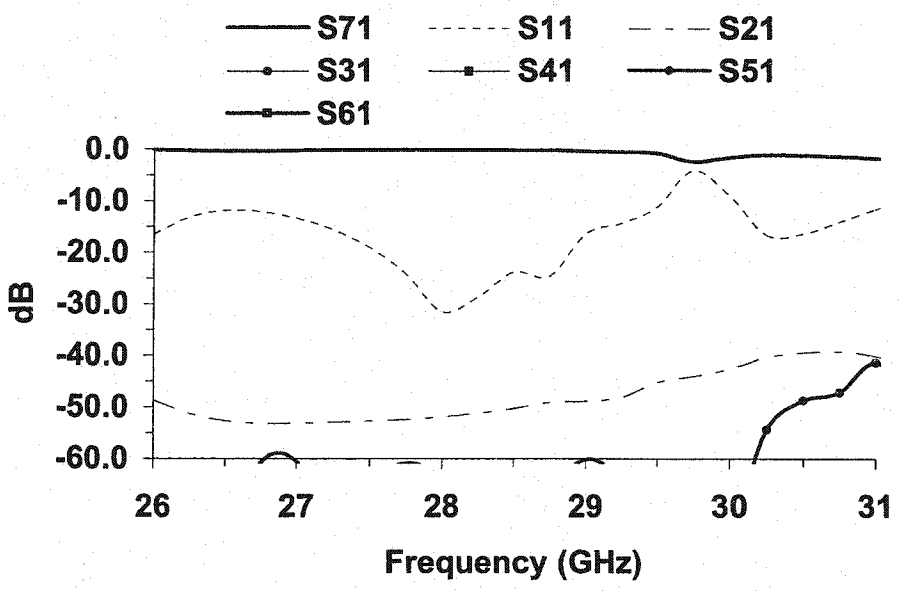

Fig. 6.2 Simulation and extracted transmission and return losses of S-parameters for the proposed transition as described in Figure 6.1(a) including mode conversion effects

6.3 Spurious mode-suppressing techniques for the integrated microstrip-to-surface-mounted NRD-guide transition

In chapter V, the integration scheme of a surface-mounted NRD-guide with a microstrip circuit located on a separate layer is described in Figure 5.4. The transmission and return losses of the principal modes for the transition from microstrip to surface-mounted NRD-guide are plotted in Figure 5.5.

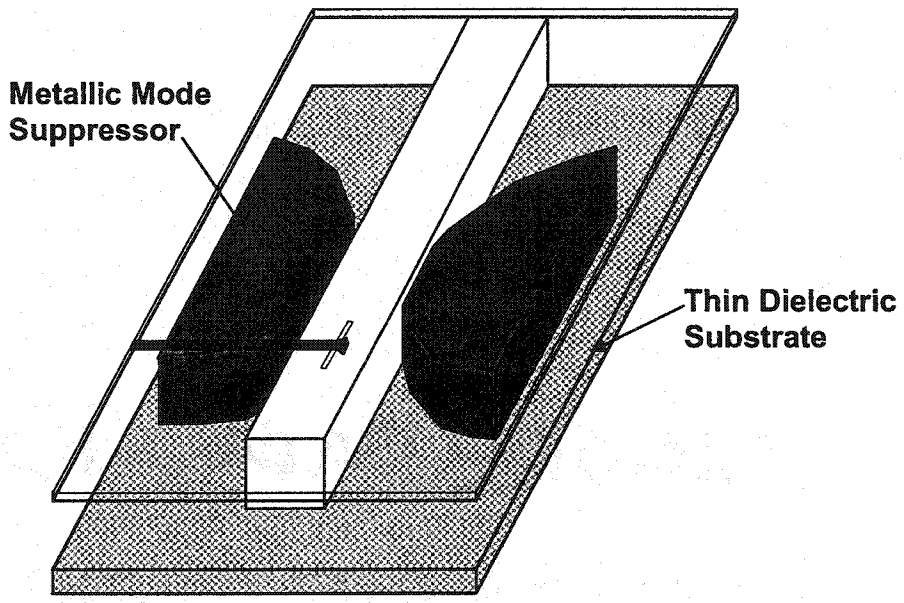

Fig. 6.3 3-D transparent view of the microstrip-to-surface-mounted-NRD-guide integrated transition involving the proposed spurious mode suppressor

Figure 6.3 illustrates our proposed transition of two dissimilar structures to handle the spurious modal responses, which involves a conventional transition combined with a mode suppressor. The concept of the spurious mode suppression is the same as that used in the integrated microstrip-to-NRD-guide (standard) transition that has been presented in the section 2. Please note that, in this case, the NRD-guide is directly deposited on top of a thin substrate, the higher order spurious modes excited in the core NRD strip are not the same as that in the structure without thin dielectric substrate.

For the structure shown in Figure 5.4, based on the previously results and discussions, we can find out, that this structure has a feature inherent to reject the unwanted LSE_{01} and TE_{10} modes. Similarly, the subsequent consideration in the design is reduced to how to suppress the spurious TE_{20}-mode, which is in fact also very simple to implement. Again, the easiest way is to use a section of a cutoff waveguide relative to the TE mode together with match sections, while this suppressor has little or negligible effect on the fundamental LSM_{01} mode in the NRD-guide. The design guideline of the mode suppressor is similar to that used for the microstrip to standard NRD-guide transition, which is described in section 2.

In this design, the proposed mode suppressor is designed to suppress the remaining higher-order spurious modes, especially the TE_{20} and TE_{40} modes in this case. The center straight length is designed to be about a half wavelength of the fundamental LSM_{01} mode

in the surface-mounted NRD-guide. The position of the mode suppressor is then optimized to match with the fundamental LSM_{01} mode.

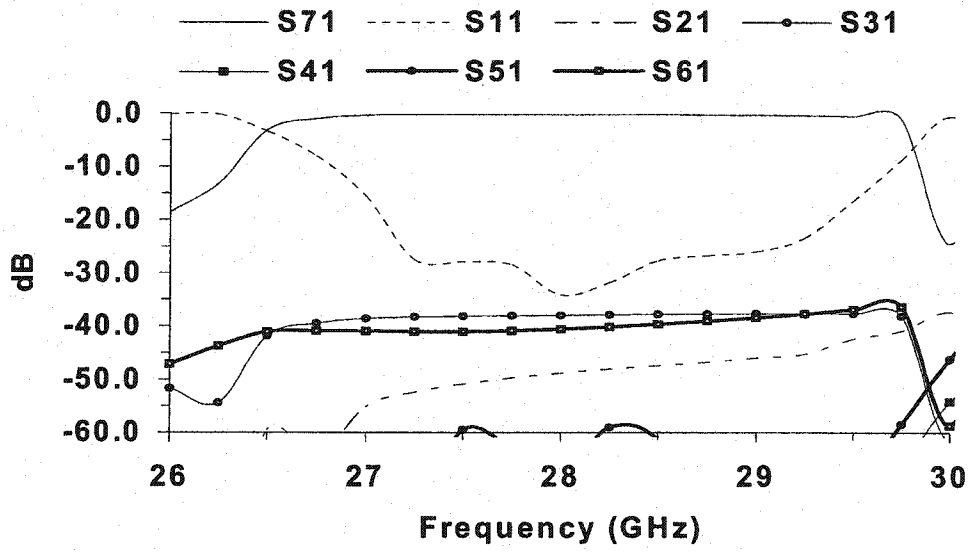

Fig. 6.4 Simulation and extracted transmission and return losses of S-parameters for the proposed transition as described in Figure 6.3 including mode conversion effects

Figure 6.4 plots simulated transmission and return losses for this performance-enhanced transition. We can observe now that the return loss is better than -20 dB over the frequency band of interest from 27.5 to 28.5 GHz. The worst spurious modes excited in this case are TE_{20} and LSE_{40} modes but they are all suppressed to be better than –35 dB over the frequency range. Therefore, the proposed technique should be useful for low-loss hybrid integration of planar and NRD-guide at millimeter-wave frequency band, and in particular for hybrid planar NRD filter design that requires a stringent out-of-the-band rejection.

6.4 Compact design of mode suppressing structures

In this section, a compact spurious mode suppresser for hybrid planar/NRD-guide integrated circuits is presented. The proposed mode suppressing technique with embedded metallic plate/film is used in the hybrid design that is compact and easy to implement. It is found through our investigation that the rejection to all the spurious modes (including TE and LSE modes) is better than –32 dB for a single transition of planar-to-NRD-guide over a broadband frequency of interest, and the performance could be further enhanced. This new technique also provides an alternative solution to the inherent problem of spurious modes (especially TE modes) in the standard design procedure of NRD-guide circuits.

In this study, the microstrip line and the NRD-guide are made of 10 mil Duroid substrate (ε_r = 10.2) and TMM 6 (ε_r = 6), respectively. The width and the height of the NRD-

guide strip are 100 mil and 150 mil, respectively.

Figure 6.5 illustrates our proposed prototype transition with two dissimilar structures to handle the spurious modal responses, which involves a conventional transition combined with a metallic film mode suppresser. This mode suppresser is designed to suppress the remaining higher-order spurious modes, especially in this case, the TE_{20} and TE_{40} modes. The design of such a mode suppresser is very simple, and again no metallic sheet insertion into the NRD-guide core strip is needed in this design. As shown in the figure, the distance between the two metallic films of the mode suppresser is selected to reject the TE_{20} mode, and the length is designed equal to about half wavelength of the fundamental LSM_{01} mode (in the mode suppresser section). The whole structure is then optimised to match with the fundamental LSM_{01} mode. Figure 6.6 plots the transmission and return losses for this new structure.

We can observe now that the return loss is better than -15 dB over the frequency band of interest from 27.5 to 28.5 GHz. The worst spurious modes excited in this case are TE_{10} and LSE_{01} modes but they are all lower than –32 dB over the frequency range of interest. Therefore, the proposed structure should be useful for low-loss hybrid integration of planar and NRD-guide at millimetre-wave frequency that is in particular important for hybrid planar NRD filter design.

For the practical implementation consideration, the metallic thin plate as shown in Figure 6.7 may replace the metallic film. With proper optimization, as shown in Figure 6.8, good performance can be obtained.

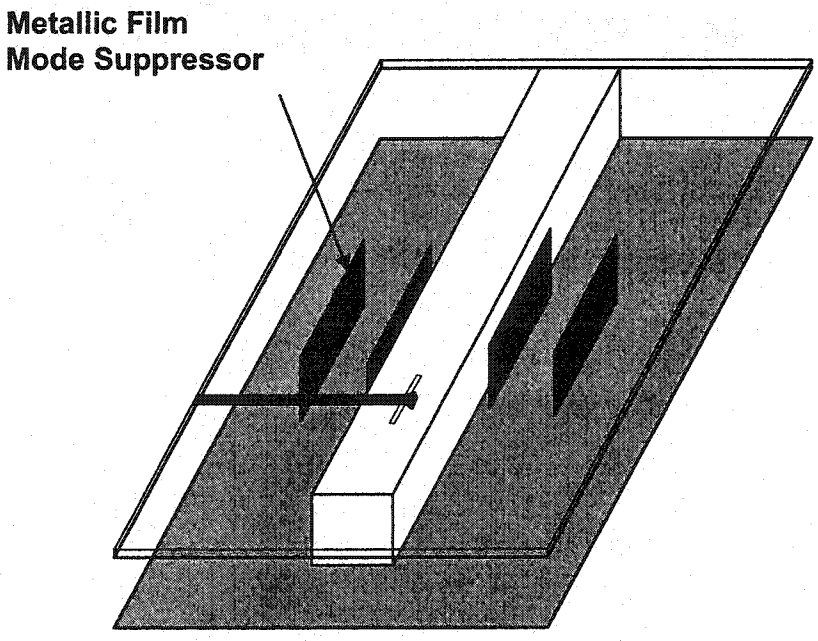

Fig. 6.5 Three-dimensional (3-D) topological view of the proposed microstrip-to-NRD-guide integrated transition involving a metallic film higher-order mode suppressor

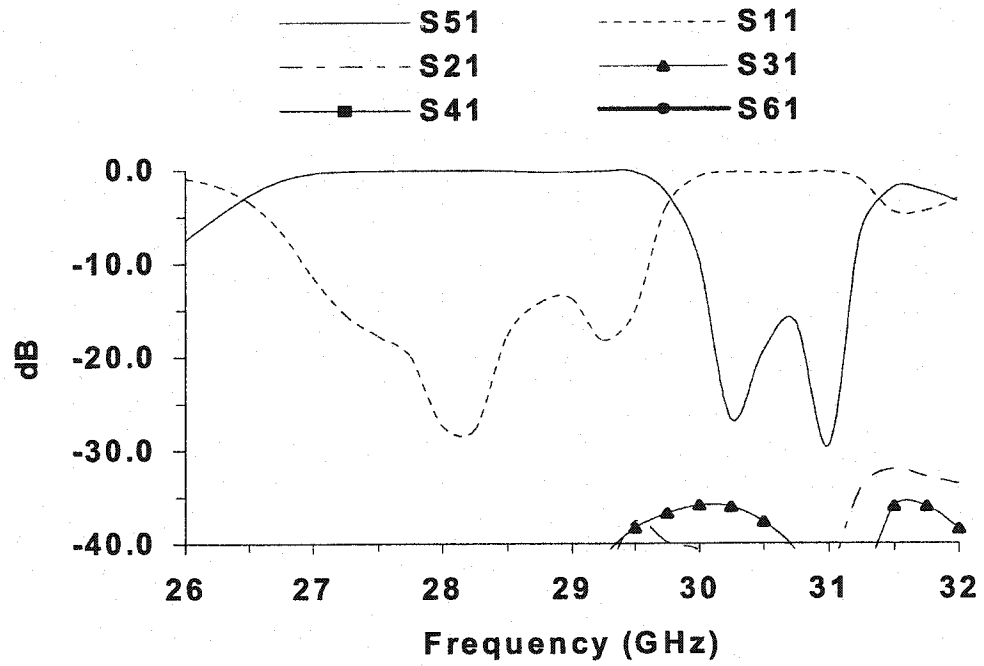

Fig. 6.6 Transmission and return losses of the proposed transition described in Figure 6.5

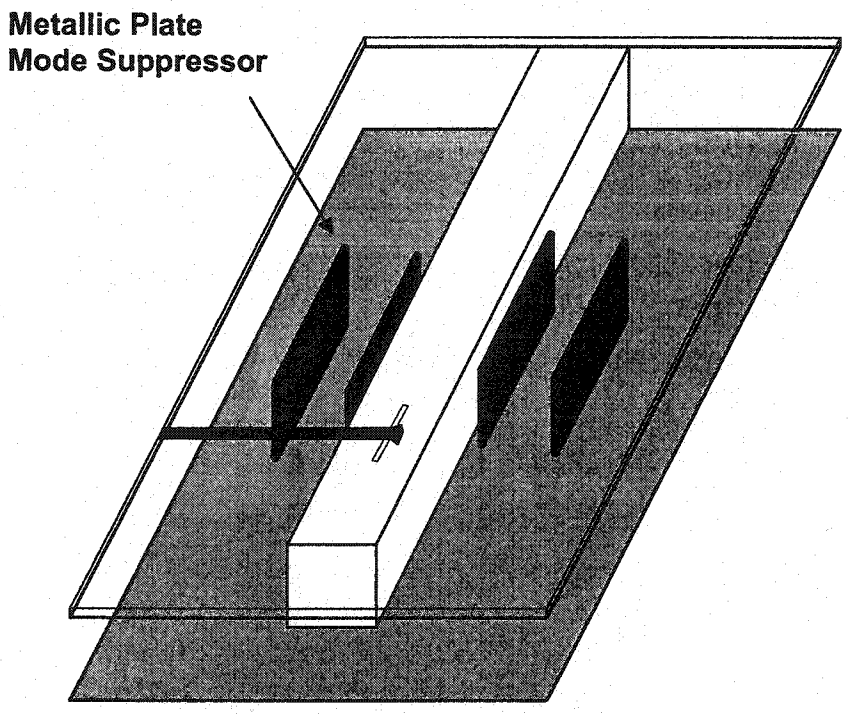

Fig. 6.7 Three-dimensional (3-D) topological view of the proposed microstrip-to-NRD-guide integrated transition involving a metallic plate higher-order mode suppressor

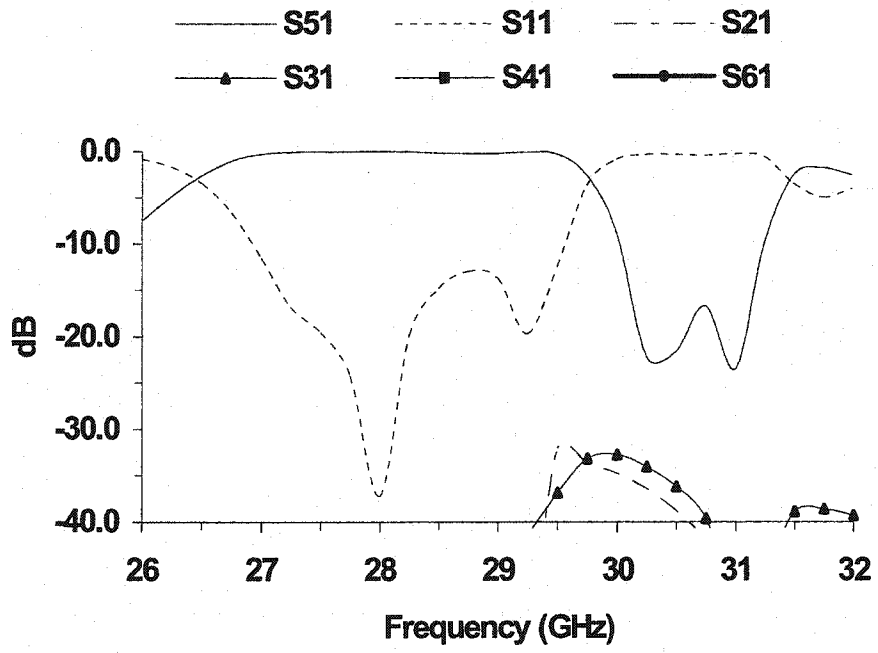

Fig. 6.8 Transmission and return losses of the proposed transition described in Figure 6.7

6.5 Experimental evaluation of the proposed technique

To demonstrate the features and usefulness of the proposed spurious mode suppressing technique, several experimental examples, in connection with the design of millimeter-wave integrated planar/NRD-guide filters, are used to evaluate the new mode suppressor. The first experimental example deals with a microstrip/NRD-guide filter without the use of the proposed suppressor, while the second experimental example investigates effects of the spurious modes on the performance of the filter made in the first experiment. In this way, we hope to gain insight into how the spurious modes affect the electrical performance of such a hybrid filter. Finally, an integrated microstrip/NRD guide filter is presented with the proposed spurious-mode suppressor.

In this work, a five-pole NRD-guide filter (the width and the height of the NRD-guide strip are 168 mil and 180 mil, respectively) is designed for the fundamental LSM_{01} mode with 1 GHz bandwidth. It is used as our example for evaluation of the proposed scheme. The filter is optimized with a method reported in [27], as illustrated in Figure 6.9. Measured insertion and return losses of the filter are presented in Figure 6.10. We can observe that the out-of-band rejection around 29.5 GHz is about –20 dB, which is much worse than -38 dB designated for the NRD-filter. This problem is essentially caused by the spurious modes excited in the structure that severely deteriorate the out-of-band performance. The following experiment will help us to further understand the problem relative to spurious-modes.

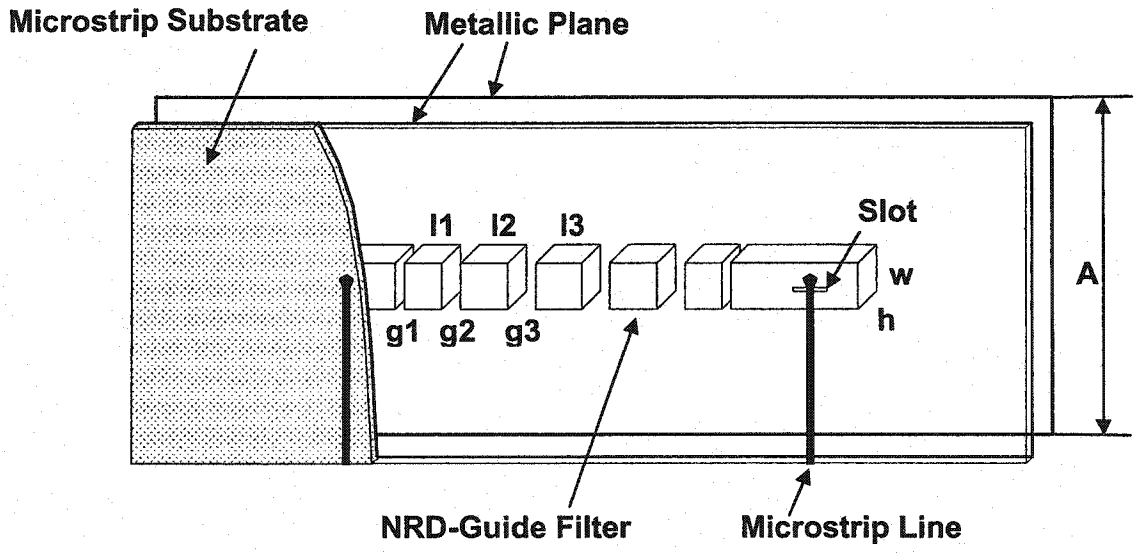

Fig. 6.9 Structural arrangement of the conventional five-pole integrated microstrip/NRD-guide filter without the use of the proposed mode suppressing technique

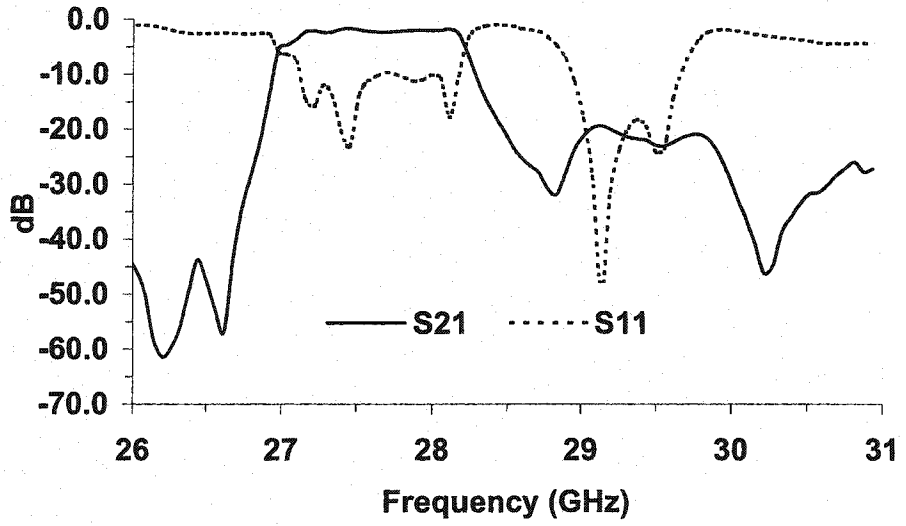

Fig. 6.10 Measured insertion and return losses of the conventional integrated microstrip/NRD-guide filter as described in Figure 6.9

In our second example, the bilateral sides along the cross-section of the NRD-guide filter of Figure 6.9 are electrically shielded with metallic plates (with width A = 950 mil). First, the shielding has little influence on the fundamental LSM_{01} mode propagating along the filter. The measured insertion and return losses are presented in Figure 6.11. We can find that the upside stop-band of the filter becomes even worse as compared to the results displayed in Figure 6.10. This is due to the fact that the shielding plates are sensitive to the spurious modes excited in the structure, and they cause serious cross-sectional reflections because of certain leakages of the spurious modes. Note that the NRD-guide filter itself presents no particular capacity of rejecting the spurious modes. Therefore, the first and second experimental examples clearly indicate that the spurious modes are responsible for the degradation of the out-of-band rejection because they in fact generate leakages. The spurious mode effects create a number of problems including excessive loss, and unwanted backward and/or forward coupling that certainly deteriorates the performance of filter.

Figure 6.12 depicts our planar/NRD-guide filter designed with the proposed spurious mode suppressing technique. In this case, the similar five-pole NRD-guide filter as in the previous experiments is reassembled for the LSM_{01} mode operating at the center frequency 27.9 GHz with 1 GHz bandwidth. Note that the shift of the center frequency in the previous two experiments is due to a scale error with our PCB process. Parameters of the filter are given by g_1 = 47.6 mil, g_2 = 100.8 mil, g_3 = 126.0 mil, l_1 = 224.7 mil, l_2 = 233.4 mil and l_3 = 234.6 mil that are described in Figure 6.12. For the purpose of

evaluation, only one suppressor is used in this experiment. Figure 6.13 plots measured frequency response of the designed filter. We can see that in addition to a reasonably good band-pass performance, the out-of-band relative to the upside frequency range is greatly improved, the worst rejection level is around –35dB. Of course, the bandpass performance should be further improved that is beyond the scope of this paper. The minor difference between the measured out-of-band rejection and the designed level of the NRD-guide filter is mainly due to the unsatisfactory accuracy in our filter fabrication process. In any case, this experiment confirms the usefulness of our proposed technique for effective suppression of spurious modes. In addition, it indicates that it is necessary to take extra-measure to prevent out-of-band rejection from leakage problems in the design of high-quality NRD-guide filters.

6.6 Conclusions

A simple but effective technique for suppressing spurious mode is proposed and presented for millimeter-wave planar/NRD-guide integrated circuits. Design considerations are provided with experimental validations. Our simulated and measured results confirm well the feasibility and interesting features of the proposed technique. This scheme is essential to successful applications of the hybrid planar/NRD-guide circuits. Our results indicate that the rejection to all the spurious modes (including TE and LSE modes) can be better than –35 dB for a single transition over a wide frequency range of interest, and the electrical performance could be greatly improved. This new

technique also provides an alternative solution to the inherent problem of spurious modes (especially TE modes) in the standard NRD-guide circuit design.

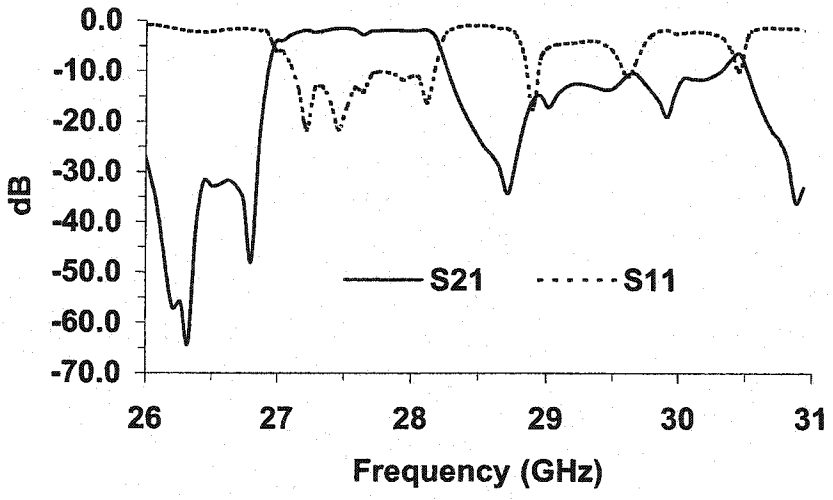

Fig. 6.11 Measured insertion and return losses of the conventional integrated microstrip/NRD-guide filter as shown in Figure 6.9, considering that the bilateral cross-sectional sides are shielded with metallic plates (width A = 950 mils)

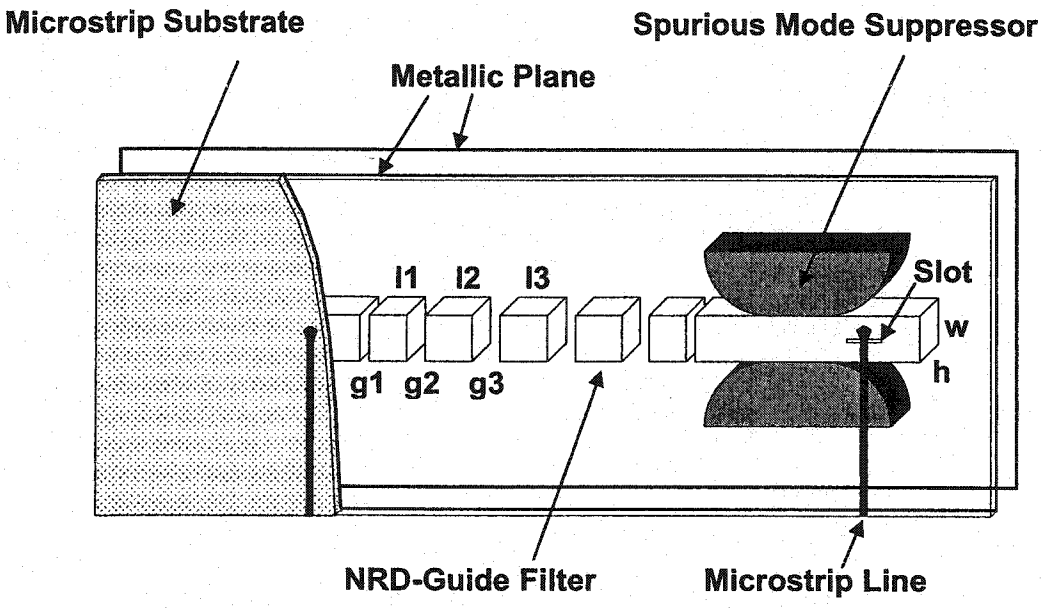

Fig. 6.12 Graphical description of the five-pole integrated microstrip/NRD-guide filter that involves a mode suppressor proposed in this work

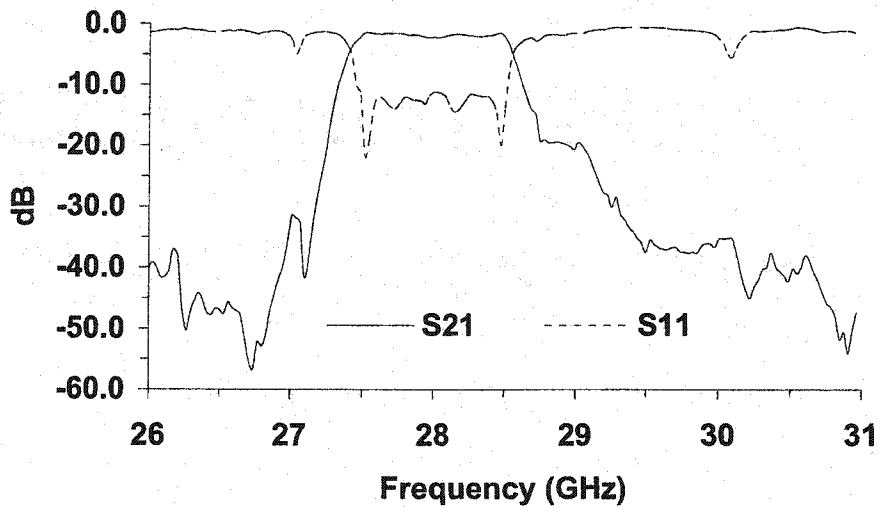

Fig. 6.13 Measured insertion and return losses of the integrated microstrip/NRD-guide filter as shown in Figure 6.12, which confirm the usefulness of the proposed scheme for suppressing spurious modes

CHAPTER VII

DESIGN AND APPLICATIONS OF SURFACE-MOUNTED CPW /NRD-GUIDE INTEGRATED CIRCUITS

7.1 Introduction

We proposed in previous chapters a three-dimensional (3-D) co-layered integration scheme involving surface-mounted nonradiative dielectric (NRD) waveguide and coplanar waveguide (CPW). The proposed planar and non-planar integration technique allows for the low-cost design of millimeter-wave circuits, systems and high-performance is expected. As an application example, in this chapter, an innovative CPW-fed surface-mounted NRD-guide antenna that includes hybrid CPW/NRD-guide transition has been presented. Analysis results demonstrate that low transmission loss and good return loss can be achieved with the proposed concept.

In the second part of this chapter, a spurious mode suppressing technique for the performance enhancement in the design of a broadband CPW-to-NRD-guide transition is presented. This work also reveals some interesting and unique electrical and mechanical features of the proposed building blocks in 3-D design.

7.2 CPW fed antenna scheme and the preliminary analysis results

The example scheme is simply a surface mounted NRD-guide antenna fed by a CPW line as shown in Figure 7.1. The CPW and the surface mounted NRD-guide are made of 10 mil Duroid substrate (ε_r=2.33) and Polystyrene dielectric block (ε_r=2.56), respectively. The dimensions of NRD-guide are designed with $a \times b \times c = 830 \times 230 \times 160$ (unit = mil). Its simulated results are given in Figure 7.2 together with its far field plots in Figure 7.3 and Figure 7.4. It is found that the directivity of the new radiating structure is 8.63 dB at around 26.7GHz, and its gain is 8.59 dB.

The above results have shown the attractive properties of this new scheme, which allows for innovative design of millimeter-wave building blocks. The results have also demonstrated the usefulness of the proposed concept. It is expected that this work will add new features and new horizons in the hybrid integration technology of planar circuits/NRD-guide for the design of 3D multilayered ICs and millimeter-wave MMICs.

7.3 Spurious mode suppressing technique for the integrated CPW to NRD-guide transition

In this section, we present a spurious mode suppressing technique for the performance enhancement in the design of a broadband CPW-to-NRD-guide transition. To begin with, the spurious modes behaviors of a conventional CPW-to-NRD-guide integrated transition

are investigated using a method similar to that described in previous chapters, which has been designed to suppress all of the inherent higher order spurious modes. The investigation results indicate that both the hybrid CPW-to-NRD transition and the mode suppresser can reduce all the spurious modes to a level required for practical applications.

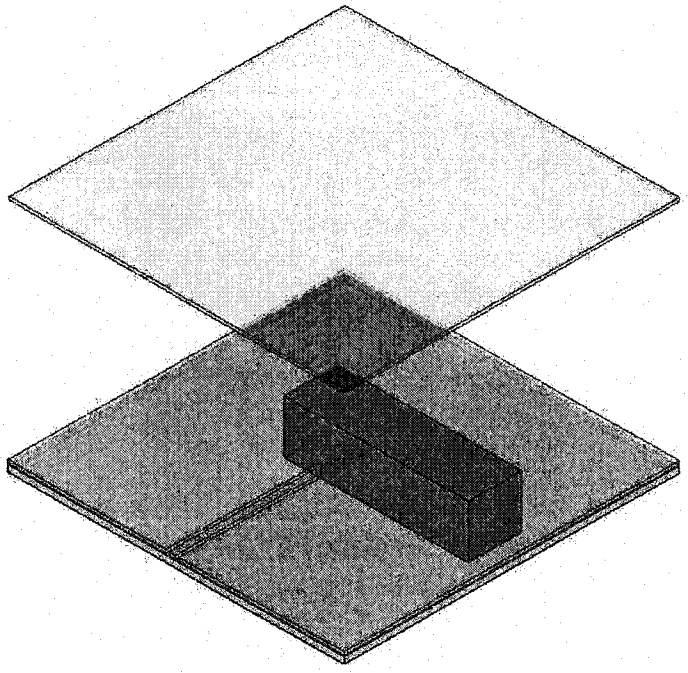

Fig. 7.1 Novel integration scheme of the surface mounted NRD-guide antenna with CPW as feed line

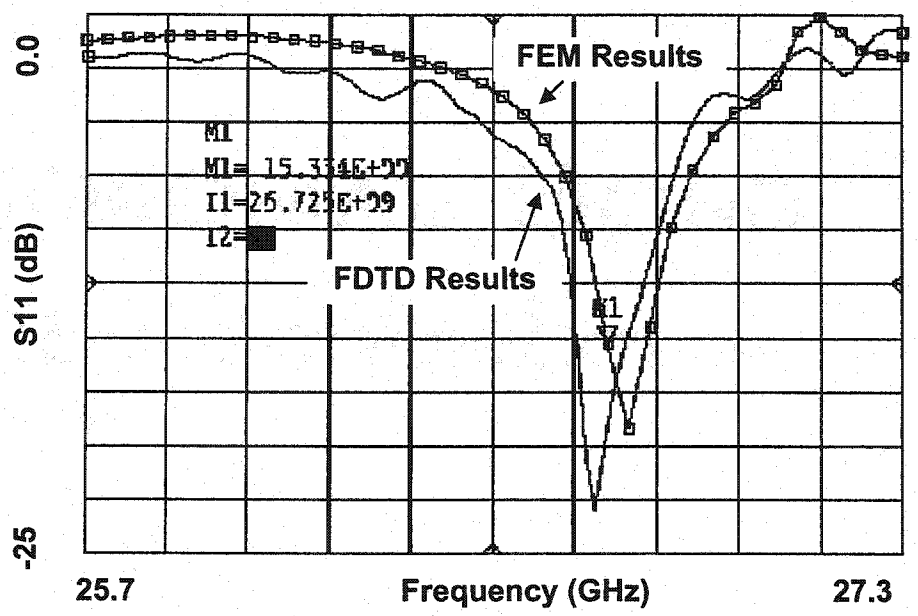

Fig. 7.2 Simulation input return losses of CPW-fed surface-mounted NRD-guide antenna

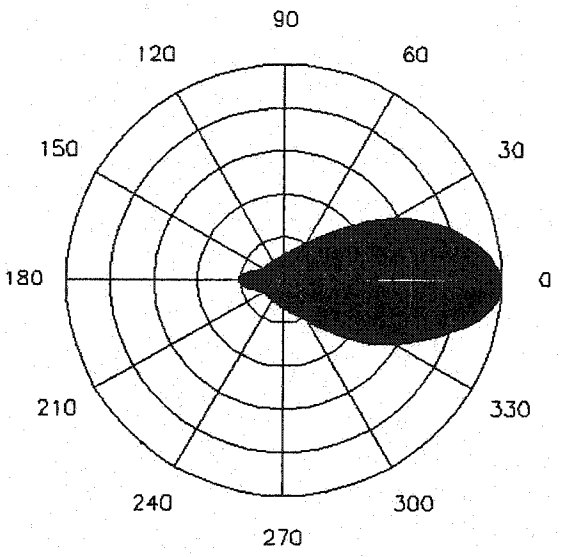

Fig. 7.3 Far field plots of proposed novel CPW-fed surface-mounted NRD-guide antenna: top view (E-plane)

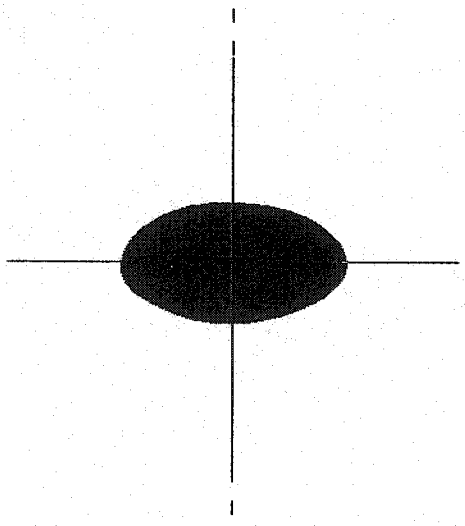

Fig. 7.4 Far field plots of proposed novel CPW-fed surface-mounted NRD-guide antenna: side view (H-plane)

Figure 7.5 shows the integration scheme of CPW-to-NRD-guide. In this study, the CPW and the surface-mounted NRD-guide are made of 10 mil Duroid substrate ($\varepsilon_r = 2.94$) and TMM6 dielectric block ($\varepsilon_r = 6$), respectively. Similarly, the core dielectric strip of the NRD-guide is orthogonal in space with respect to the CPW line in order to excite the wanted LSM_{01} mode. The width and the height of the NRD-guide strip are 100mil and 168 mils, respectively, which are selected on the basis of a technique reported in [28].

The integration between the CPW and the NRD-guide involves two dissimilar structures. In this case, the quasi-TEM mode in the CPW may excite TE_{10}, LSE_{01}, TE_{20}, LSM_{01}, TE_{30}, TE_{40}, and LSM_{02} modes among others in the NRD-guide. We can use an equivalent one-port to multi-port network as sketched in Figure 7.6 to represent the CPW-to-NRD-guide transition as described in Figure 7.5. Principal modes generated in this hybrid CPW-to-NRD-guide structure can be modeled and extracted.

The transition shown in Figure 7.5 may be good enough for certain applications. Nevertheless, the spurious modes appear to quickly emerge and become significant especially in the out-of-the band. These spurious modes are responsible for making the filter upper stop-band performance deteriorated. In the following, parameters S_{21}, S_{31}, S_{41}, S_{51}, S_{61}, and S_{71} represent the conversion losses from the input TEM mode to TE_{10}, LSE_{01}, TE_{20}, LSM_{01}, TE_{30} and TE_{40} modes, respectively.

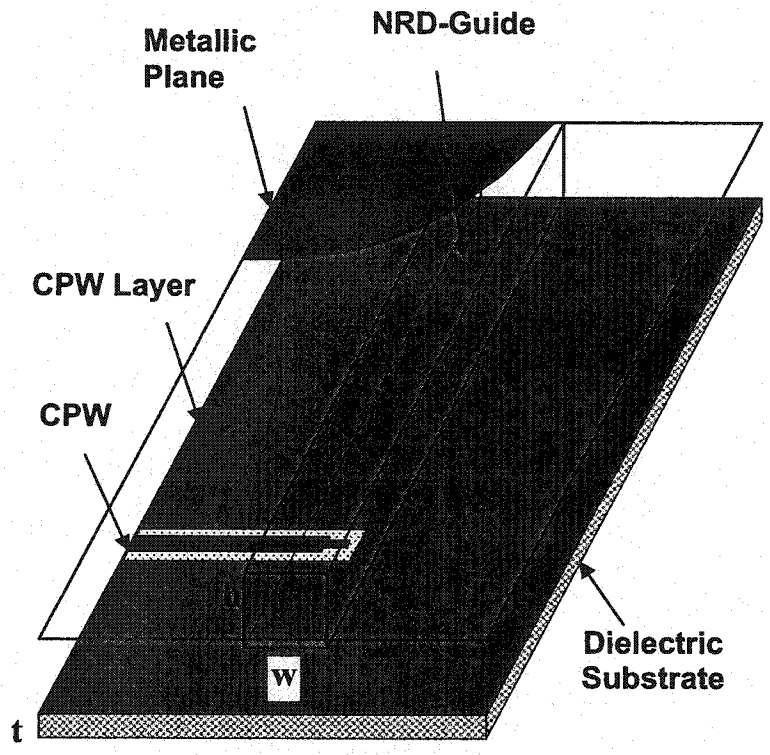

Fig. 7.5 Three-dimension (3-D) topological view of integrated CPW-to-NRD-guide transition

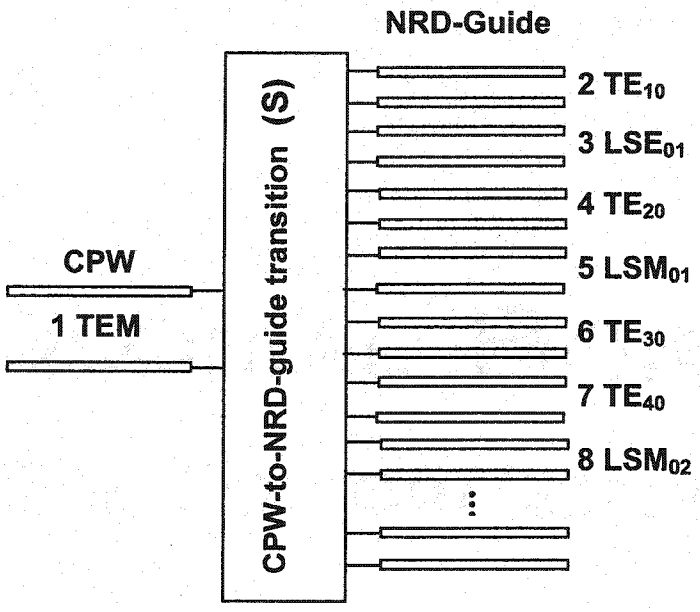

Fig. 7.6 Equivalent network for the CPW-to-NRD-guide transition, which takes into account the quasi TEM mode in the CPW to a multi-modes coupling in the NRD-guide

The complete modal conversion in this hybrid structure is modeled with a commercial package (HFSS). Modal transmission and return losses are plotted in Figure 7.7. Note that both TE_{10} and LSE_{01} modes become an important part of the spurious modes.

The spurious mode suppressing structure used in previous section is not able to suppress the TE_{10} mode, and a new structure has to be considered. Figure 7.8 illustrates our proposed transition with two dissimilar structures to handle the spurious modal response, which involves a conventional transition combined with a mode suppressor. This mode suppressor is designed to suppress all the higher-order spurious modes, especially in this particular case, the TE_{10}, TE_{20} and TE_{40} modes. As shown in the figure, the center width of the mode suppressor is selected to reject the TE_{10} mode, and the center straight length is designed to be equal to about a half wavelength of the fundamental LSM_{01} mode. The NRD-guide within the suppressor should be modified as shown in the figure. The whole mode suppressor is then optimized so to match with the fundamental LSM_{01} mode. Figure 7.9 plots the transmission and return losses for this new structure. We can observe now that the return loss is better than -15 dB over the frequency band of interest from 27 to 30 GHz. The worst spurious modes excited in this case are all lower than –50 dB over the frequency range of interest. Therefore, the proposed structure should be useful for low-loss hybrid integration of CPW and NRD-guide at millimeter-wave frequency that is in particular important for integrated CPW/NRD filter design.

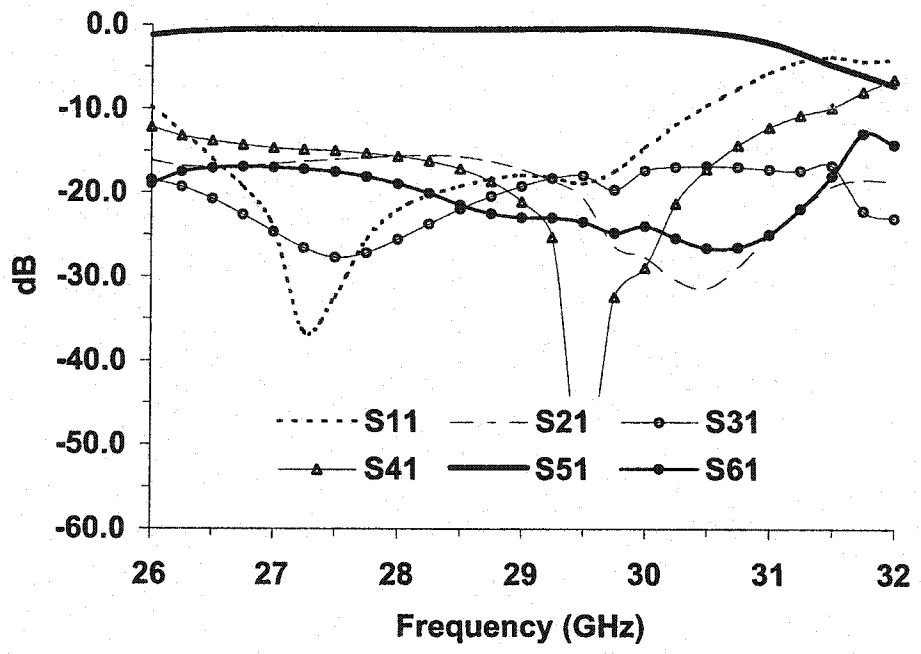

Fig. 7.7 Transmission and return losses of an optimized transition as shown in Figure 7.5

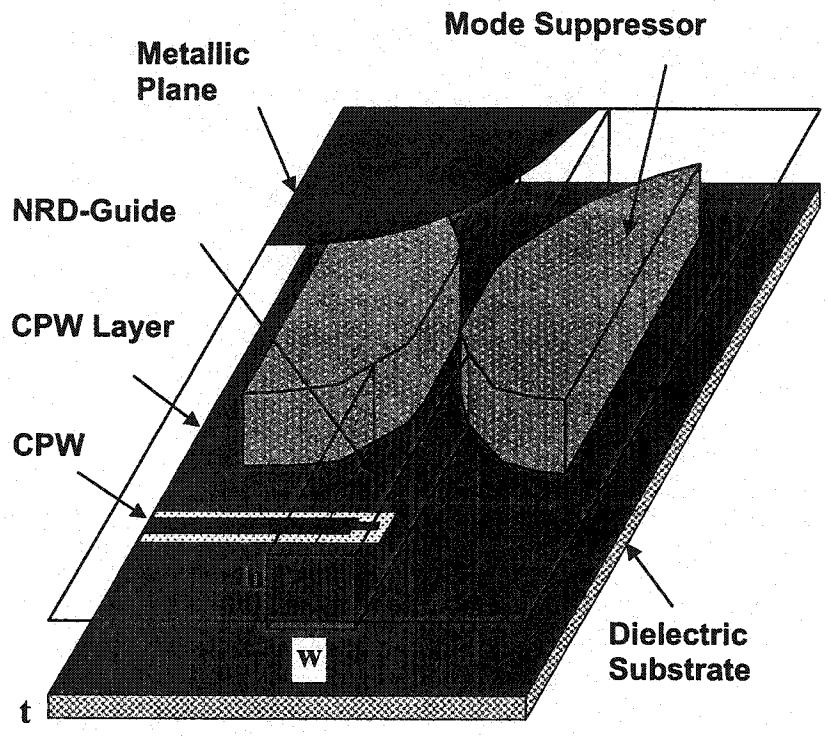

Fig. 7.8 Three-dimensional (3-D) topological view of the proposed CPW-to-NRD-guide integrated transition that involves a performance-enhanced mode suppressor

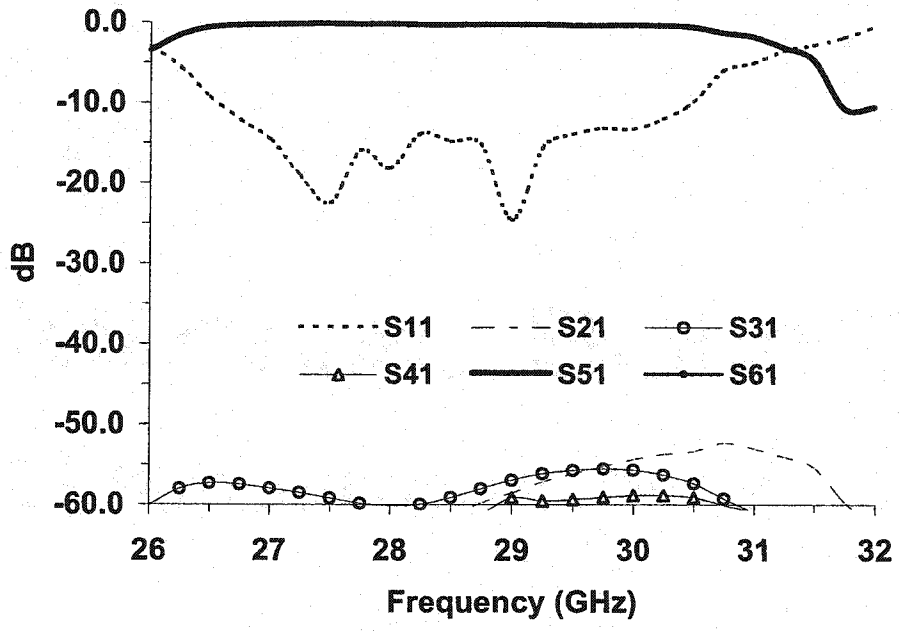

Fig. 7.9 Simulation transmission and return losses of our proposed transition as described in Figure 7.8

7.4 Conclusion

An innovative CPW-fed surface-mounted NRD-guide antenna that includes hybrid CPW/NRD-guide transition has been presented. Analysis results demonstrate that low transmission loss and good return loss can be achieved with the proposed concept.

For the performance enhancement in the design of a broadband CPW-to-NRD-guide transition, a spurious mode suppressing technique is presented. Based on the investigation results, it is found that the rejection to all the spurious modes (including TE and LSE modes) are very effective over a broadband frequency of interest, and the performance could be further enhanced. This work once again reveals usefulness of our proposed spurious mode-suppressing technique.

CHAPTER VIII

BROADBAND PLANAR INTERCONNECT TECHNIQUES FOR CO-LAYER MULTI-CHIP MODULE (MCM) OF MICROWAVE AND MILLIMETER-WAVE CIRCUITS

8.1 Introduction

Worldwide effort in research and development of advanced high-speed electronics and broadband radio-frequency systems in commercial sectors is to search for new concepts and innovative techniques in driving down design and production costs while preserving or enhancing stringently demanded electrical and mechanical performance. Multi-chip modules (MCM) are commonly used today and they are considered as one of the most enabling technologies available in the design of microwave and millimeter-wave circuit building blocks. Due to tolerances or inconsistency in chip sizes and other factors such as thermal expansion, gap may remain between two substrates to be connected. Therefore, reliable and broadband transmission line-type interconnects of chip-to-chip are of great importance in the design of monolithic and/or hybrid circuits based MCM [29-31]. As it is known, such interconnects for hybrid circuits at millimeter wave frequencies may behave like discontinuities that are difficult to design. Since most of the present MMICs or hybrid circuits are based on microstrip, low-cost ribbon bonding technique has been widely used for interconnects and/or packaging. Nevertheless, because of potential

parasitic effects of the bonding ribbon, unwanted resonance may take place that usually deteriorates the chip-to-chip coupling efficiency at higher frequency range [31]. Special bonding schemes such as the use of turning stub with line width compensation [29], and the use of a bonding ribbon together with a dielectric pad were reported [32].

In this Chapter, we present a very effective but rather simple scheme of ribbon interconnects for applications in the broadband design of co-layer multi-chip module (MCM) of planar circuits at microwave and millimeter-wave frequencies. The interconnect does not require the modification of the shape of microstrip lines.. This new concept is stemmed from the principle of sectional impedance matching. A field-based analysis and experimental verification have validated the proposed technique. Our work shows that excellent low-loss broadband performance could be achieved up to 35 GHz and beyond by using this simple and low-cost technique.

8.2 Overview of the conventional ribbon bonding techniques

Figure 8.1 (a) shows a typical geometry of the conventional ribbon interconnects technique; microstrip lines on two different substrates are bridged over a gap of 1.6 mm in this example. Simulated S-parameters with a numerical simulator are shown in Figure 8.1 (b), which are in good agreement with the results given in [32] from 0 to 8 GHz (not shown in the figure). As expected, residual parasitic effects of the ribbon rapidly deteriorate performance of the ribbon as frequency increases.

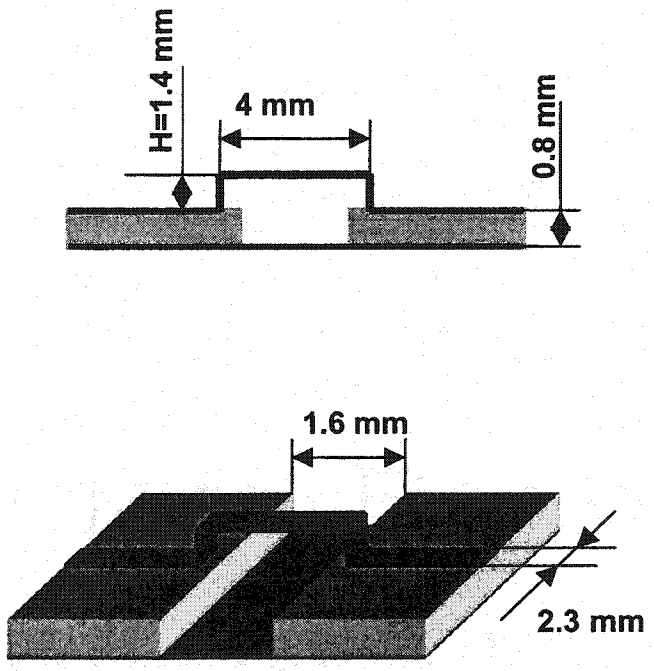

Fig. 8.1 (a) Geometry of the conventional ribbon interconnect with H =1.4 mm

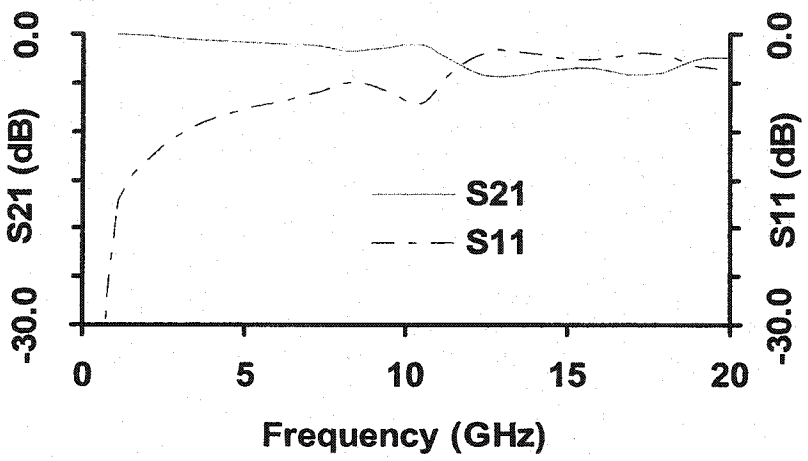

Fig. 8.1 (b) Simulation insertion and return losses of conventional ribbon interconnect with H =1.4 mm

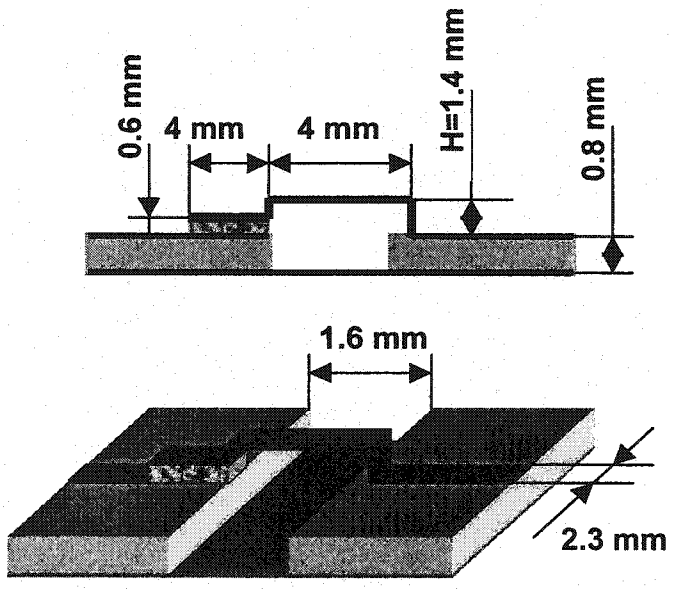

Fig. 8.2 (a) Geometrical view of resonant type of ribbon interconnects

Figure 8.2 (a) shows the resonant coupling type interconnects scheme proposed by M. Hotta et al., consisting of a single ribbon and a companion rectangular dielectric pad. The ribbon and dielectric pad constitute a series LC resonator so that a high efficient connection is achieved at resonance. As a result, both simulation and experiments reveal very low return loss and excellent connection over the predicted resonant frequency region [32]. Figure 8.2 (b) shows our simulated results of this kind of interconnect. It is however observed that this kind of resonant coupling-type interconnects are not suited to broadband application.

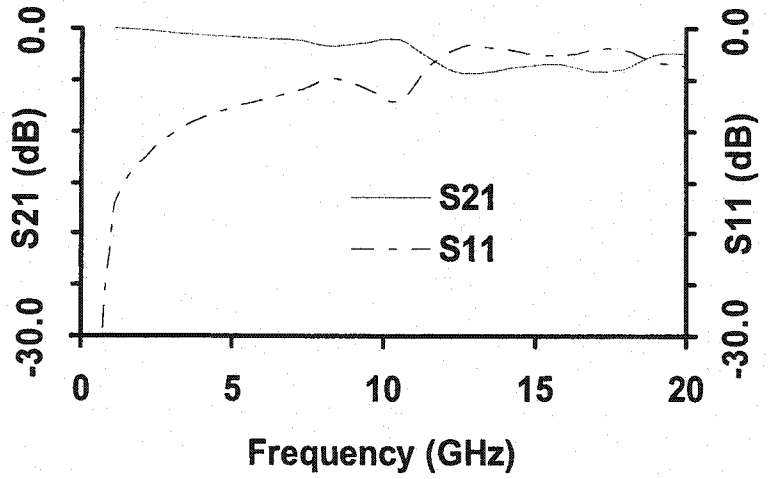

Fig. 8.2 (b) Simulation insertion and return losses of resonant type of ribbon interconnects

8.3 The proposed scheme of effective ribbon interconnects

Our following investigations show how overall performance of co-layer chip-to-chip interconnects can greatly be improved by a simple modification of the ribbon bonding. The proposed scheme of the ribbon bonding is sketched in Figure 8.3 (a). Instead of using the conventional upward bonding shape, this ribbon is bent downward towards the ground plane.

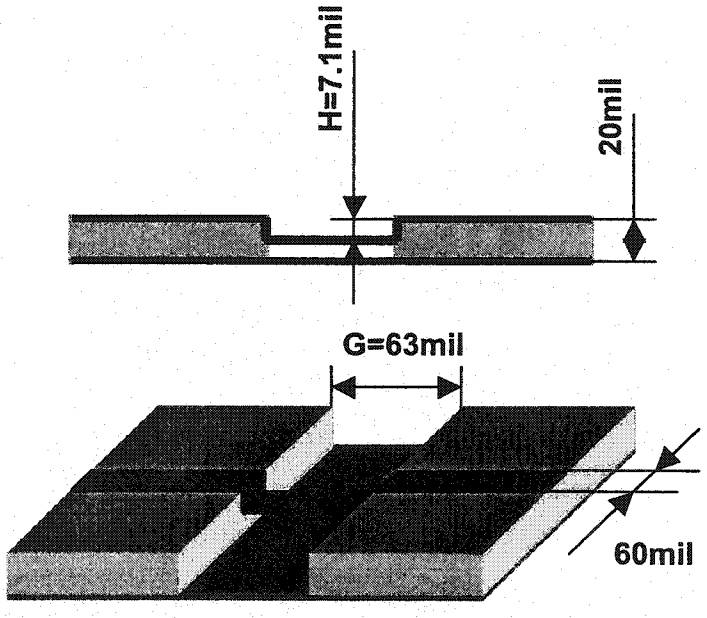

Fig. 8.3 (a) Geometrical view of proposed interconnects scheme

8.3.1 Circuit model and numerical results

The effectiveness of this new scheme can easily be explained with the help of its basic circuit model as shown in Figure 8.3 (b). To compensate low-pass performance of this kind of interconnects; it is necessary to reduce the parasitic effects to a minimum or negligible level. In our intuitive sense, the new scheme has a flexible compensation and it is very easy to implement. The dimension and shape of the ribbon interconnects can be adjusted to achieve a low-loss transmission that relies on the gap size as well as substrate material and thickness.

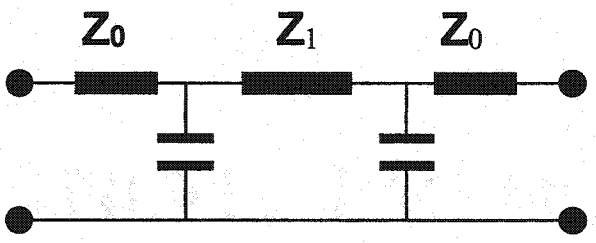

Fig. 8.3 (b) Equivalent network of the proposed interconnects scheme

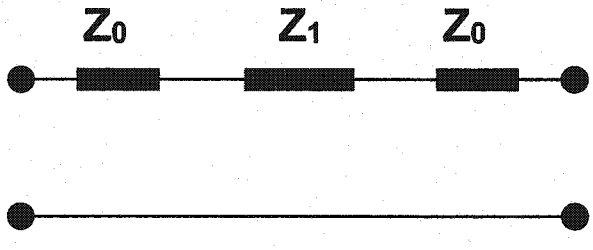

Fig. 8.3 (c) Simplified circuit model of the proposed interconnects

This simple scheme can be modeled by a simplified circuit model as described in Figure 8.3 (c) to determine the dimension of the proposed ribbon interconnects, the required impedance and relevant dimension of the ribbon interconnects can be calculated by an impedance matching concept. To verify our assumption, Figure 8.3 (d) also shows simulated results via a numerical simulator. We observe that an excellent compensation has indeed been achieved with this very simple technique. To compare the effect of the ribbon shape, the ribbon interconnects shown in Figure 8.4 (a) and 8.5 (a) are also modeled, and the results are shown in Figure 8.4 (b) and 8.5 (b), respectively. Our results indicate that the proposed scheme can achieve the low-loss broadband interconnects without compromise.

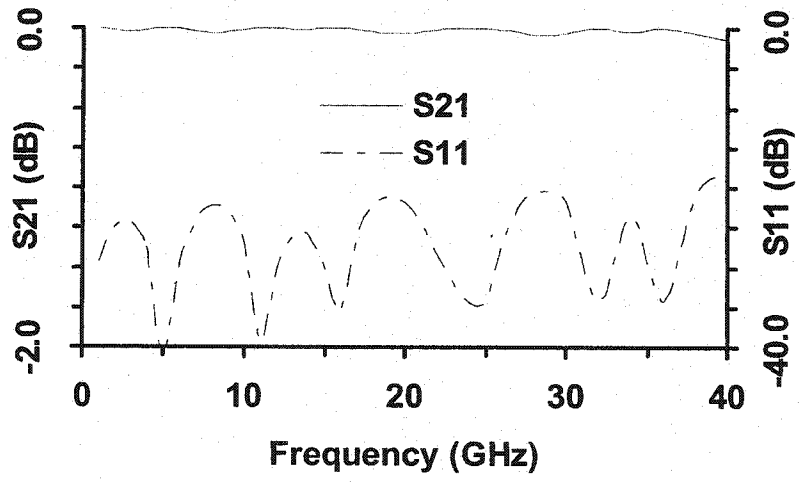

Fig. 8.3 (d) Simulation insertion and return losses of the proposed interconnects

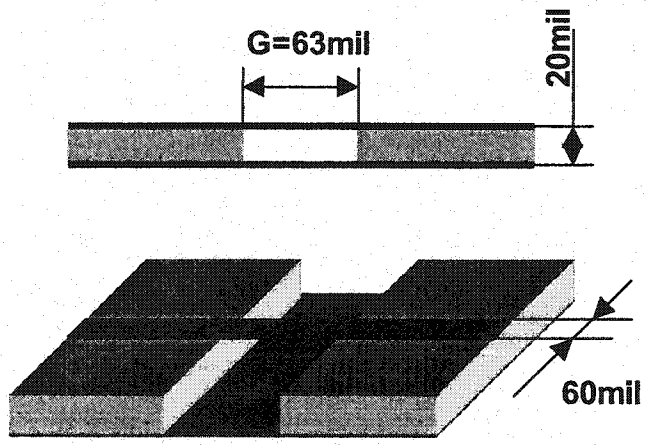

Fig. 8.4 (a) Geometrical view of chip-to chip aligned ribbon interconnects

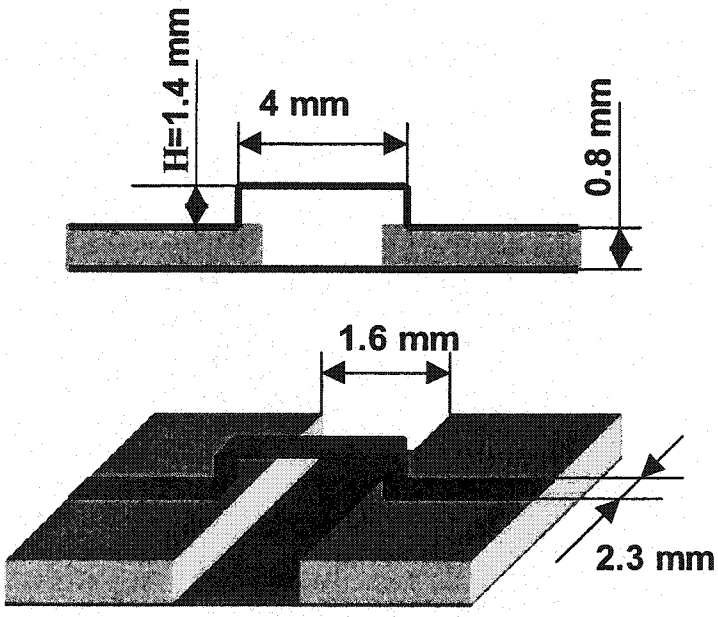

Fig. 8.4 (b) Geometrical view of conventional ribbon interconnects

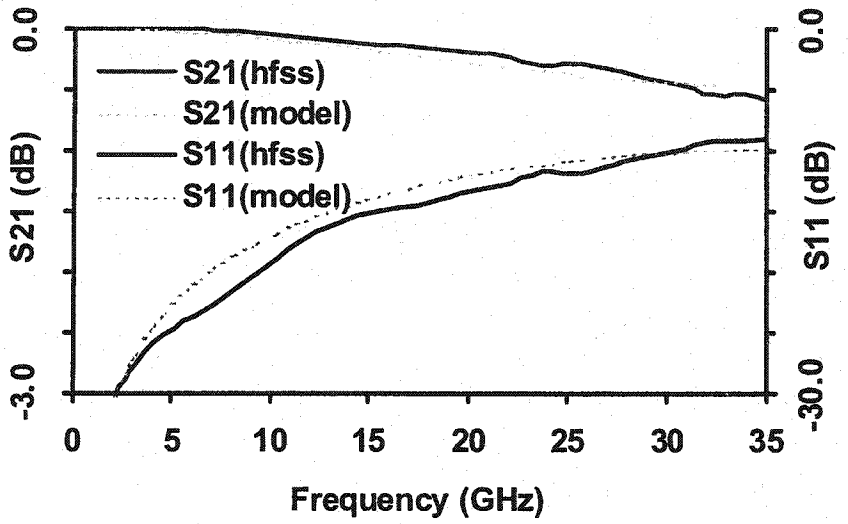

Fig. 8.5 (a) Simulation insertion and return losses of chip-to-chip aligned ribbon interconnects

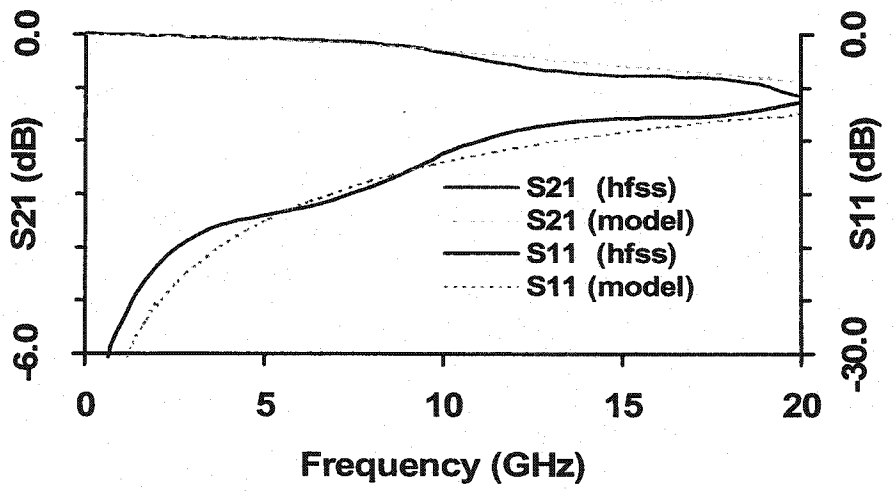

Fig. 8.5 (b) Simulation insertion and return losses of conventional ribbon interconnect with H =10 mil

8.3.2 Measurement results

In our experiments, the microstrip lines are fabricated on 20 mil Duroid substrate (ε_r = 2.33) with h = 20 mil. The geometry in Figure 8.3 (a) is fabricated and measured with a HP8510C vector network analyzer (VNA). A thru-reflect-line (TRL) calibration technique is applied in the measurements, and the standards are fabricated on the same substrate used for the microstrip lines.

Measured results covering the calibration-kit allowable broadband frequency range from 0.9 GHz to 35 GHz are presented in Figure 8.6. It is found that an excellent insertion loss can easily be obtained with S21 better than 0.3 dB within 16 GHz, better than 0.65 dB up to 28 GHz, and better than 1 dB within 35 GHz. While the return loss S11 is below -15 dB except a small rise around 32 GHz. Note that the ribbon bonds are handled by hands in a very rough manner. It is expected that a further improvement on performance can be achieved by utilizing this technique over the millimeter-wave range.

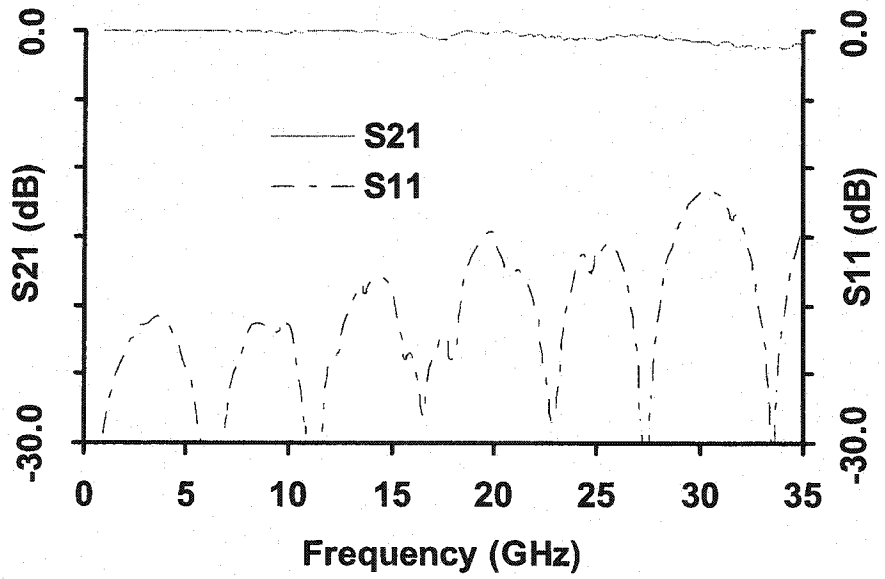

Fig. 8.6 Measured insertion and return losses of proposed interconnect with H = 7.1 mil

CHAPTER IX

CONCLUSIONS AND SUGGESTIONS FOR FUTURE WORK

9.1 Conclusions

This thesis has presented new concept and technology of hybrid integration and interconnects for the applications in microwave and millimeter wave integrated circuits, which are based on a class of new low loss surface mounted NRD-guide structures. The associated circuit building blocks are based on the novel co-layered arrangement of dissimilar structures, which allows the NRD-guide in direct contact with (or surface mounted on) the planar circuits, such as microstrip line and coplanar waveguide (CPW) planar circuits. Several co-layered integration and interconnects structures and spurious suppressing techniques have been proposed, analyzed and verified both theoretically and experimentally. Following is a summary of the work addressed in this thesis.

Chapter I is the introduction of the thesis. Chapter II is a general presentation of .a class of surface mounted dielectric guides; the proof of concept has been provided with analysis results. In chapter III, guided-wave characteristics of the new hybrid or composite structure, which is surface-mounted on a relatively thin dielectric substrate, are studied numerically and experimentally. Detailed results provide a basic guideline for the design of low-loss hybrid planar/NRD-guide millimeter-wave circuits using the proposed

composite building block. It is demonstrated that the proposed transmission line can preserve low-loss and almost non-radiating advantages of the conventional NRD-guide. The experiments further verify the low-loss characteristics of the structure. In chapter IV, the new concept of hybrid integration between planar circuits and non-radiative dielectric (NRD) waveguide is presented. Two basic building block schemes are presented that involve microstrip line and coplanar waveguide (CPW) with the NRD-guide. This approach utilizes co-layered arrangement of the two dissimilar structures, which allows the NRD-guide in direct contact with (or surface-mounted on) the planar circuits. Preliminary experimental verification results have been provided. In chapter V, principal modes generated in the hybrid planar/NRD-guide structure are modeled. Results for transmission and return loss are presented for different transitions. The investigation indicates that an optimized but uncompensated hybrid planar/NRD-guide integrated transition should be good enough for many applications over a certain frequency band. For broadband applications, however, spurious mode suppressors in the design of eliminating unwanted modes are required. In chapter VI, a new spurious mode suppressing technique is first presented, concerned with an integrated microstrip-to-NRD-guide transition and a mode suppressor. The design guideline and procedures are then addressed. With some simple modifications, this spurious mode-suppressing concept can be extended and applied to a class of integrated planar to surface-mounted NRD-guide transitions. General spurious mode-suppressing techniques for the integrated microstrip-to-surface-mounted NRD-guide transition (NRD-guide surface-mounted on the top of a relatively thin planar substrate) have also been investigated. A compact

spurious mode suppresser for hybrid planar/NRD-guide integrated circuits is also presented in this chapter. The proposed mode suppressing technique with embedded metallic plate/film is used in the hybrid design that is compact and easy to implement. It is found through our investigation that the rejection to all the spurious modes (including TE and LSE modes) is better than –32 dB for a single transition of planar-to-NRD-guide over a broadband frequency of interest, and the performance could be further enhanced. This compact design technique also provides an alternative solution to the inherent problem of spurious mode (especially TE modes) in the standard NRD-guide circuit design. Practical examples in the design of millimeter-wave planar/NRD-guide filter are exploited to evaluate features of the proposed technique that yields expected good results. It is found through analysis and experiments that the rejection to all the spurious modes (including TE and LSE modes) can be better than –35 dB for a single microstrip-to-NRD-guide transition over a broadband frequency of interest.

In chapter VII, an innovative CPW-fed surface-mounted NRD-guide antenna that includes hybrid CPW/NRD-guide transition has been presented. Analysis results demonstrate that low transmission loss and good return loss can be achieved with the proposed concept. In the second part of this chapter, a spurious mode suppressing technique for the performance enhancement in the design of a broadband CPW-to-NRD-guide transition is presented. This work also reveals some interesting and unique electrical and mechanical features of the proposed building blocks in 3-D design.

From the theoretical analysis, the simulations and the experiment results, this work provides engineers with new methods in the design and development of microwave and millimeter wave integrated circuits.

In Chapter VIII, broadband planar interconnect for co-layer multi-chip module (MCM) has been presented. It is a very effective but rather simple technique for applications at microwave and millimeter-wave frequencies. Excellent performance has been theoretically and experimentally demonstrated.

9.2 Suggestions for future work

The new integration and interconnects techniques have been presented, and the associated advanced features in the applications in microwave and millimeter wave integrated circuits have been demonstrated in this work. The future work associated with this thesis should include the following aspects:

The proposed integration and interconnect concept makes possible the effective integration, however, only available dielectric substrates and materials were used in the evaluation of the new concept and integration and interconnect techniques proposed in the work, and the prototype modules for the evaluation purposes were fabricated manually. It is highly recommended that further work should be associated with the available advanced processing technologies and packaging materials such as LTCC (Low

Temperature Co-fired Ceramic), HTCC (High Temperature Co-fired Ceramic), MEMS (Micro-Electro-Mechanical systems), and plastic injection. Future work should also be focused on how the circuits are designed and manufactured, thereby, greatly expanding the design and application space.

In the design of planar circuits to co-layered NRD guide transitions, more convenient methods should be further studied for the fast design and practical development.

In the design and implementation of spurious mode suppressors, new configurations should be further studied to adapt to the advanced processing technology.

This thesis has addressed the issues in separate application cases. One obvious extension is to use these basic circuits for the applications in developing more complicated functional blocks such as electro-optical transceivers. For example, the integrated millimeter wave duplexers in the transceivers can be realized using the proposed techniques.

REFERENCES

[1] WU K., (1998), Hybrid three-dimensional planar/non-planar circuits for microwave and millimeter-wave applications: the state-of the art and challenge, FACTA Universitatis, Series: Elect. And Energ., Vol. 11, No.1, pp. 87-101.

[2] FATHY A., PENDRICK V., AYERS G., GELLER B., NARAYAN Y., THALER B., CHEN H. D., M. LIBRATORE J., PROKOP J., CHOI K. L., and SWAMINATHAN M. (1998), Design of embedded passive components in low-temperature cofired ceramic on metal (LTCC-M) technology, IEEE MTT-S International Microwave Symposium Digest, Baltimore, vol. 3, pp. 1281-1284.

[3] GRABHERR W., HUDER B., and MENZEL W., (1995), Microstrip to waveguide transition compatible with mm-wave integrated circuits, IEEE Trans. Microwave Theory Tech., vol. 42, pp. 1842-1843.

[4] VILLEGAS F. J., STONES D. I., and HUNG H. A., (1997), A novel microwave-to microstrip transition for low-cost millimeter-wave and MMIC applications, IEEE MTT-S International Microwave Symposium Digest, Denver, vol. 1, pp. 739-742.

[5] WU K. and MAURIN D., (1997), Alternated multilayered CPW/slotline/microstrip hybrid techniques for compact RF and microwave circuits, (invited paper) PIERS, Hong Kong, pp. 444.

[6] YONEYAMA T., and NISHIDA S., (1981), Nonradiative dielectric waveguide for millimeter wave integrated circuits, IEEE Trans. Microwave Theory Tec., vol. 29, pp.1188-1192.

[7] YONEYAMA T., (1984), Nonradiative dielectric waveguide, Infrared and Millimeter Waves, Vol. 11, K. J. Button, Ed. New York: Academic, Ch. 2, pp. 61-98.

[8] YONEYAMA T., FUJITA S., and NISHIDA S. (1983), Insulated nonradiative Dielectric waveguide for millimeter-wave integrated circuits, IEEE Trans. Microwave Theory Tec., vol. 31, pp. 1002-1008.

[9] YONEYAMA T., (1992), Recent development in NRD-guide technology, Ann. Telecommun., vol. 47, nos. 11-12, pp. 508-514.

[10] YONEYAMA T., (1989), Millimeter-wave transmitter and receiver using the nonradiative dielectric waveguide, IEEE MTT-S International Microwave Symposium Digest, Long Beach, CA, pp. 1083-1086.

[11] HUANG J., WU K. WU, KUROKI, F., and YONEYAMA T., (1996), Computer-aided design and optimization of NRD-guide mode suppressors, IEEE Trans. Microwave Theory Tec., vol. 44, pp.905-910.

[12] WU K., and HAN L. (1997), Hybrid integration technology of planar circuits and NRD-guide for cost effective microwave and millimeter-wave applications, IEEE Trans. Microwave Theory Tec., vol. 45, pp. 946-954.

[13] XU S. J., ZENG X. Y., WU K., and LUK K. M., (1998), Leaky-wave characteristics of trapezoidally shaped NRD-guide suitable for design of millimeter-wave antenna, IEEE MTT-S International Microwave Symposium Digest, Baltimore, vol. 2, pp. 659-662.

[14] TANG J., ZENG X. Y., XU S. J., and WU K., (2000), Low-loss millimeter-wave propagation characteristics of NRD-guide surface-mounted on planar substrate for hybrid integrated circuit, IEEE MTT-S International Microwave Symposium Digest, Boston, pp.1679-1682.

[15] TANG J., DESLANDES, D., ZENG X.; XU S.; WU K.(2001), Substrate-Mounted Non-Radiative Dielectric (NRD)-Guide For Low-Loss Millimeter-Wave Integrated Circuits, IEE Proceedings - Microwaves, Antennas and Propagation, Vol. 148, No. 5, pp. 291-294.

[16] HARRINGTON R. F. (1961), Time Harmonic Electromagnetic Fields, New York: McGraw_hill.

[17] MITTRA R., HOU Y., JAMNEJAD V., (1980), Analysis of open dielectric waveguides using mode-matching technique and variational methods, IEEE Trans. Microwave Theory Tech. Vol. MTT-28, pp.36-43.

[18] COLLIN R. E. (1960), Field Theory of Guided Waves, New York: McGrawHill, Ch.6

[19] ALTSHULER H. M., GOLDSTONE L. O., (1959), On network representations of certain obstacles in waveguide regions, IRE IEEE Trans. Microwave Theory Tech. Vol. MTT-7, pp.213-221.

[20] PENG S.T., OLINER A.A., (1981), Guidance and leakage Properties of a Class of Open Dielectric Waveguides, Part I: Mathematical Formulations, IEEE Trans. Microwave Theory Tech. Vol. MTT-29, pp.843-855.

[21] OLINER A.A., PENG S.T., HSU T., SANCHEZ A., (1981), Guidance and leakage Properties of a Class of Open Dielectric Waveguides, Part II: New Physical Effects, IEEE Trans. Microwave Theory Tech. Vol. MTT-29, pp.855-869.

[22] DAWN D., and SACHIDANANDA M., (1990), Analysis and design of strip line to NRD guide transition, The 3rd Asia-Pacific Microwave Conference Proceedings, Tokyo, pp. 15-18.

[23] WILSON A., JR. ARTUZI, and YONEYAMA T., (1990), A HEMT amplifier for NRD guide integrated Circuits, 3rd Asia-Pacific Microwave Conference Proceedings, Tokyo, pp. 147-150.

[24] TANG J., and WU K. (1999), New millimeter-wave circuit building block concept using innovative surface-mounted nonradiative dielectric (NRD) waveguide, Proc. SPIE, Terahertz and Gigahertz Photonics, vol. 3795, p. 631-638.

[25] TANG J., and WU K. (2000), Co-layered integration and interconnect of planar circuit and non-radiative dielectric (NRD) wave-guide, IEEE Trans. Microwave Theory Tech., vol. 48, pp.519-524.

[26] TANG J., and WU K. (2000), Integrated microstrip to NRD-guide transition using a spurious mode suppressing technique, IEEE MTT-S International Microwave Symposium Digest, Volume: vol. 3, pp. 1805--1808.

[27] BOONE F., HINDSON D., CARON M., ABDULNOUR J., and WU K., (1999), Design and properties of integrated millimeter-wave bandpass filters using nonradiative dielectric waveguide for broadband wireless system, SPIE Symposium Digest, Sept., Boston.

[28] BOONE F., and WU K., Mode conversion and design consideration of integrated non-radiative dielectric (NRD) components and discontinuities, accepted by *IEEE Trans. Microwave Theory Tec.*

[29] MENZEL W., (1997), Packaging and interconnects for millimeter wave circuits: a review, Ann. Telecommun., vol. 51, no. 3-4, pp. 145-154.

[30] MENZEL W., and STRAUSS G., (1996), Millimeter-wave monolitic integrated circuit interconnects using electricmagnetic field coupling, IEEE Trans. Comp., Packag. And Manufact. Technol. part B, vol. 19, no. 2, pp. 278-282.

[31] JIN H., VAHLDIECK R., HUANG J. and RUSSER P., (1993), Rigorous analysis of mixed transmission line interconnects using the frequency domain TLM method, IEEE Trans. Microwave Theory Tec., vol. 41, no.12, pp. 2248-2255.

[32] HOTTA M., QIAN Y. AND ITOH T., (1998), Resonant coupling type microstrip line interconnect using a bonding ribbon and dielectric pad, IEEE MTT-S International Microwave Symposium Digest, vol. 1, pp. 797-802